UNIVERSIDADE ESTADUAL DE CAMPINAS

Fernanda Cristina Alcântara dos Santos

REGULAÇÃO HORMONAL DA PRÓSTATA DE FÊMEAS DO GERBILO: AVALIAÇÃO ESTRUTURAL, CITOQUÍMICA E IMUNOCITOQUÍMICA

Tese apresentada ao Instituto de Biologia para obtenção do Título de Doutor em Biologia Celular e Estrutural, na área de Biologia Celular.

Orientador: Prof. Dr. Sebastião Roberto Taboga

Campinas, 2006

FICHA CATALOGRÁFICA ELABORADA PELA
BIBLIOTECA DO INSTITUTO DE BIOLOGIA – UNICAMP

Sa59r

Santos, Fernanda Cristina Alcântara dos
Regulação hormonal da próstata de fêmeas do gerbilo: avaliação estrutural, citoquímica e imunocitoquímica / Fernanda Cristina Alcântara dos Santos. -- Campinas, SP: [s.n.], 2006.

Orientador: Sebastião Roberto Taboga.
Tese (doutorado) – Universidade Estadual de Campinas, Instituto de Biologia.

1. Próstata feminina. 2. Morfologia (Animais). 3. Andrógenos. 4. Estrógenos. 5. Imunocitoquímica. I. Taboga, Sebastião Roberto. II. Universidade Estadual de Campinas. Instituto de Biologia. III. Título.

(scs/ib)

Título em inglês: Hormonal regulation of the gerbil female prostate: morphology, cytochemistry and immunocytochemistry.
Palavras-chave em inglês: Female prostate; Morphology (Animals); Androgens; Estrogens; Immunocychemistry.
Área de concentração: Biologia Celular.
Titulação: Doutora em Biologia Celular e Estrutural.
Banca examinadora: Sebastião Roberto Taboga, José Carlos Mesquita, Renée Laufer Amorin, Wilma de Grava Kempinas, Sérgio Luis Felisbino.
Data da defesa: 10/11/2006.
Programa de Pós-Graduação: Biologia Celular.

Campinas, 10 de novembro de 2006.

BANCA EXAMINADORA

Prof. Dr. Sebastião Roberto Taboga (Orientador)

Assinatura

Prof. Dr. José Carlos Mesquita

Assinatura

Profa. Dra. Renée Laufer Amorim

Assinatura

Profa. Dra. Wilma De Grava Kempinas

Assinatura

Prof. Dr. Sérgio Luís Felisbino

Assinatura

Profa. Dra. Patrícia Maluf Cury

Assinatura

Prof. Dr. Francisco Eduardo Martinez

Assinatura

Prof. Dr. Classius de Oliveira

Assinatura

Agradecimentos

Ao meu orientador, Prof. Dr. Sebastião Roberto Taboga, por vários motivos... Primeiro, por ter acreditado no meu trabalho e ter me dado a oportunidade de chegar até aqui. Segundo, por ter despertado em mim a incansável paixão pela pesquisa... Por fim, e mais importante, por ser um grande amigo em todos os momentos...

Ao Prof. Dr. Sérgio Luis Felisbino por ter me encaminhado para o meu primeiro estágio de iniciação científica e por ter acompanhado minha formação profissional.

Ao Prof. Dr. Hernandes Faustino Carvalho por toda orientação e colaboração durante todos estes anos de trabalho.

À Profa. Dra. Rejane Maira Góes pelo auxílio na elaboração e discussão dos trabalhos.

À Líliam Panagio, por toda atenção e auxílio durante estes anos de pós-graduação.

À CAPES pela bolsa de estudos concedida.

À FAPESP pelo auxílio técnico e financeiro.

A todos os meus companheiros de pesquisa: Renato, Sérgio, Silvana, Cristiani, Lara, Welerson, Daniela, Maê, Ricardo, Manoel, Rodrigo, Sabrina, Cláudia... sou muito grata à todos, pois esta tese é fruto de um trabalho em equipe.

Ao meu querido técnico do coração, Luiz Roberto Falleiros Júnior, por todo auxílio, amizade e dedicação. Você é a prova de que o amor pela profissão é o segredo do sucesso!

À minha querida Ana Maria, que é a irmã que a vida me deu...

Aos meus amigos-compadres, Sérgio e Silvia, por todo carinho, amparo nos momentos difíceis e pela alegria de me darem um afilhado e uma sobrinha!

A todos os meus amigos do coração, em especial, Cristiane Tomazeli, Gilmara, Matheus Marques, Rose Nunes, Silvia, Miliane, Ricardo Sobreira, Patrícia Vilamaior, Valéria Stranguetti, Jonas Duarte... sem o carinho e o apoio de vocês tudo teria sido mais difícil!

A todos os meus familiares que tanto torcem por mim! Em especial ao meu querido primo Armênio, por ser em minha vida um grande exemplo de perseverança!

Aos meus irmãos, Aline e Alexandre, por serem presença constante de amor em minha vida.

Aos meus amados pais, Alcina e Sérgio, por toda dedicação, amor e apoio em todos os momentos da minha vida. Tudo deu certo por que vocês foram os primeiros a acreditar!

A Deus, que me ama e se faz presente em todos os momentos.

Sumário

Resumo

A próstata feminina é uma glândula funcionalmente ativa encontrada em diversas espécies de mamíferos, incluindo humanos e roedores. Em fêmeas adultas de gerbilos, a próstata apresenta localização parauretral, exibindo íntimo contato com a parede da uretra mediana e distal. Esta glândula é homóloga a próstata ventral de roedores machos, sendo formada por um conjunto de glândulas e ductos inseridos em um estroma fibromuscular. Em machos, a fisiologia prostática é regulada por hormônios esteróides, principalmente andrógenos e estrógenos. Em fêmeas, os fatores que influenciam a atividade prostática são pouco conhecidos, embora existam indícios de que alterações hormonais decorrentes da senescência estejam associadas à instalação de lesões prostáticas. Assim, o objetivo deste trabalho foi avaliar os fatores que promovem a regulação hormonal da próstata feminina do gerbilo (*Meriones unguiculatus*) em condições de hiperandrogenismo e de supressão da atividade estrogênica. Os resultados obtidos com as análises estruturais, ultra-estruturais, sorológicas e imunocitoquímicas permitiram concluir que a próstata feminina do gerbilo é sensível à ação de andrógenos e de agentes anti-estrogênicos. O estímulo androgênico provocou crescimento anormal da próstata, aumento da atividade secretória, além de causar displasia prostática e síndrome de ovário policístico. O tratamento com letrozol resultou em aumento dos níveis séricos de testosterona, hiperplasia glandular, incremento da atividade secretória e crescimento displásico, simulando os efeitos causados por andrógenos exógenos. Os efeitos causados pelo tamoxifeno indicam que este agente endócrino atuou como agonista estrogênico na próstata, causando hipertrofia glandular, diminuição da

atividade secretória e desenvolvimento de lesões prostáticas, tais como prostatites e adenocarcinoma. Deste modo, pode-se concluir que a utilização de drogas hormonalmente ativas resulta em uma série de efeitos complexos que comprometem a fisiologia de órgãos hormônio-dependentes, como a próstata feminina e os ovários. O desequilíbrio hormonal provocado pela administração destas drogas causa profundas alterações na morfologia prostática, de maneira muito similar ao que ocorre durante o desenvolvimento de lesões espontâneas em mulheres no período pós-menopausa. Assim, essas terapias devem ser utilizadas com cautela, visto que longos períodos de tratamento podem resultar em lesões malignas da próstata feminina.

Abstract

The female prostate is a functionally active gland found in several species of mammals, including humans and rodents. In adult female gerbils, the prostate presents a paraurethral location, showing close contact with the wall of urethra in its median and distal portions. This gland is homologue to the ventral prostate of male rodents and it is formed by a cluster of glands and ducts inserted into a fibermuscular stroma. In males, the prostatic physiology is regulated by steroid hormones, mainly androgen and estrogen. In females, the factors that influence the prostatic activity are unclear, although there are evidences that the hormonal alterations caused by aging are associated with the installation of prostatic lesions. Thus, the objective of this work is to evaluate the factors that promote the hormonal regulation of the gerbil (*Meriones unguiculatus*) female prostate in hyperandrogenic conditions and estrogenic activity suppression. The results obtained with the structural, ultrastructural, serologic and immunocytochemical analyses showed that the gerbil female prostate is responsive to androgenic and the anti-estrogenic action. The androgenic stimulus has caused an abnormal prostatic growth, increase in secretory activity, and has also caused prostatic dysplasia and polycystic ovary syndrome. The letrozole treatment has stimulated an increase in testosterone serum levels, glandular hyperplasia, increment of the secretory activity and dysplasic growth, simulating the effects provoked by exogenous androgens. The effects caused by tamoxifen indicate that this endocrine agent has acted as an estrogenic agonist on the prostate, causing glandular hypertrophy, decrease in secretory activity and prostatic lesions. Hence, it is possible to

conclude that the use of hormonally active drugs results in a series of complex effects that endanger the physiology of hormone-dependent organs, like female prostate and ovaries. The hormonal unbalance caused by the administration of such drugs results in alterations in prostatic morphology similar to what occurs during the development of spontaneous lesions in post-menopausal women. Thus, the utilization of such therapies must occur in a careful manner because a long-term treatment can cause malignant lesions in female prostate.

1. Desenvolvimento embrionário do sistema urogenital

O sistema urogenital em desenvolvimento contém estruturas epiteliais de origem mesodérmica (ductos mesonéfricos ou de Wolf e ductos paramesonéfricos ou de Müller) e endodérmica (seio urogenital - SUG) que estão associadas ao tecido conjuntivo indiferenciado do embrião, o mesênquima (Cunha et al., 2002; Marker et al., 2003; Staack et al., 2003).

Os estágios iniciais de desenvolvimento gonadal são idênticos em embriões masculinos e femininos, sendo esta fase denominada estágio indiferenciado ou ambissexual da diferenciação sexual. Em camundongos, as gônadas masculina e feminina passam a ser distinguíveis morfologicamente apenas aos 13 dias de gestação (Staack et al., 2003).

Em machos de camundongos, após o 13º dia de gestação as células mesenquimatosas do rudimento gonadal se agregam e se condensam em cordões epiteliais que tornam-se os túbulos seminíferos. A partir do 14º dia de gestação, as células de Leydig dos testículos fetais diferenciam-se e passam a secretar testosterona (Pointis et al., 1980). A testosterona evita a morte celular programada do ducto mesonéfrico, estimulando o seu desenvolvimento para formar o epidídimo, ducto deferente, vesícula seminal e ductos eferentes. Paralelamente, as células de Sertoli iniciam a produção da substância inibidora Müleriana (MIS), que provoca a regressão do ducto paramesonéfrico.

Em fêmeas, os ovários fetais são relativamente inativos na função endócrina, não sendo requeridos para o desenvolvimento embrionário do trato urogenital feminino. Na ausência de estímulos androgênicos, o ducto mesonéfrico regride e, na ausência de MIS, o ducto paramesonéfrico se desenvolve, originando os ovidutos, cornos uterinos, canal cervical e porção superior da vagina (Staack et al., 2003).

A próstata desenvolve-se a partir do seio urogenital, que é um tubo endodérmico derivado do intestino primitivo e que termina na cloaca. O septo uroretal divide a cloaca em seio urogenital ventralmente e em canais retal e anal dorsalmente. A subdivisão da cloaca ocorre de maneira que os ductos mesonéfricos e paramesonéfricos terminam no seio urogenital. Posteriormente, o seio urogenital é subdividido em vesícula urinária e em seio urogenital definitivo. Em camundongos, os dois derivados do seio urogenital são claramente demarcados entre o 13º e 14º dias de gestação (Staack et al., 2003).

O seio urogenital é composto por uma camada epitelial (UGE) derivada da endoderme, que é circundada por uma camada mesenquimal (UGM) originada da mesoderme. Esta estrutura é encontrada na base da vesícula urinária em desenvolvimento e surge nos machos e nas fêmeas após 13 dias de concepção nos camundongos e ratos, e após 7 semanas de gestação em humanos. O seio urogenital é morfologicamente indistinguível em machos e fêmeas até o 17º-18º dia de gestação em camundongos e até a 10º-12º semana em humanos. A partir desse período, inicia-se a morfogênese prostática, um processo que é iniciado e dependente de andrógenos (Marker et al., 2003).

Em machos, o evento inicial da morfogênese prostática é o crescimento de brotos epiteliais sólidos do epitélio do seio urogenital (UGE) em direção ao mesênquima circundante do seio urogenital (UGM). Em roedores, a maioria dos ductos prostáticos não é

ramificada ao nascimento. Entretanto, no período neonatal, conforme esses cordões crescem invadindo o mesênquima do seio urogenital, eles começam a bifurcar-se em ramos laterais, originando três lobos prostáticos distintos: o lobo ventral, o lobo dorsolateral e a glândula coaguladora ou lobo anterior (Marker et al., 2003). Simultaneamente ao processo de morfogênese de ramificação ductal, ocorre a canalização ductal (formação do lúmen) e a citodiferenciação epitelial e estromal (Wang et al., 2001).

Sendo a morfogênese prostática dependente de hormônios esteróides, os andrógenos são necessários para iniciar o desenvolvimento prostático, para continuar o seu crescimento embrionário e neonatal e, posteriormente, para iniciar a atividade secretória prostática na puberdade (Isaacs et al., 1994). No entanto, a ação androgênica não é exercida diretamente sobre as células epiteliais. Sob a influência de andrógenos, as células mesenquimais produzem e secretam fatores parácrinos específicos que ditam o crescimento e diferenciação da glândula prostática. Assim, com a diferenciação das células epiteliais, os níveis de receptores androgênicos (AR) aumentam e a expressão de receptores estrogênicos epiteliais (ERβ) e estromais (ERα) é induzida.

Interações epitélio-mesenquima desempenham um papel chave no direcionamento do crescimento e do desenvolvimento da próstata, sendo que a sinalização parácrina do mesênquima para o epitélio é essencial para a embriogênese prostática. Desse modo, a ação de andrógenos sobre as células mesenquimais resulta em fatores parácrinos específicos que atuam sobre as células epiteliais induzindo a sua proliferação (Thomson et al., 2001). Por outro lado, também existe uma sinalização parácrina do epitélio para o mesênquima. Esta sinalização regula a diferenciação do mesênquima que circunda os brotos em formação em um estroma composto por células musculares lisas e fibroblastos (Hayward et al., 1996).

Assim, durante a morfogênese prostática, o AR é necessário no mesênquima e não no epitélio, sendo que sua expressão precede o surgimento dos brotos prostáticos. Nas células epiteliais, a função do AR se restringe à regulação de proteínas secretórias e, talvez, à diferenciação celular (Donjacour e Cunha, 1993).

Dentre os fatores parácrinos que atuam sobre a morfogênese prostática, pode-se citar os fatores de transcrição da família homeobox NKx3.1, Hoxa-13, Hoxb-13 e Hoxd-13, os fatores da família FGF (FGF-7 e -10) (Huang et al., 2004), a glicoproteína Sonic hedgehog (Shh), o receptor para Shh, patch (ptc), os fatores de transcrição da família Gli e BMP-4 (Pu et al., 2004). O gene NKx3.1 é expresso no epitélio do seio urogenital (UGE) antes do início do brotamento prostático e parece desempenhar um papel na diferenciação epitelial e determinação prostática (Bieberich et al., 1996). Hoxa-13, Hoxb-13 e Hoxd-13 são expressos no mesênquima do seio urogenital, estando envolvidos no desenvolvimento prostático. Estes fatores são expressos em altos níveis durante a vida fetal, porém seus níveis declinam após o nascimento. FGF-10 e FGF-7 são produzidos pelas células do mesênquima do seio urogenital e interagem com o mesmo receptor (FGFR2iiib), que é expresso pelas células do epitélio do seio urogenital. Em conjunto, esses fatores apresentam papel crítico no direcionamento da expansão e ramificação dos brotos prostáticos (Huang et al., 2004). A glicoproteína Shh é secretada pelas células do epitélio do seio urogenital na interface mesenquimal da próstata em desenvolvimento, ativando o seu receptor patch (ptc), que é expresso nas células mesenquimais. A ligação Shh-ptc desencadeia uma cascata de sinais moleculares que resulta no aumento dos níveis de fatores de transcrição Gli que, por sua vez, mediam os efeitos de Shh. Em vertebrados, são conhecidos três tipos de transcritos Gli (Gli-1, -2, -3) que são redundantes e compartilham a mesma função.

Acredita-se que o gene Shh esteja envolvido na iniciação do brotamento e expansão prostática. Além disso, Shh parece regular muitos outros genes envolvidos no desenvolvimento prostático, incluindo Hoxa-13, Hoxd-13 e NKx3.1 (Pu et al., 2004). As proteínas morfogenéticas BMP-4 são membros da família TGF-β e, em geral, agem inibindo a proliferação durante o desenvolvimento prostático. Na próstata de camundongos, o RNAm para BMP-4 está localizado no mesênquima, sendo que seus níveis declinam no período pós-natal. Na figura 1, propõem-se um modelo pelo qual esses fatores parácrinos atuam em conjunto para dirigir a morfogênese prostática de roedores no período pós-natal (Huang et al., 2004).

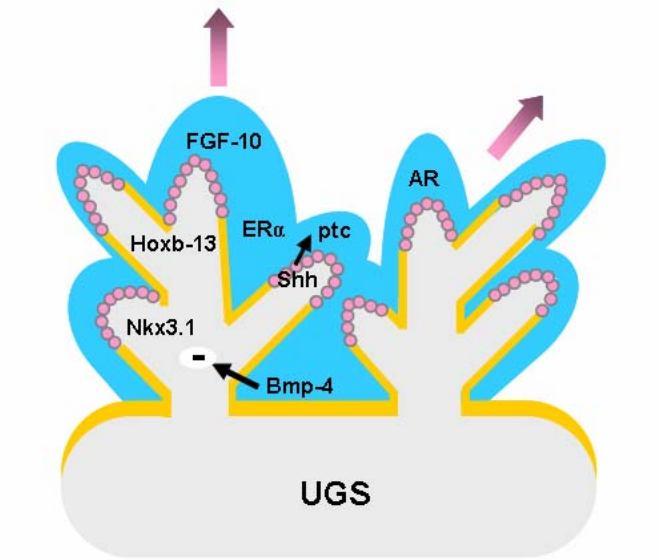

Figura 1. Na próstata masculina normal, a expressão de receptores androgênicos (AR) e estrogênicos (ERα) ocorre nas células estromais (azul) localizadas nas proximidades dos brotos prostáticos em crescimento (cinza). A expressão de BMP-4, que é alta antes do brotamento prostático, declina rapidamente após o nascimento, cessando seu efeito inibitório sobre o crescimento ductal. A glicoproteína Shh é secretada pelas células epiteliais (rosa) das pontas distais dos brotos em crescimento e ativa o receptor ptc localizado nas células estromais adjacentes. A ativação de ptc desencadeia uma série de sinalizações que provocam o crescimento e diferenciação prostática. FGF-10 é expresso pelas células mesenquimais distais e estimula o crescimento e ramificação ductal. NKx3.1 é expresso precocemente pelas células epiteliais indiferenciadas e está envolvido na iniciação prostática e na diferenciação epitelial. Hoxb-13 é expresso pelas células epiteliais e participa da manutenção de fenótipo diferenciado dessas células. Camada de músculo liso (amarelo) (modificado de Huang et al., 2004).

Em embriões de fêmeas de ratos e humanos, a ausência de testosterona induz o seio urogenital a originar a porção inferior da vagina e a uretra (Shapiro et al., 2004). O mesênquima do seio urogenital passa a circundar o epitélio uretral, sendo subdividido em três zonas: o mesênquima periuretral, a zona mesenquimal que sofre diferenciação em músculo liso e a zona que contém o mesênquima condensado ventral (VMP). Esta última estrutura apresenta localização análoga à próstata ventral masculina e representa o mesênquima do seio urogenital sem a invasão epitelial (Thomson et al., 2002).

A diferenciação de parte do mesênquima do seio urogenital em músculo liso é crucial para a morfogênese prostática em machos e fêmeas, pois é este evento que regula a sinalização parácrina entre o epitélio e o mesênquima (Thomson et al., 2002).

Durante a diferenciação do mesênquima, os andrógenos regulam a espessura e a continuidade da camada de músculo liso formada, de modo que a ausência de andrógenos em embriões femininos ocasiona a formação de uma camada muscular espessa e contínua. Esta camada separa o mesênquima condensado ventral (VMP) do epitélio uretral, impedindo que os brotos epiteliais prostáticos que estão emergindo da uretra entrem em contato direto com o VMP. Desse modo, a espessa camada de músculo liso impede a interação do mesênquima condensado ventral com os brotos prostáticos em formação, bloqueando a comunicação parácrina entre o epitélio e o mesênquima (Thomson et al., 2002). Em machos, na presença de andrógenos, a formação do músculo liso é inibida ou atrasada e os brotos prostáticos emergem da uretra e podem penetrar no mesênquima condensado ventral. Assim, a interação parácrina epitélio-mesênquima é estabelecida, ocasionando a ramificação e expansão da próstata ventral. O modelo ilustrativo da indução

prostática em machos e fêmeas foi proposto por Thomson e colaboradores (2002) e pode ser observado na figura 2.

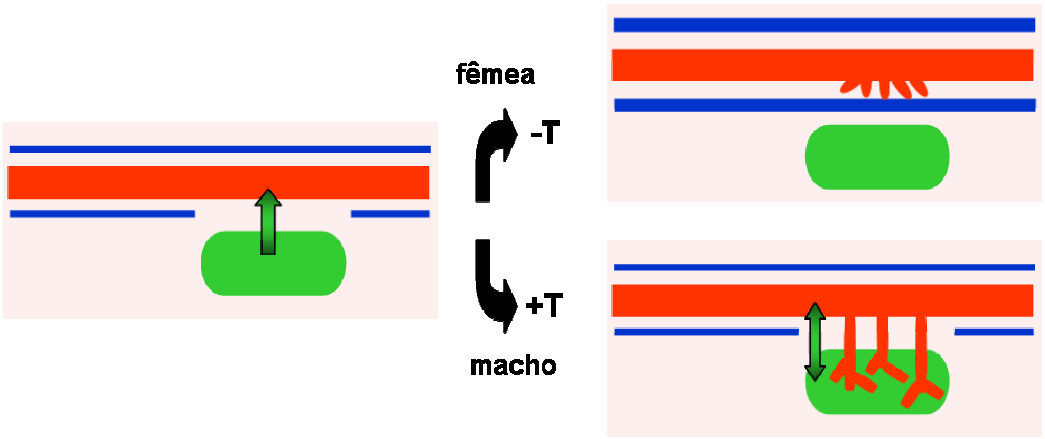

Figura 2. Modelo descritivo da indução da próstata ventral em embriões femininos e masculinos de ratos. Do lado esquerdo pode-se observar o mesênquima condensado ventral (verde) durante os estágios iniciais de indução prostática (17-18 dias de gestação). Observe que a camada de músculo liso (azul) é descontínua e permite a sinalização entre o mesênquima condensado ventral e o epitélio uretral (vermelho). Do lado direito pode-se observar a morfogênese prostática em machos e fêmeas (a partir de 21,5 dias de gestação). Em fêmeas, a ausência de testosterona permite que o músculo liso forme uma camada espessa e contínua, impedindo a sinalização parácrina entre os brotos prostáticos em crescimento (vermelho) e o mesênquima condensado ventral. Em machos, a testosterona induz a formação de uma camada muscular delgada e descontínua que permite a interação epitélio-mesenquimal. Os brotos que emergem do epitélio uretral (vermelho) invadem o mesênquima condensado ventral. No período neonatal, esses brotos sofrem bifurcações laterais dentro do mesênquima condensado ventral, originando a próstata ventral (modificado de Thomson et al., 2002).

A formação de brotos prostáticos é um processo constitutivo de machos e fêmeas, porém a ramificação e expansão desses brotos é regulada por andrógenos. Em fêmeas, o isolamento entre o mesênquima condensado ventral e o epitélio uretral, que é provocado pela camada de músculo liso, impede a formação de uma glândula prostática desenvolvida e lobulada. Desse modo, o reduzido tecido prostático observado em fêmeas de várias espécies é originário do seio urogenital que não sofreu estímulo androgênico. No entanto, embora a próstata feminina adulta seja menor que a masculina (cerca de 15% a 25% do

tamanho da próstata ventral masculina), ela apresenta um epitélio secretor diferenciado e funcional (Zaviačič et al., 2000a; Santos et al., 2003; Custódio et al., 2004). Como a próstata de fêmeas cresce e desenvolve-se em um ambiente com baixos níveis de andrógenos (apenas 5% do total de precursores androgênicos produzidos no organismo masculino), acredita-se que outros fatores além desses hormônios possam atuar no desenvolvimento e manutenção da função dessa glândula em adultos (Timms et al., 1999).

A freqüência de desenvolvimento de uma glândula prostática funcional em fêmeas é muito elevada. Na espécie humana, cerca de 90% das mulheres desenvolvem um tecido prostático maduro e ativo nos processos de secreção (Zaviačič et al., 2000b). Em fêmeas de roedores, a morfogênese prostática parece ser influenciada pela posição intrauterina dos animais durante a gestação (Clark et al., 1991; Timms et al., 1999). Assim, em fetos femininos de ratos, o desenvolvimento de brotos prostáticos é mais freqüente quando a gestação ocorre entre duas fêmeas (gestação 2F - 67% de ocorrência de próstata), e mais raro quando a gestação ocorre entre dois machos (gestação 2M - 29% de freqüência de próstata). Isso acontece por que animais de gestação 2F e 2M apresentam diferenças naturais nos níveis de testosterona (T) e estrógeno (E). As fêmeas com gestação 2F apresentam maiores níveis de E, que é o hormônio responsável por modular os efeitos dos andrógenos sobre a próstata em desenvolvimento, induzindo um maior crescimento dos brotos prostáticos durante a morfogênese glandular (Timms et al., 1999).

2. Próstata feminina: novos conceitos e mudança de paradigmas

O primeiro relato a respeito da "próstata feminina" ocorreu em 1672, quando Reinier de Graaf usou este termo para descrever um conjunto de glândulas localizadas ao redor da uretra, as quais, segundo ele, apresentavam grande homologia com a próstata masculina (de Graaf, 1672). Dois séculos depois, Alexander Skene redescreveu a próstata feminina como sendo formada por dois ductos parauretrais principais que se abrem em orifícios de ambos os lados da uretra, e que são desprovidos de função secretória (Skene, 1880). Desde então, este conjunto de glândulas passou a ser chamado de "glândulas parauretrais de Skene" e, por um longo tempo, esta glândula foi considerada como um órgão vestigial, sem nenhuma importância biológica para o organismo feminino (Zaviačič e Ablin, 2000).

No entanto, a partir de 1950 novas pesquisas retomaram a discussão a respeito da próstata feminina, principalmente com relação ao papel biológico que este órgão poderia desempenhar no organismo da mulher (Huffman, 1948, 1951; McCrea, 1952; Tepper et al., 1984; Wernet et al., 1992; Zaviačič, 1993; Zaviačič et al., 1993; 1997a; b; 2000a; b). Destes trabalhos, destacam-se os de Zaviačič e colaboradores que juntos editaram um livro que descreve amplamente a próstata feminina humana, abordando principalmente seus aspectos estruturais e funcionais, bem como suas implicações sexológicas (Zaviačič, 1999).

Zaviačič apresenta a próstata feminina humana como um conjunto parauretral de numerosas glândulas e ductos que estão inseridas em um estroma fibromuscular (Zaviačič et al., 2000a). As glândulas são revestidas por um epitélio secretor maduro e diferenciado, que apresenta dois tipos principais de células: as basais, que são células fonte responsáveis

pela manutenção da população de células prostáticas, e as secretoras ou luminais que produzem continuamente o líquido prostático (Zaviačič et al., 2000b). As células luminais são as mais numerosas e expressam o antígeno específico da próstata (PSA) e a fosfatase ácida prostática (PSAP), dois importantes marcadores prostáticos (Zaviačič et al., 1993).

Paralelamente aos estudos com material humano, diversas pesquisas têm demonstrado a ocorrência de próstata em fêmeas de diversos roedores como *Praomys natalensis* (Smith et al., 1978; Gross e Didio, 1987), *Rattus novergicus* (Shehata, 1980; Vilamaior et al., 2005), *Lagostomus maximus maximus* (Flamini et al., 2002), *Meriones libycus* (Shehata, 1974; 1975) e *Meriones unguiculatus* (Santos et al., 2003; Custódio et al., 2004). Estes trabalhos demonstraram a existência de grande semelhança entre a próstata feminina de roedores e humanos. Além disso, as características morfológicas apresentadas por estas pesquisas indicaram que a próstata feminina dessas espécies é equivalente à próstata ventral masculina, e que suas células epiteliais exibem um fenótipo de células funcionalmente ativas.

O exato papel biológico que a próstata desempenha no organismo feminino ainda não foi totalmente esclarecido. Estudos bioquímicos demonstraram que o líquido prostático liberado durante a ejaculação feminina apresenta a mesma constituição química do líquido prostático masculino. Dentre os componentes do ejaculado feminino humano, os mais abundantes são o PSA, PSAP, zinco e frutose (Zaviačič, 1993; 1999). Evidências indicam que a frutose produzida por esta glândula escoa em pequenas quantidades da uretra para a vagina, desempenhando importante papel para a reprodução. Assim, como a frutose é a principal fonte de energia para os espermatozóides, a fêmea também garante o sucesso da fertilização dos ovócitos. Além disso, estudos recentes confirmaram a detecção de níveis de

PSA no soro e na urina de mulheres (Zaviačič e Ablin, 2000; Schmidt et al., 2001). Estes trabalhos indicaram que a próstata é a principal produtora de PSA nas fêmeas, embora existam outras fontes extraprostáticas para sua expressão (Diamandis e Yu, 1997; Yu e Berkel, 1999; Galadari et al., 2004; Kocak, 2004; Sauter et al., 2004).

Outro campo de exploração para as possíveis funções da próstata feminina é a sua importância na manifestação do comportamento sexual feminino (Zaviačič, 1993). Alguns trabalhos têm associado a próstata feminina ao ponto de Gräfenberg (ponto-G), ressaltando a importância do estímulo deste ponto para que o fenômeno de ejaculação feminina aconteça (Schubach, 2002). Pela definição de Gräfenberg, o ponto-G se refere a uma "área" ou "zona" ricamente inervada presente na parede ântero-superior da vagina, através da qual a próstata feminina pode ser acessada (Gräfenberg, 1950). No entanto, artigos polêmicos defendem que a próstata feminina e o ponto G são as mesmas estruturas (Addiego et al., 1981; Hines, 2001).

Além das implicações biológicas e comportamentais acima expostas, o principal foco de interesse sobre a próstata feminina advém de sua capacidade em desenvolver lesões severas durante a senescência. Trabalhos recentes têm relatado a ocorrência de cânceres de uretra, cujo foco de origem é a próstata feminina (Dodson et al., 1994; 1995; Ali et al., 1995; Ebisuno et al., 1995; Sloboda et al., 1998; Islam et al., 2001; Sharifi-Aghdas e Ghaderian, 2004; Kato et al., 2005; McCluggage et al., 2006). Além disso, existem evidências de que outras desordens prostáticas, tais como prostatites e hiperplasia benigna prostática acometam a próstata feminina com o mesmo grau de potencialidade observado na próstata masculina (Zaviačič, 1999). Cistites severas são a forma mais comum de infecção do trato urinário feminino, e a incidência desta lesão em mulheres jovens nos EUA

é de 0,5-0,7 episódios por pessoa por ano. Atualmente sabe-se que o foco de origem dessas cistites é a próstata feminina. Como existe uma comunicação do sistema de glândulas prostáticas com a uretra e a parede anterior da vagina, quando ocorre a inflamação da próstata (prostatites ou Skenites), esta se dissemina por todo o trato reprodutor feminino, caracterizando as conhecidas útero-prostato-cistites (Zaviačič, 1999).

A partir das colocações acima expostas, torna-se inviável considerar a próstata feminina como um órgão vestigial e insignificante e, desse modo, a definição de Skene deve ser reavaliada. Embora a próstata feminina seja menos desenvolvida que a masculina, ela é um órgão ativo nos processos de secreção e merece os cuidados que qualquer outro órgão do organismo feminino, uma vez que alterações em sua fisiologia podem comprometer a saúde e a qualidade de vida das mulheres. Assim, são necessários estudos que permitam o melhor entendimento dos processos que mantém a homeostase dessa glândula, visto que pouco se sabe a respeito dos eventos fisiológicos que mantém a funcionalidade da próstata feminina tanto em condições normais quanto em patológicas.

3. Próstata feminina: experimentos com roedores

A morfologia da próstata feminina, tanto humana quanto de roedores, já foi descrita por vários pesquisadores (Shehata, 1980; Gross and Didio, 1987; Zaviačič, 1999; Flamini et al., 2002). No entanto, nenhum desses trabalhos investigou efetivamente os mecanismos que regem o funcionamento da glândula prostática feminina.

Os experimentos com material humano são muito limitados, pois a próstata feminina só pode ser obtida a partir de necrópsias de mulheres que sofreram morte cerebral

(Zaviačič, 2000a). Assim, torna-se necessária a adoção de modelos experimentais que apresentem uma glândula prostática semelhante à da mulher, a fim de se extrapolar os dados para a espécie humana.

A adoção do gerbilo da Mongólia (*Meriones unguiculatus,* Gerbilinae, Muridae, figura 3) como modelo experimental tem trazido resultados muito satisfatórios, uma vez que a próstata feminina deste roedor apresenta grande homologia com a próstata feminina humana (figura 4) e com a próstata ventral do gerbilo macho (Taboga et al., 2001). Além disso, a ocorrência de próstata em fêmeas desses animais é muito elevada, sendo que cerca de 80% das fêmeas apresentam uma glândula prostática bem desenvolvida e ativa nos processos de secreção (Santos et al., 2003).

Figura 3. Gerbilo da Mongólia (*Meriones unguiculatus*).

Anatomicamente, a próstata feminina do gerbilo é composta por um conjunto de glândulas e ductos que se concentram em ambos os lados da uretra mediana. Os ductos estão inseridos na musculatura envolvente da uretra, e se abrem em vários pontos da luz uretral (Santos et al., 2003)

A porção secretora da próstata de fêmeas adultas do gerbilo é revestida por um epitélio que varia de cúbico simples a colunar pseudoestratificado. As células epiteliais são

de dois tipos: as basais, que formam uma camada descontínua de células-fonte para a manutenção do crescimento prostático, e as secretoras que apresentam um citoplasma rico em organelas envolvidas nos processos de síntese e secreção de glicoproteínas (figura 4) (Santos et al, 2003). As glândulas e os ductos prostáticos estão associados a um estroma fibromuscular composto por células musculares lisas e fibroblastos, fibras de colágeno e elásticas, e muitos vasos sangüíneos (Santos et al., 2001).

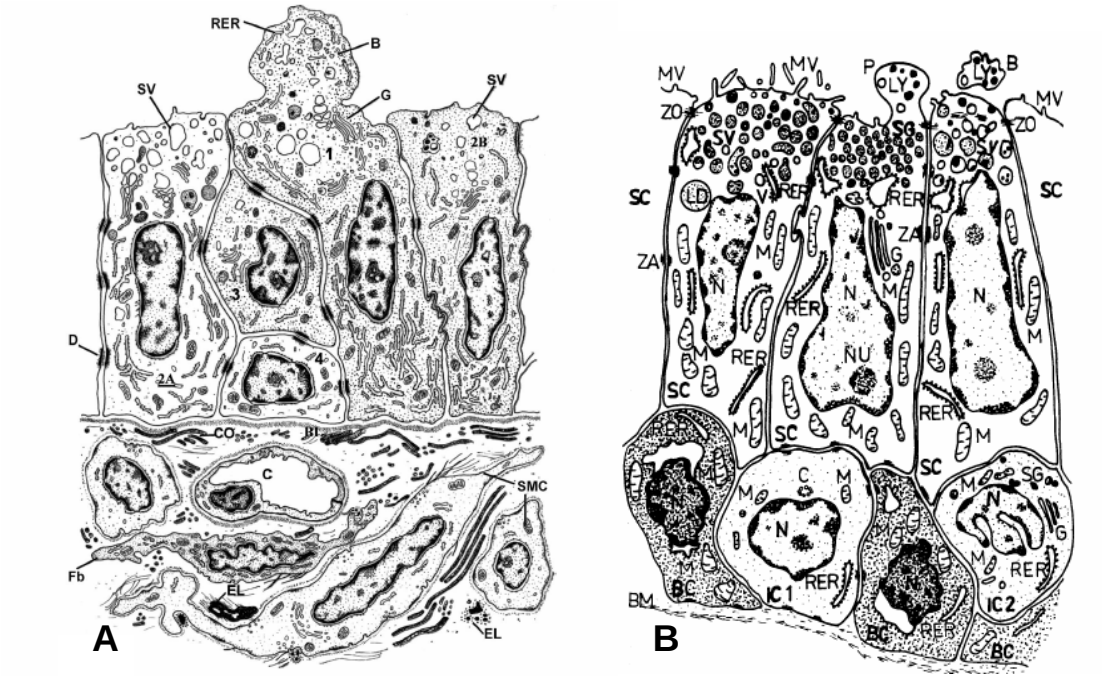

Figura 4. Aspectos ultra-estruturais da próstata feminina do gerbilo (A – Santos et al., 2003) e humana (B - Zaviačič et al., 2000a). A próstata feminina adulta do gerbilo apresenta grande semelhança com a humana. Os mesmos tipos epiteliais são observados em ambas as espécies. O compartimento estromal da próstata feminina do gerbilo é denso, sendo composto por células musculares lisas (SMC) e fibroblastos (Fb), além de muitas fibras de colágeno (CO) e elásticas (El) **A** – 1: célula secretora apócrina; 2A: célula secretora merócrina clara; 2B célula secretora merócrina típica; 3: célula intermediária; 4: célula basal. **B** – SC: célula secretora; BC: célula basal; IC1 e IC2 células intermediárias. B: "blebs" apicais; BM: membrana basal; C: capilar; G: complexo de Golgi; M: mitocôndrias; RER: retículo endoplasmático rugoso; SV: vesículas de secreção.

As características morfofuncionais da próstata feminina adulta normal do gerbilo demonstram que esta glândula é madura e fisiologicamente ativa, embora a produção de andrógenos no organismo feminino seja muito reduzida (Santos et al., 2003). Desse modo, acredita-se que outros fatores como, por exemplo, os estrógenos, influenciem a fisiologia prostática. Assim, torna-se fundamental compreender os fatores que regulam a diferenciação, crescimento e secreção da próstata feminina, uma vez que alterações nestes fatores podem levar à instalação de lesões malignas.

4. Reguladores endócrinos da atividade prostática

Os fatores que regulam o desenvolvimento e atividade da próstata feminina são pouco conhecidos, mas muitos estudos sugerem que os hormônios esteróides desempenham um importante papel na manutenção da fisiologia prostática (Zaviačič et al., 2000a, b; Santos et al., 2003).

Assim como a próstata de machos pós-púberes, a próstata feminina do gerbilo adulto pode ser considerada como um órgão maduro, uma vez que apresenta um epitélio glandular diferenciado. No entanto, ela é menos desenvolvida que a próstata masculina, devido aos baixos níveis androgênicos presentes no organismo feminino (Zaviačič et al., 2000b).

No organismo feminino existe uma baixa concentração de testosterona circulante, que é produzida pelos ovários e pela glândula adrenal (Staub e Beer, 1997). A glândula adrenal secreta primariamente os precursores androgênicos, como por exemplo, o sulfato de

diidroepiandrosterona (DHEA-S), a diidroepiandrosterona (DHEA) e a androstenediona, que são convertidos pelos tecidos periféricos em suas formas fisiologicamente ativas. Os andrógenos secretados pelos ovários são a androstenediona, a DHEA e a testosterona. Comparados à glândula adrenal, os ovários produzem aproximadamente 25% do total de testosterona circulante no organismo de fêmeas em idade reprodutiva. Na espécie humana, com a conversão dos precursores androgênicos em testosterona, a produção diária desse hormônio em mulheres adultas pode chegar a 0,35mg. Isso demonstra que os níveis de testosterona circulante no organismo feminino são muito inferiores aos apresentados pelo organismo masculino, que são de aproximadamente 7mg/dia (Staub e Beer, 1997).

Receptores para testosterona têm sido identificados nos ovários, ovidutos e útero, indicando que os andrógenos exercem um significativo papel na regulação e desenvolvimento do aparelho reprodutor feminino (Staub e Beer, 1997). Estudos imuno-histoquímicos demonstraram que os receptores para andrógenos também estão presentes na próstata feminina humana, podendo estar relacionados com a manutenção da estrutura desta glândula no organismo feminino (Wernet, 1992).

Atualmente, muitos trabalhos têm investigado a influência do estrógeno sobre o metabolismo da próstata de machos (Timms et al., 1999; Härkönen & Mäkelä, 2004; García-Flórez et al., 2005; Risbridger et al., 2003), uma vez que este hormônio está envolvido na modulação dos efeitos dos andrógenos, na proliferação glandular e na etiologia de doenças prostáticas. No entanto, até o momento nenhuma pesquisa avaliou se os estrógenos participam direta ou indiretamente do controle fisiológico da próstata feminina. Assim, é de fundamental importância que se desenvolvam estudos que

verifiquem a influência do estrógeno sobre a próstata feminina, visto que ela está exposta aos altos níveis estrogênicos presentes no organismo feminino.

5. Terapias endócrinas e inibição da atividade estrogênica

Nas últimas décadas, diversas terapias anti-estrogênicas foram desenvolvidas com o objetivo de interromper a progressão de tumores malignos estrógeno-positivos. Dentre os agentes terapêuticos mais indicados atualmente, destacam-se o tratamento com o tamoxifeno (Cabot et al., 1996) e o letrozol (Berstein et al., 2002; Haynes et al., 2003; Smith, 2003), ou a combinação de ambos (Dixon et al., 2003; Ingle e Suman, 2003; Miller et al., 2003). Estas drogas também estão sendo apontadas como benéficas na supressão do câncer prostático, cujas células tornam-se altamente proliferativas pela ação combinada de andrógenos e estrógenos (Block et al., 1996).

O tamoxifeno é um trifeniletileno não-esteroidal que exibe função mista agonista/antagonista sobre o estrógeno (figura 5), dependendo da espécie e do órgão analisado (Berstein et al., 2003; Zhang et al., 2005).

Em humanos, o tamoxifeno atua como antagonista estrogênico na mama, sendo amplamente utilizado como primeira linha de tratamento do câncer mamário positivo ao receptor estrogênico (Gradishar, 2004). Ele também é um antagonista do metabolismo de glicolipídeos, os quais exercem uma grande influência sobre o crescimento e diferenciação celular, além de desempenhar um importante papel na diminuição de ocorrência de metástases (Cabot et al., 1996).

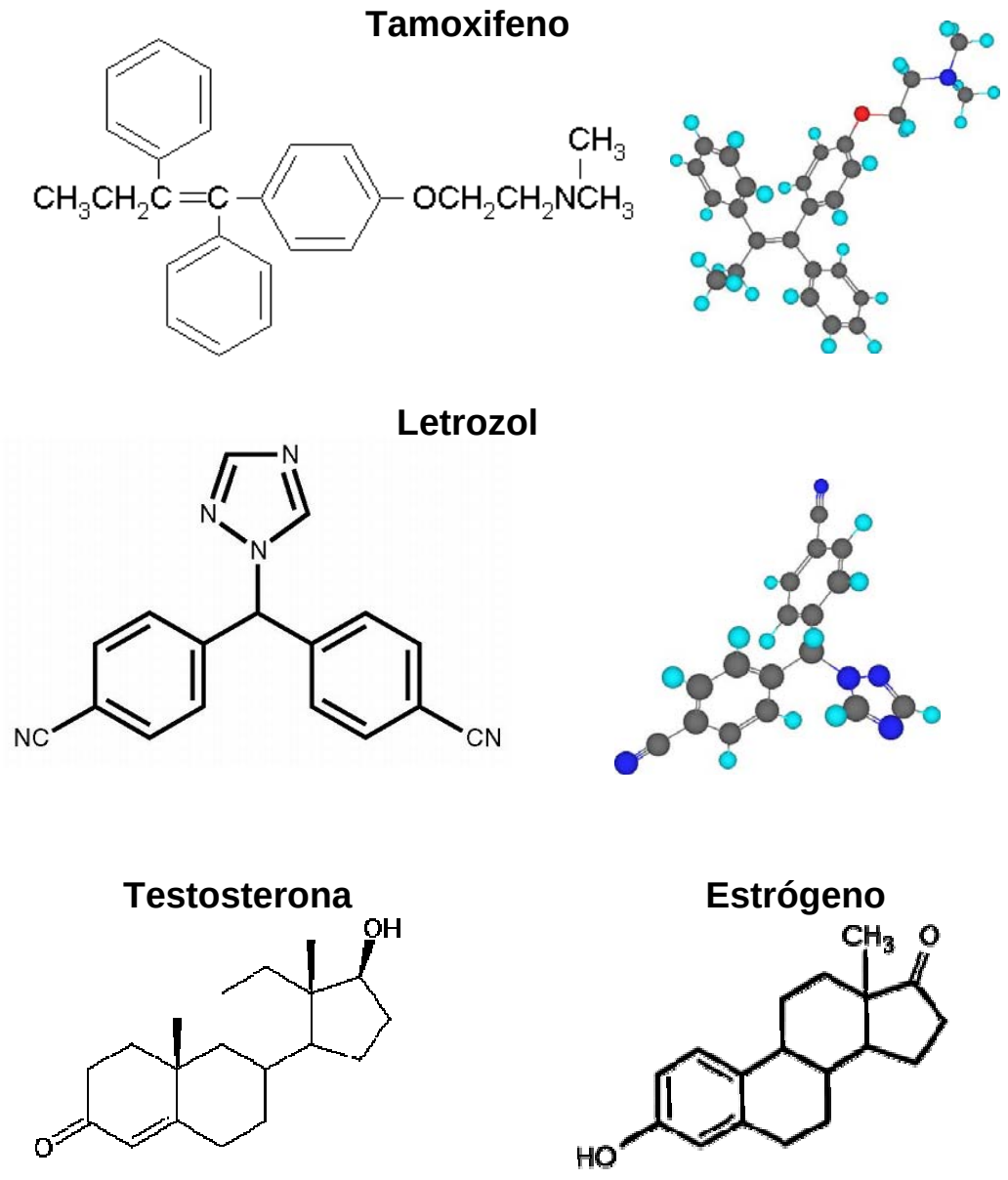

Figura 5. Forma molecular e arranjo tridimensional dos anti-estrogênicos tamoxifeno e letrozol. O tamoxifeno compete com o estrógeno para ligar-se aos receptores estrogênicos alfa e beta. O letrozol liga-se ao sítio ativo da enzima aromatase, impedindo que a testosterona seja aromatizada em estrógeno.

Em fêmeas de camundongos, o tamoxifeno exerce o mesmo efeito antagonista na mama, porém atua como agonista estrogênico no útero e na vagina (Taguchi, 1987).

Estudos com camundongos machos demonstraram que o tamoxifeno age como agonista parcial do ERα na próstata ventral, causando lesões similares às encontradas em roedores machos estrogenizados neonatalmente (Singh e Handelsman, 1999).

O letrozol é um inibidor não-esteroidal da enzima aromatase capaz de evitar até 99% da conversão periférica de andrógenos em estrógenos (figura 5) (Haynes et al., 2003). Estudos com fêmeas de ratos adultos demonstraram que o letrozol (0,3–1mg/kg/dia) interrompe completamente a ciclicidade ovariana e reduz o peso uterino e as concentrações de estradiol no soro, da mesma forma como ocorre com a ovariectomia (Bhatnagar et al., 1990). Em estudos de carcinogeneticidade, o letrozol diminuiu significativamente a incidência de tumores espontâneos do trato reprodutivo de fêmeas de ratos (Gunson et al., 1996; Markovits e Sahota, 2000).

O uso de ambas as drogas levam a drásticas alterações hormonais que podem influenciar a fisiologia de todos os órgãos regulados por hormônios. Como a próstata feminina do gerbilo se mostra sensível às alterações dos níveis de hormônios esteróides, torna-se relevante avaliar o efeito destas drogas sobre a manutenção da homeostase glandular.

O presente estudo teve o objetivo de investigar os eventos fisiológicos que promovem a regulação hormonal da próstata de fêmeas adultas do gerbilo *Meriones unguiculatus*, abordando os seguintes aspectos:

1. Avaliar a resposta da próstata feminina adulta ao estímulo androgênico.

2. Observar a sensibilidade da glândula a agentes endócrinos exógenos (anti-estrógenos sintéticos) capazes de alterar o equilíbrio homeostático do organismo feminino.

3. Investigar como os andrógenos e anti-estrógenos atuam sobre a morfo-fisiologia dos diferentes tipos de células epiteliais e estromais da glândula prostática feminina.

Para cumprir estes propósitos foram utilizados métodos morfológicos, ultra-estruturais, sorológicos e imunocitoquímicos. Os resultados obtidos com esta pesquisa foram divididos em quatro artigos científicos, que estão apresentados nos próximos capítulos.

Artigo: Testosterone stimulates growth and secretory activity of the female prostate in the adult gerbil (*Meriones unguiculatus*), publicado pelo periódico *Biology of Reproduction* em setembro de 2006. Este trabalho foi publicado como capa da revista do mês de setembro.

?1 BIOLOGY OF REPRODUCTION 75, 000–000 (2006)
Published online before print 17 May 2006.
DOI 10.1095/biolreprod.106.051789

Testosterone Stimulates Growth and Secretory Activity of the Female Prostate in the Adult Gerbil (*Meriones unguiculatus*)[1]

Fernanda C.A. Santos,[3] Rodrigo P. Leite,[3] Ana M.G. Custódio,[3] Karina P. Carvalho,[4] Luiz H. Monteiro-Leal,[4] Adriana B. Santos,[5] Rejane M. Góes,[5] Hernandes F. Carvalho,[2,3] and Sebastião R. Taboga[6]

Department of Cell Biology,[3] State University of Campinas, Campinas, São Paulo, Department of Histology and Embryology,[4] State University of Rio de Janeiro, Rio de Janeiro, Departments of Computational Sciences and Statistics[5] and Biology,[6] IBILCE, State University of São Paulo, São José do Rio Preto, São Paulo, Brazil.

ABSTRACT

?2 ?3 ?4 **The prostate of the female gerbil (*Meriones* sp.) is similar to the human female prostate (Skene gland) and, despite its reduced size, it is functional and shows secretory activity. However, virtually nothing is known about its physiological regulation. This study was thus undertaken to evaluate the behavior of the gerbil female prostate in a hyperandrogenic condition. Adult females received subcutaneous injections of testosterone cypionate (1 mg/kg body weight every 48 h) up to 21 days. Circulating levels of testosterone and estradiol were monitored, and the prostate and ovaries subjected to structural and immunocytochemical analyses. The treatment resulted in sustained high levels of circulating testosterone, and caused a transient increase in estradiol. At this early stage, there was an increase in epithelial cell proliferation accompanied by significant reorganization of the epithelium and an apparent reduction in secretory activity, followed by a progressive increase in luminal volume density and accumulation of secretory products. Immunocytochemistry identified the expression of androgen receptor and a prostate-specific antigen (PSA)-related antigen in prostatic epithelial cells. A circulating PSA-related antigen was also found, and its concentration showed strong negative correlation with circulating estrogen. Epithelial dysplasia was detected in the prostate of treated females. Analysis of the ovaries showed the occurrence of a polycystic condition and stromal cell hyperplasia. The results indicate that testosterone has a stimulatory effect on the female prostate, inducing epithelial cell proliferation, differentiation, secretory activity, and dysplasia. The results also suggest that prostatic growth and activity, polycystic ovaries, and ovarian stromal cell hyperplasia are related to a hyperandrogenic condition in females.**

androgen receptor, female reproductive tract, ovary, prostate, testosterone

INTRODUCTION

The adult gerbil female prostate shows a paraurethral location, exhibiting intimate contact with the urethral wall in the distal and median portions. Two types of secretory cells have been recognized by histology and ultrastructural analysis. The first is a typical prostatic secretory cell. The second is characterized by a unique set of secretory organelles and was named clear secretory cell because of its pale color after HE staining. Although reaching a very limited size in adulthood, the gerbil female prostate has been found to be morphologically similar to the ventral lobe of the prostate of postpubertal males [1]. The histochemical and ultrastructural aspects of the gland permitted us to assume that it secretes glycoproteins functionally and constitutively [1, 2].

Despite an increasing number of reports on the structural characteristics of the female prostate of different species [3–8], including humans [9, 10], reference to this organ is still a matter of controversy among people dealing with women's health. Moreover, its small size led some authors to conclude that the female prostate is a vestigial gland [4, 11, 12].

Androgens regulate the growth, differentiation, and survival of male prostatic cells [13, 14]. Testosterone and its derivative, dihydrotestosterone, along with other hormones, such as estrogen and prolactin, regulate prostate physiology during both development and adulthood [15–18]. Although Zaviačič [9] has suggested that the activity of this gland is regulated by steroid hormones, the influence of androgens on this organ is unclear.

Androgens play an important role in the regulation and development of the female urogenital system. This is supported by the fact that androgen receptors have been identified in various organs, such as ovaries, oviduct, and uterus [19]. Immunohistochemical studies have demonstrated that androgen receptors are also present in the human female prostate (Skenes paraurethral gland), suggesting a role for androgens in the maintenance of the structure and functional state of the prostate in the female organism [10, 12].

It seemed important to us to investigate whether androgens regulate the growth and activity of the female prostate gland by comparing the effects of these hormones with those seen in males. Furthermore, this model may have some clinical implications, because 1) women suffer from steroid hormone imbalances after menopause, 2) hyperandrogenism is not unusual in some populations, 3) the use of androgens for adjuvant therapy of female-to-male transsexuals is common [20], and 4) its administration to bodybuilders and female high-performance athletes is a common (although yet illegal) procedure.

Thus, the objective of the present study was to evaluate the response of the adult gerbil female prostate to the experimental administration of testosterone, simulating a hyperandrogenic condition, using a series of structural and immunocytochemical analyses.

The results presented here demonstrate that the epithelial cells of the gerbil female prostate express the androgen receptor and secrete a prostate-specific antigen (PSA)-related antigen. Most importantly, our results show that exogenous testosterone

[1]Supported by São Paulo State Research Foundation (FAPESP) grants to S.R.T. and H.F.C., and National Research Council (CNPq) grants to H.F.C. F.C.A.S., and A.M.G.C. were recipients of fellowships from CNPq and CAPES, respectively.
[2]Correspondence: Hernandes F. Carvalho, Department of Cell Biology–IB–UNICAMP, CP6109, 13083–863 Campinas SP, Brazil.
FAX: 55 19 3788 6111; e-mail: hern@unicamp.br

Received: 17 February 2006.
First decision: 3 March 2006.
Accepted: 15 May 2006.

ISSN: 0006-3363. http://www.biolreprod.org

induces prostate growth resulting from the proliferation, differentiation, secretory activity, and dysplasia of epithelial cells, and affects the concentration of circulating estradiol and PSA, which showed a high negative correlation to one another. Moreover, we also observed that testosterone treatment leads to a polycystic ovarian condition, ovarian stromal cell hyperplasia, and urethral wall thickening. Taken together, the results suggest that, in addition to many side effects, the administration of androgens to females may also result in abnormal growth and dysplasia of the prostate gland.

MATERIALS AND METHODS

Animals and Experimental Design

Eighty seven 3-month-old female gerbils (*Meriones unguiculatus*, *Gerbillinae*: *Muridae*) were employed in this study. Seventy-one animals received intradermic testosterone injections (1 mg/kg testosterone cypionate [Novaquímica/Sigma Pharma, Hortolândia, São Paulo, Brazil] in 0.25 ml corn oil) every other day after the beginning of treatment [21] and were divided in to groups that were subjected to the different analyses. The control animals received corn oil injections every other day for 21 days. The treated animals were killed after 3, 7, 14, or 21 days of treatment. After being anesthetized by CO_2 inhalation, the animals were weighed and immediately decapitated. Blood samples from some of them were collected for serological analysis, and the prostatic complex (urethra and adjacent tissues) was dissected out, weighed, and fixed according to different protocols, as specified below. Those that were not easily dissected out of adherent tissue were not weighed. The ovaries were also collected to assess histological changes due to testosterone administration. Animal handling and experiments were done according to the ethical guidelines of the State University of Campinas, following the *Guide for Care and Use of Laboratory Animals* (unpublished). The large sample size used in this work was justified by the minute size of the organ and the large number of analytical procedures employed.

Plasma Total Testosterone, Estradiol, and PSA Levels

Circulating plasma testosterone, estradiol, and PSA levels were determined by immunochemical assays. Blood was collected by cardiac puncture immediately before death and 24 h after the last injection of testosterone (except for Day 14, the sample for which was collected 48 h after the last injection). Plasma was separated by centrifugation and stored at −20°C for subsequent assays. Measurements were done in duplicate using automated equipment from Vitros-ECi-Johnson & Johnson (XXX, XXX) for ultrasensitive chemiluminescence detection. The sensitivity was 0.1–150 ng/ml for testosterone, 0.1–3 814 pg/ml for estradiol, and 0.1–100 ng/ml for human PSA. The intraassay variations were 1%, 1.1%, and 0.97%, and the interassay variations were 2.1%, 1.5%, and 1.75%, for testosterone, estradiol, and human PSA, respectively.

Morphological Analysis

The urethra and adhering tissues and ovaries were fixed by immersion in Karnovsky solution (5% paraformaldehyde, 2.5% glutaraldehyde in 0.1 M phosphate buffer, pH 7.2), or in Bouins solution, for 24 h. After fixation, the tissues were washed under running tap water, dehydrated in an ethanol series, cleared in xylene, embedded in paraffin (Histosec; Merck, Darmstadt, Germany) or glycol methacrylate resin (Historesin embedding kit; Leica, Nussloch, Germany), and cut into 3-μm sections with a Leica RM2155 automatic rotatory microtome. Sections from the female prostate and ovaries were stained with hematoxylin-eosin [22]. The Feulgen reaction for DNA was used to count mitotic cells. Neutral carbohydrates were identified by the periodic acid-Schiff (PAS) test [22]. The specimens were analyzed and photographed with a Zeiss Jenaval (Zeiss-Jenaval, Jena, Germany) or an Olympus BX60 light microscope (Olympus, Hamburg, Germany).

Morphometry and Stereology

The relative volume of the tissue compartments was determined according to the procedure of Weibel [23] using a 168-point grid test system, as applied to the rat male prostate by Huttunen et al. [24] and Garcia-Florez et al. [25]. Twenty microscopic fields were chosen at random. The volume density was calculated after counting the number of points that coincided with each of the tissue compartments (epithelium, lumen, or stroma). Absolute volumes could not be determined because it was not possible to separate the female prostate from adhering tissue and to determine its weight.

The number of acinar profiles per prostate was counted after serial sectioning. The relative sectional area of the lumen was measured using the NIH Image J software (available at http://rsb.info.nih.gov/ij/; National Institutes of Health, Bethesda, MD). Briefly, the lumen was artificially stained and its sectional area was measured in square pixels. The number of secretory, clear, and basal epithelial cells per alveolus was counted, and the individual contribution of each cell type is expressed as a percentage. Morphometric analysis also included the determination of epithelial cell height, nucleus/cytoplasm ratio, nuclear area (μm^2), nuclear perimeter (μm), and form factor (4p.nuclear area/[nuclear perimeter]^2).

For the quantification of mitotic cells, Feulgen-stained sections were examined and 10 acini were digitized. The total number of nuclei per acinus and the number of mitotic figures were counted. Results are reported as the percentage of mitotic cells.

Immunocytochemistry

Sections of Bouin-fixed prostates were subjected to immunocytochemistry for the detection of PSA and androgen receptor (AR), as described elsewhere [26, 27]. Mouse monoclonal immunoglobulin G1 anti-PSA and rabbit polyclonal anti-AR (SC-7316 and SC-816, respectively; Santa Cruz Biotechnology, Santa Cruz, CA) antibodies were employed at a dilution of 1:100. Peroxidase-conjugated specific antibodies (Sigma Chemical Co., Saint Louis, MO) and 3,3′-diaminobenzidine were used as secondary antibodies and peroxidase substrate, respectively. Sections were counterstained with Harrys hematoxylin or methyl green.

Three Dimensional Reconstruction

After histological processing, whole prostates (control and testosterone-treated) were serially sectioned at 5 μm and stained with hematoxylin-eosin, as described above. Image capture and processing were carried out using the Analysis 3.2 software (Build 743; Digivision–SIS, San Diego, CA). After image alignment, the urethra and prostatic ducts and alveoli were isolated in each image and then processed to obtain an interface boundary in each section, thus generating a three dimensional (3-D) model [28]. It is important to mention at this point that this software was unable to deal with dead-end structures, such as the prostatic acini, and the images show blunt ends at the tips.

TABLE 1. Body and prostatic complex weight in control and testosterone-treated females (mean ± SEM).

Parameter	Control (vehicle)*	Testosterone treatment*			
		3 Day	7 Day	14 Day	21 Day
Body weight (g)	59.1 ± 4.2[a] (n = 6)	58.0 ± 1.3[a] (n = 7)	62.6 ± 1.5[a] (n = 9)	63.7 ± 1.7[a] (n = 6)	67.7 ± 1.4[b] (n = 9)
Prostatic complex weight (g)	0.091 ± 0.011[a]	0.091 ± 0.008[a]	0.139 ± 0.008[b]	0.136 ± 0.013[b]	0.157 ± 0.009[b]
Relative weight†	0.0015 ± 0.0001[a]	0.0016 ± 0.0001[a]	0.0022 ± 0.0001[b]	0.0022 ± 0.0002[b]	0.0023 ± 0.0001[b]
Relative weight variation (%)‡	—	+3.6	+47.1	+41.7	+52.3

* Statistically significant differences between control and treatments; superscript letters (a, b) represent statistically significant differences between the experimental groups.
† Relative weight corresponds to the ratio between the weight of the prostate and that of the whole body.
‡ Relative weight variation is shown with respect to the control, which was taken as 100%.

Statistical Analysis

Data were analyzed using Statistica 6.0 software (StarSoft, Inc., Tulsa, OK). The hypothesis tests used to determine statistical significance were the Kruskal-Wallis test, ANOVA, Tukeys multiple comparison test, or the median test, with the level of significance set at 5% ($P \leq 0.05$). Values are presented as median or mean ± 1 SD (low number of measurements) or SEM (high number of measurements), or as box-plots, as required for clearer presentation of the data. ?11

RESULTS

Body Weight and Prostatic Complex Weight

Table 1 shows the variation in body and prostatic complex weights. There was a 14.6% increase in body weight after 21 days of testosterone treatment. Significant increase in the prostatic complex weight, including the whole urethra and prostate gland, was observed after 7 days of treatment. The relative weight of the prostatic complex showed an ~ 52% increase after 21 days of treatment, demonstrating a marked specificity in prostatic complex growth.

Serum Steroid Hormone and PSA-Related Antigen Levels

Serum steroid hormone and PSA-related antigen levels are shown in Figure 1. As expected, exogenous testosterone administration resulted in sustained high levels of circulating testosterone, reaching as much as 19 ± 2.1 ng/ml after 21 days of treatment. This sustained level was about 12 times the normal circulating testosterone level of female gerbils (Fig. 1A). Testosterone treatment caused a significant rise in circulating estradiol levels, corresponding to double the concentration observed in the control on the third day of treatment. However, this increase was transient, and, despite sustained high levels of testosterone, estradiol returned to control levels after 21 days of treatment, with no significant difference being observed by day 7 of treatment (Fig. 1B).

Serum PSA-related antigen concentration in control females was 0.156 ng/ml (Fig. 1C). Testosterone treatment caused a subtle decrease in PSA levels, which progressively returned to control levels within the duration of the experiment, with no difference compared to control being observed after 7, 14, or 21 days (Fig. 1C). Although no significant correlation was observed between testosterone and PSA-related antigen concentration, there was a high negative correlation between estradiol and PSA-related antigen levels ($r = -0.98$). On the other hand, the correlation between estradiol and testosterone levels was very low. This low correlation was due to a marked dissociation between the highest testosterone concentrations, which were associated with a decline in estradiol levels. Lower circulating testosterone concentrations showed a positive correlation with estradiol levels ($r = 0.86$). This effect was more evident in the testosterone concentration range of 13–17.5 ng/ml, presenting a very high correlation coefficient ($r = 0.99$).

Morphological Aspects and Alterations Caused by Testosterone Treatment

The gerbil female prostate established a close contact with the median and distal portions of the urethral wall. This organ was formed by a small group of glands and ducts dispersed in a dense stroma. The glands were lined by small cuboidal to moderately tall prismatic cells (Fig. 2, A and B). These glands generally enclosed a voluminous lumen containing PAS-positive secretion (Fig. 2C). Two distinct types of epithelial cells were identified: secretory and basal cells (Fig. 2B). Secretory cells were in contact with the glandular lumen and predominated in the prostatic epithelium. These cells were characterized by large, parabasal nuclei and an acidophilic cytoplasm. PAS-positive secretory material was found to be accumulated close to the apical surface (Fig. 2C). Some chromophobic secretory cells, previously named clear cells [1], ?12 were interspersed amongst common secretory cells. Basal cells were located between the secretory cells. These cells were smaller and less frequent than the secretory cells, and had an irregular elliptical shape.

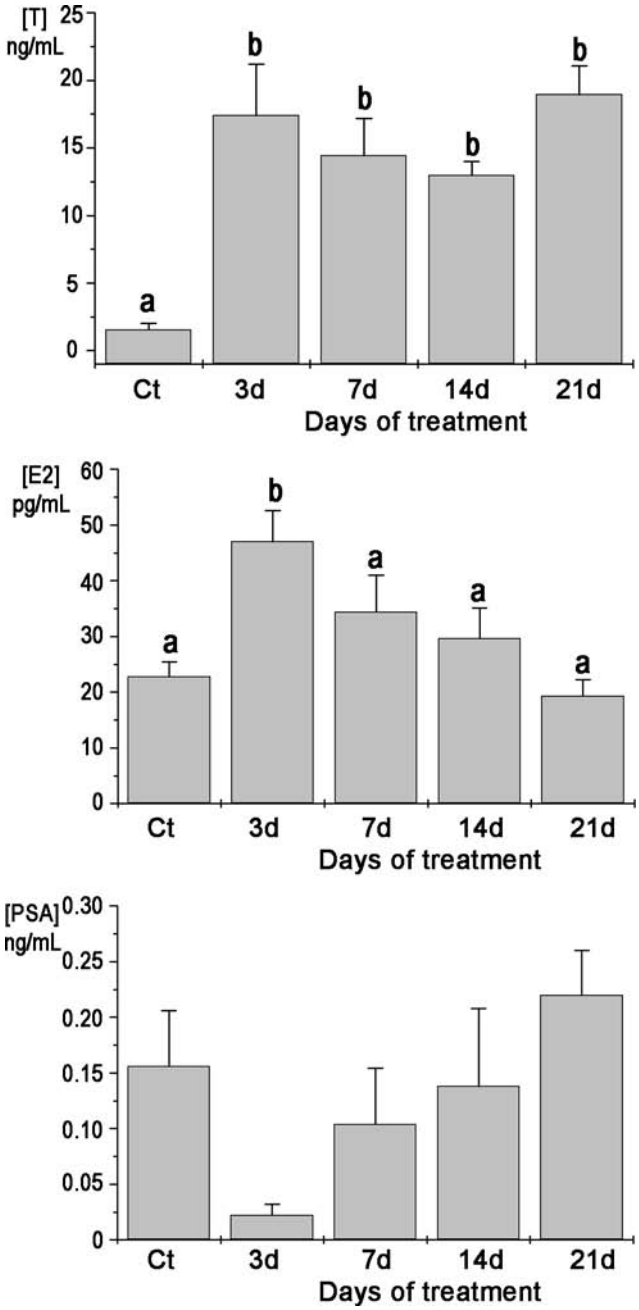

FIG. 1. Absolute variation in serum testosterone (**A**), Estradiol (E2) (**B**), and PSA-related antigen levels (**C**) in the female gerbil during testosterone treatment. Observe the significant increase in E2 only at the earliest point (3 days) of treatment, and that there was no significant variation in PSA-related antigen levels, although a decrease was noted at the beginning of testosterone administration. The lack of significance is, to a large extent, due to the high individual variation in PSA-related antigen levels. Values are means ± SEM (n = 5).

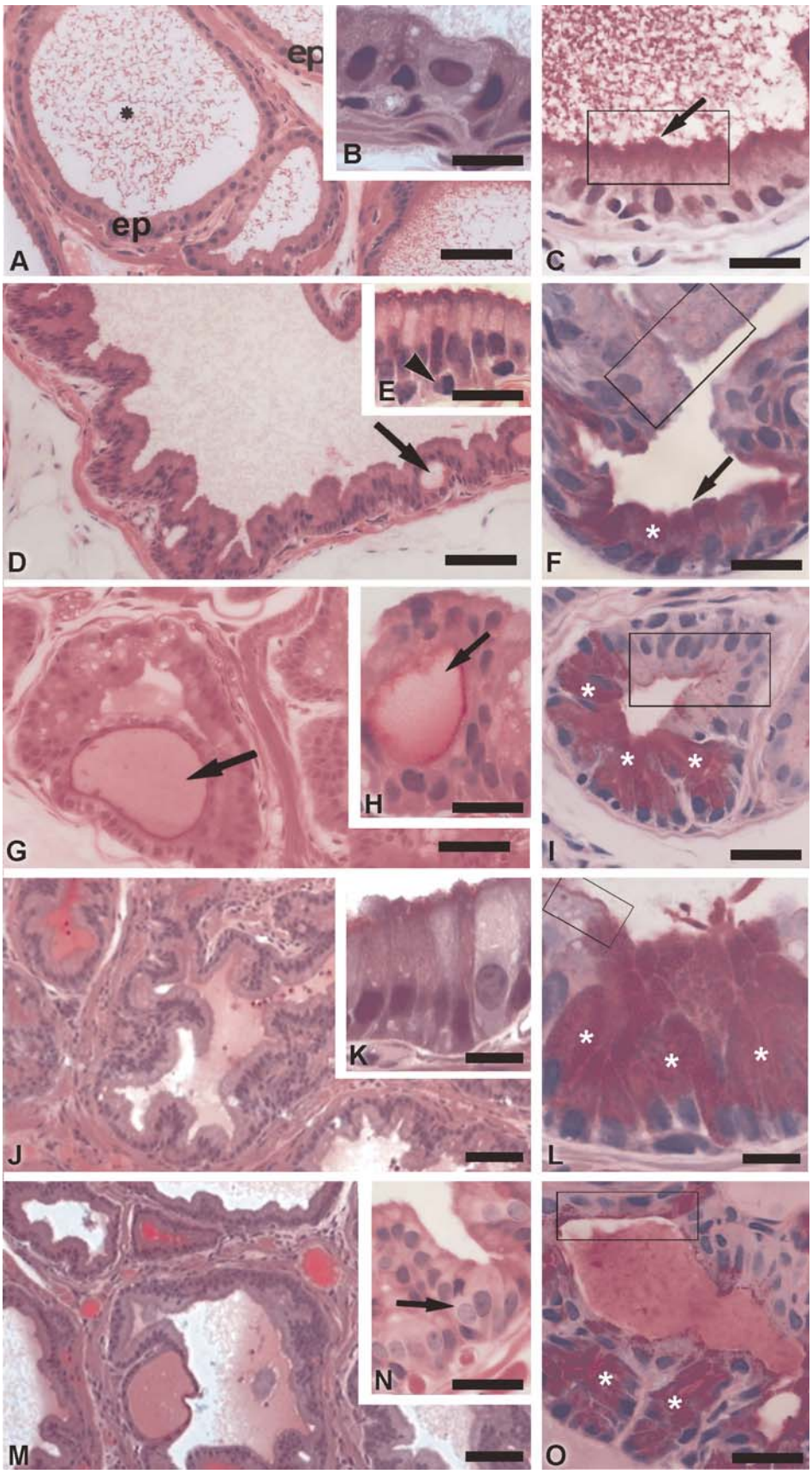

FIG. 2. Histological sections of the normal female prostate stained with hematoxylin-eosin or PAS (**C**, **F**, **I**, and **L**). **A**) General view of the prostate gland exhibiting a small cuboidal epithelium (ep) and a voluminous lumen, where secretion products are deposited (asterisk). **B**) Detail of the epithelium showing the principal epithelial cells. In the stroma, a multilayered arrangement of smooth muscle cells is observed. **C**) PAS staining of the prostatic epithelium shows the presence of secretory material rich in neutral polysaccharides accumulated in the apical portion of epithelial cells (box and arrow) and in the lumen. **D**) Aspect of the female prostate gland 3 days after the beginning of treatment. Note that the epithelium is hyperplastic, showing many foldings and the presence of intraepithelial vesicles (or arcs [arrow]). **E**) A higher magnification of the epithelium demonstrates that the cells are taller and accumulate a basophilic material in the apical portion of the cytoplasm. The arrowhead points to a basal cell. **F**) PAS staining of the epithelium showing a decrease in the staining of the apical portion of the principal epithelial cells (box), and an increase in the number of clear cells (arrow) that appear intensely stained for neutral polysaccharides (asterisk). **G**) Aspect of the prostate epithelium of a female treated for 7 days with testosterone. Note the increase in epithelial cell density and their less organized arrangement in the epithelial layer. The arrow points to an intraepithelial vesicle. **H**) Detail of the epithelial layer, supporting the aspects observed at low magnification. **I**) PAS staining of the epithelium. The box shows some principal epithelial cells containing very little PAS-positive material compared to control cells. The asterisks indicate some clear cells that became more frequent in the epithelium after testosterone treatment. **J**) Aspect of the prostate gland after 14 days of testosterone treatment. Note the high density of epithelial cells in the epithelial layer. **K**) Detail of tall epithelial cells containing some basophilic material in the apical portion of the cytoplasm and many unstained vesicles scattered throughout the cell. **L**) PAS staining demonstrates that the epithelial cell slowly recovers the staining observed in control cells (box) and that the number of intensely PAS-stained clear cells (asterisks) is still larger. **M**) General view of the prostate gland after 21 days of testosterone treatment. Note the presence of small epithelial structures and the presence of intraepithelial vesicles. The detail shows that the epithelial cells are smaller at this time point. The arrow points to a clear cell. **O**) PAS staining reveals the presence of PAS-positive material in the apical portion of the principal epithelial cells (box), more closely resembling what was observed in the control. The number of clear cells is still larger (asterisks). Bars = 50 μm (**A**, **D**, and **G**), 15 μm (**B**, **C**, **E**, **F**, **H**–**J**, and **M**–**O**), 10 μm (**K** and **L**).

Many morphological alterations were observed in the epithelial compartment of the female prostate glands after experimental testosterone administration. After 3 days of treatment, a marked increase in prostatic epithelial height was observed, with the epithelium being of the pseudostratified columnar type, with a predominance of tall epithelial cells arranged in frequent epithelial infoldings (Fig. 2, D and E). The secretory cells exhibited a readily observed chromophobic

TABLE 2. Epithelial cell types and morphometric and karyometric data obtained for the female prostate during testosterone treatment (mean ± SD).

Parameter	Control (vehicle)*	Testosterone treatment*			
		3 Day	7 Day	14 Day	21 Day
Frequency of epithelial cell types (%)†					
Secretory cells	90.4 ± 2.2[a]	86.1 ± 2.1[b]	86.1 ± 2.0[b]	86.7 ± 1.2[b]	84.9 ± 2.3[b]
Clear secretory cells	1.6 ± 1.2[a]	5.7 ± 1.8[b]	5.3 ± 1.2[b]	5.4 ± 1.1[b]	7.2 ± 2.4[c]
Basal cells	8.0 ± 1.8	8.2 ± 1.6	8.6 ± 1.3	7.9 ± 0.9	7.9 ± 1.4
No. of epithelial cells/acinus	92.7 ± 5.8[a]	89.3 ± 12.3[a]	156.2 ± 12.8[b]	126.5 ± 8.4[b]	132.8 ± 8.3[b]
Morphometric data‡					
Secretory cell height (μm)	14.4 ± 3.9[a]	21.8 ± 5.7[b]	23.6 ± 4.9[c]	23.3 ± 4.8[c]	14.8 ± 4.2[a]
Karyometric data‡					
Nucleus/cytoplasm ratio	0.24 ± 0.05[a]	0.23 ± 0.05[a]	0.23 ± 0.05[a]	0.20 ± 0.03[b]	0.22 ± 0.04[a]
Nuclear area (μm^2)	23 ± 5.4[a]	28.8 ± 7.0[b]	29.6 ± 6.6[b]	30.3 ± 6.1[b]	27.8 ± 6.5[b]
Nuclear perimeter (μm)	19.5 ± 2.5[a]	21.9 ± 2.7[b]	22 ± 2.6[b]	22.1 ± 2.4[b]	20.9 ± 2.6[c]
Nuclear form factor	0.76 ± 0.08[a]	0.75 ± 0.08[a]	0.77 ± 0.10[a]	0.78 ± 0.09[b]	0.8 ± 0.08[b]

* Statistically significant differences between control and treatment periods; superscript letters (a, b, c) represent statistically significant differences between the experimental groups.
† n = 30 alveoli/group
‡ n = 200 measurements in five animals/group.

supranuclear area and an apical accumulation of acidophilic material (Fig. 2E), which was not observed in control specimens. One of the most evident epithelial alterations caused by 3 days of testosterone treatment was the appearance of intraepithelial vesicles in the prostatic acini (Fig. 2D, arrow), which were observed between two epithelial layers. In most cases, the apical surface of the lower cell layer was in contact with the content of the vesicle, whereas the basal surface of the upper cell layer delimited the vesicle, and its apical surface was in contact with the main glandular lumen. Basal cells were commonly seen in the epithelium (Fig. 2E), but were not observed in the cell layers that formed the intraepithelial vesicles. PAS staining revealed the loss of apical staining observed in most secretory cells of the vehicle-treated prostate, and the appearance of groups of secretory cells whose cytoplasm was filled with neutral glycoconjugates (Fig. 2F).

Longer exposure to exogenous testosterone resulted in further growth of the gland. The histological aspects described for the third day were more prominent after 7 and 14 days of treatment (Fig. 2, G, H, J, and K, respectively). Secretory cells were even taller by Day 14, and the frequency of epithelial infoldings and epithelial vesicles was higher (Fig. 2, G and J). Also, the number of deeply stained PAS-positive cells was increased (Fig. 2, I and L).

Striking reorganization of the gland was observed after 21 days of treatment. The epithelial cells were considerably shorter (Fig. 2, M and N) despite preservation of the chromophobic supranuclear area. The number of clear cells, which were rare in the normal prostate and had increased by the 7th and 14th days, was also elevated after 21 days of treatment. Intraepithelial vesicles were scarce at this stage. The increased acidophilic apical staining observed in the epithelial secretory cells had almost disappeared (Fig. 2N). Likewise, the disappearance of the apical PAS staining was also transient and, by Day 21, the secretory cells again showed this apical staining. Foci containing PAS-positive cells were smaller but very frequent (Fig. 2O).

Morphometry

The morphometric results are presented in Table 2. There was a significant increase in the mean number of epithelial cells per acinar profile after 7 days of testosterone treatment. The larger number was maintained up to Day 21 of treatment. Clear cells were more frequent among the epithelial cells, and corresponded to 7.2% of the epithelial cells after 21 days of testosterone treatment compared to 1.6% in the control tissues. This increased frequency resulted in a significantly reduced percentage of secretory cells. On the other hand, the number of basal cells remained relatively constant, ranging from 7.9% to 8.5% of the epithelial cells. Epithelial height changed significantly during testosterone treatment, ranging from ~ 14.4 μm in controls to 23.6 μm after 14 days of treatment. After 21 days of treatment, shortening of the epithelium was observed, which became indistinguishable from the controls.

The cell nucleus/cytoplasm ratio showed a transient reduction by Day 14 of treatment (Table 2). Changes in nuclear structure were also detected. Nuclear area and perimeter showed a progressive increase up to the 14th day of treatment, followed by a small reduction in these nuclear parameters on Day 21. The form factor, an expression of nuclear roundness, was slightly increased after longer periods of testosterone treatment (i.e., 14 and 21 days). Values close to 1 indicate that the cell nucleus is more round and less elliptic, as observed after 14 and 21 days of treatment. The changes in nuclear area, perimeter, and form factor were statistically significant (Table 2).

Volume Density of Tissue Compartments

The stereological data obtained for normal and treated prostates are shown in Table 3. In the prostate of control animals, the stroma occupied most of the prostatic volume (~ 40%), and remained relatively constant throughout treat-

TABLE 3. Volume density variation in the epithelial, luminal, and stromal compartments of the female prostate during exogenous testosterone treatment (mean ± SEM).

Tissue	Control (vehicle)*	Testosterone treatment*			
		3 Day	7 day	14 Day	21 Day
Epithelium	27.5 ± 2.2[a]	38.7 ± 2.7[b]	46.3 ± 2.3[c]	43.0 ± 3.0[c]	26.3 ± 2.0[a]
Lumen	31.9 ± 3.1	18.0 ± 2.0	14.9 ± 1.8	17.0 ± 3.0	42.7 ± 2.9
Stroma	40.6 ± 3.0	43.3 ± 3.1	38.8 ± 3.2	40.0 ± 3.0	31.0 ± 2.4

*Statistically significant differences between groups; superscript letters (a, b, c) indicate statistically significant differences between the experimental groups.

TABLE 4. Variations in the number of acinar profiles and in the sectional luminal area of the female prostate following testosterone treatment.

Treatment	Median no. of acinar profiles	Sectional area of the lumen* (square pixels x10^3) (mean ± SEM)	Product of the median number of acinar profiles and the sectional luminal area (x10^3)
Control	13	1.0 ± 0.8	27.3
Testosterone			
3 Day	24	1.7 ± 0.6	41.2
7 Day	37	1.3 ± 0.4	49.4
14 Day	25	7.3 ± 1.9	176.8
21 Day	19	42.9 ± 16.0	814.2

*Statistically significant differences between the control and experimental groups.

ment, showing a small, nonsignificant reduction after 21 days of treatment. The remaining volume was almost equally shared by epithelium and lumen (27.5% and 32%, respectively) in control animals. Testosterone treatment caused an increase in epithelial volume density, which reached about 46% and 43% of the glandular volume after 7 and 14 days of treatment, respectively, returning to control levels by Day 21. The increase in epithelial volume density was counterbalanced by a decrease in luminal volume density which, however, became more prominent than in the control animals after 21 days of treatment. ANOVA revealed that the changes observed in the epithelial compartment during the period of testosterone treatment were significant. Application of Tukeys parametric test demonstrated a significant difference between groups. No significant differences were observed between the group treated for 21 days and the control group, or between the groups treated for 7 and 14 days. As there were no group differences in stromal volume density, no paired test could be applied to compare time points with the control. However, there was an evident variation in luminal volume with treatment. ?13

Number of Acinar Profiles and Luminal Area

Analysis of the median number of acini per gland revealed that testosterone induced an increase in the number of acini up to Day 7 of treatment. In the normal prostate, the number of acinar profiles ranged from 7 to 14 (median = 13). Prostates treated for 3 days had 21–29 acini (median = 24), and those treated for 7 days had 35–48 acini (median = 37). Thereafter, there was a gradual decline in the number of acinar profiles per gland. Prostates treated with testosterone for 14 days had 19–30 acini (median = 25), whereas those treated for 21 days had 14–20 acini (median = 19). The use of the median was necessary because, for each prostate, only the medial section was counted, and resulted in a very low number of measurements. Although the test of the median showed no marked differences, the application of the Kruskal-Wallis test ?14 revealed significant differences between the control and experimental groups. On the other hand, the sectional luminal area showed a marked increase on Days 14 and 21, demonstrating progressive enlargement of the lumen and the accumulation of secretory products (Table 4). The product of the median number of acinar profiles multiplied by the sectional luminal area demonstrated that the decline in the number of acini did not correspond to a decrease in luminal volume (Table 4).

Cell Proliferation

Mitotic cells were rare in the epithelium of the prostate of control animals, ranging from 0.7% to 1.3% of all epithelial cells (Fig. 3). A large oscillation in the frequency of mitotic cells was observed in the prostates of animals treated for 3 days, with a large deviation to higher figures (up to 3.6%). The frequency of mitotic cells remained constant at about the same values obtained for the control after longer periods of testosterone treatment. No statistically significant differences in the median number of mitotic cells were observed between the different periods of treatment according to the median and Kruskal-Wallis tests. Thus, the differences between groups were due to variation within the group treated with testosterone for 3 days, which showed an ~ 4-fold higher SD (1.1%) than those obtained for the other groups (control SD = 0.3%; 7 days = 0.5%; 14 days = 0.2%; and 21 days = 0.2%).

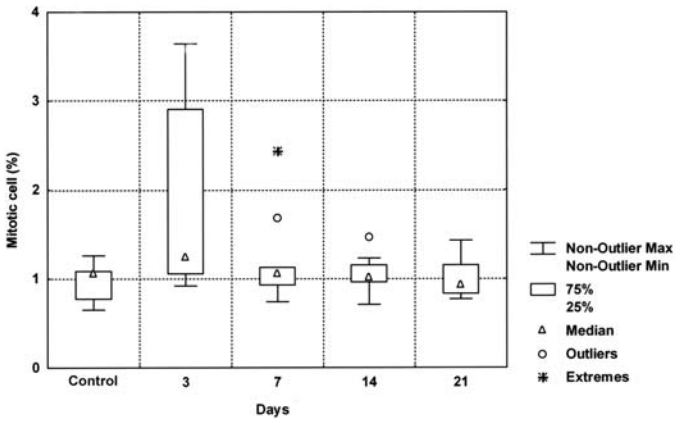

FIG. 3. Box-plot representations of the median percentage of mitotic cells per acinus in control and testosterone-treated female prostates. The experimental groups are sequentially represented according to time of testosterone administration, where 0 = control. The plots correspond to counts of 10 acini for each experimental group.

3-D Structure

Figure 4 presents the 3-D reconstruction of the prostate and urethra of control and testosterone-treated female gerbils. In both situations, the glandular structures were concentrated in the median portion of the urethra, which was 0.8–1.2 mm long and 0.06–0.1 mm thick. In control animals (Fig. 4, A and C), the prostate was characterized by a ductal system that was inserted into the urethral wall, connecting the organ to the urethra. The alveoli were aligned with the urethra and showed different lengths and thicknesses. Testosterone treatment (Fig. 4, B and D) resulted in an increased number of acini, which seemed to be larger than in control animals. In addition to the growth of the prostate gland, which contributed to the thickening of the urethral wall, it became evident that the wall musculature itself was hypertrophic. Both prostate growth and urethral wall thickening resulted in marked collapse of the urethra. ?15

Immunolocalization of PSA-Related Antigen and AR

A PSA-related antigen was detected in the female gerbil prostate by immunocytochemistry, regardless of the concentration of circulating testosterone. In control animals, the reaction was diffuse in the secretory material accumulated in the lumen, and was found almost exclusively in the apical cytoplasm. The immunocytochemical reaction was not uniform, with some epithelial cells showing no staining at all. Testosterone treatment did not affect this distribution (Fig. 5A). However, after 14 days of treatment, the concentration of this anti-human PSA reactive molecule was higher in the vesicles close to the apical portion of the cell (Fig. 5B). ?16

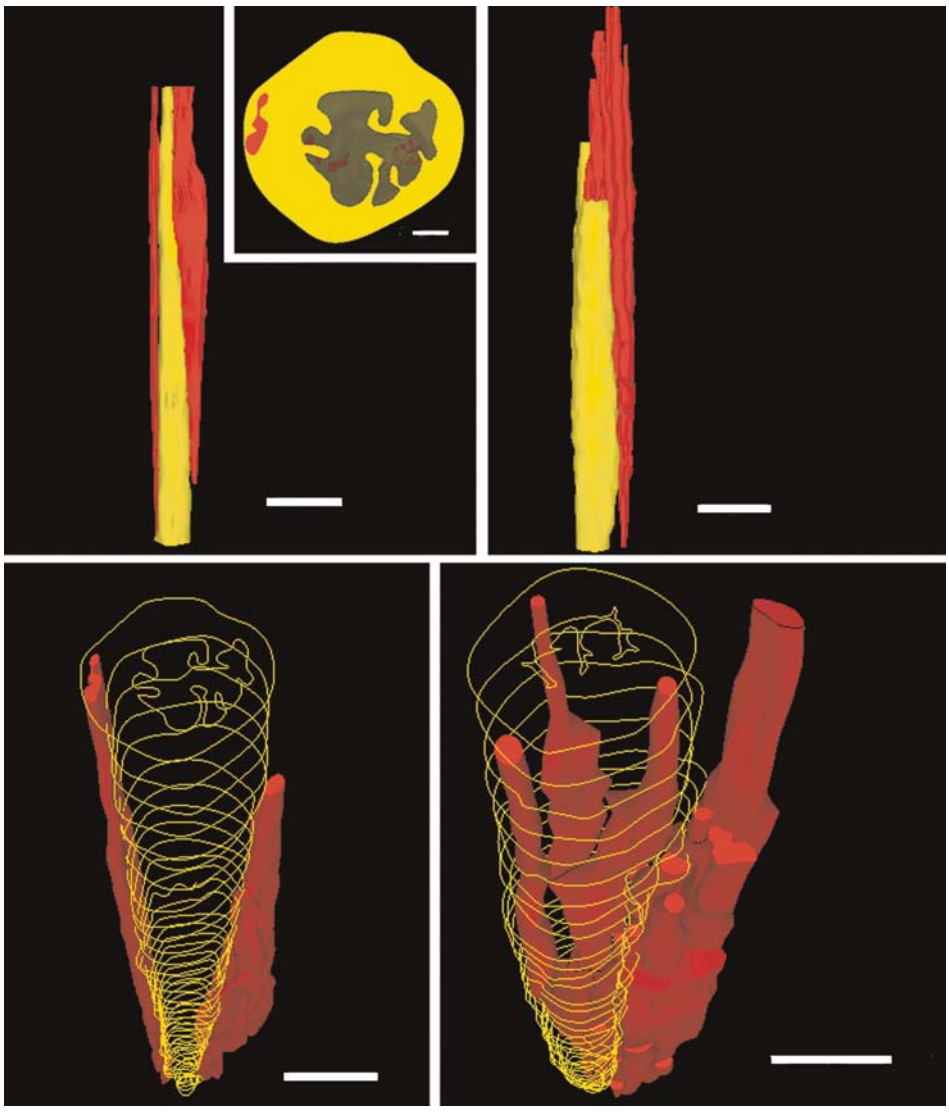

FIG. 4. 3-D reconstruction of the prostate gland and associated segment of the urethra in female gerbils that received vehicle (control; **A** and **C**) or testosterone (**B** and **D**) for 21 days. The increase in the number of acini and volume is apparent. The inset in **A** demonstrates the presence of ducts crossing the muscular wall on their way to the urethra. In **C** and **D**, only the limits of the urethral wall are shown to permit a better view of the prostatic acini. The 3-D reconstruction demonstrates that the urethral wall became thicker and that the urethra seemed to be collapsed after exogenous testosterone administration. **A**–**P** corresponds to the anteroposterior axis of the urethra. Bars = 600 μm (**A** and **C**), 60 μm (inset in **A**), and 150 μm (**B** and **D**).

The immunocytochemical reaction to AR showed that it was concentrated in the nuclei of epithelial cells of the prostate of vehicle-treated control females (Fig. 5C). Basal epithelial cells and stromal cells were also reactive. After 14 days of treatment, the same reaction pattern was identified, except for one in which immunocytochemical staining for AR was detected in the cytoplasm of many, but not all, cells (Fig. 5D). This pattern was maintained for the longer treatment period.

Dysplastic Prostate Growth

Figure 6 shows some aspects of the dysplastic growth of the epithelium in testosterone-treated female gerbils. Abnormal epithelial growth was observed in 100% of the animals treated with testosterone for 21 days. The most common lesions were prostatic intraepithelial neoplasia, atypical hyperplasia, and mucinous adenocarcinomas (Fig. 6).

Ovarian Structure

Figure 7 presents the histological aspects of the ovaries of control and testosterone-treated female gerbils. Two main aspects became visible with the androgen treatment. First, we observed the structure of a polycystic ovary, which was more evident after 14 days of testosterone treatment. Second, there was marked hyperplasia of stromal cells. Because these animals presented no Reinke crystals, we were unable, at the time, to determine whether they correspond to Leydig cells.

DISCUSSION

This study demonstrates that the administration of testosterone to female gerbils causes important alterations in the prostate gland. The major alterations involved the epithelial compartment of the gland, which presented a dual behavior during testosterone treatment, represented by an initial proliferative response followed by a secretory burst.

The experimental protocol employed here resulted in circulating levels of testosterone 12 times higher than those measured in untreated females. The resulting circulating testosterone concentration was also about four times the circulating levels determined for male gerbils, corresponding to about 4.8 ng testosterone/ml plasma (unpublished results), and was thus considered hyperandrogenic.

We have followed the effect of high testosterone on estradiol levels to check how the hypothalamus-pituitary-gonad axis was affected. Indeed, it appeared unaffected within the time line of the experiment. The transient increase in estradiol may have resulted from an immediate conversion of testosterone via aromatase. This was reinforced by the high

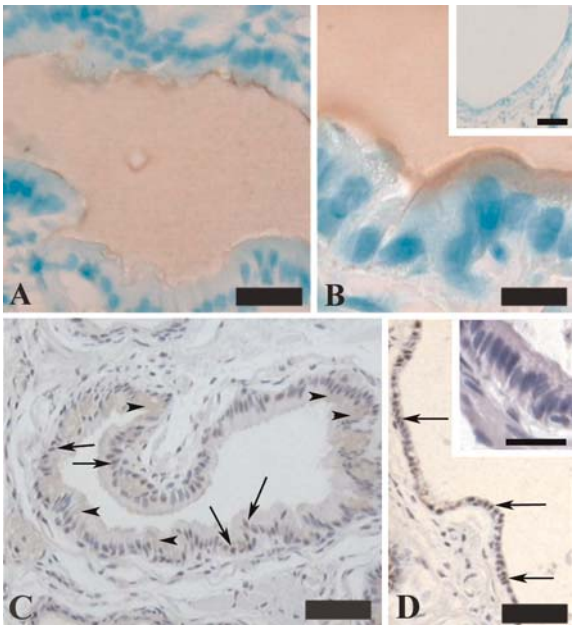

FIG. 5. Immunocytochemical identification of the PSA-related antigen (**A** and **B**) and androgen receptor (**C** and **D**) in the prostate of control (**A** and **C**) and testosterone-treated (**B** and **D**) female gerbils. PSA-related antigen immunostaining was restricted to the apical portion of the cytoplasm of epithelial cells. A diffuse reaction was also observed in the luminal secretion (**A**). The same pattern was observed after 21 days of testosterone treatment (**B**). The inset shows the control reaction. The androgen receptor was detected by immunocytochemistry in both epithelial and stromal cells. Immunostaining was irregularly observed in both cell nucleus (arrows) and cytoplasm (arrowheads) of the control prostate (**C**), whereas the reaction was mainly nuclear (arrows) in the testosterone-treated prostate (**D**). Bars = 25 μm (**A** and inset in **D**), 10 μm (**B**), and 50 μm (**C**, **D**, and inset in **B**)

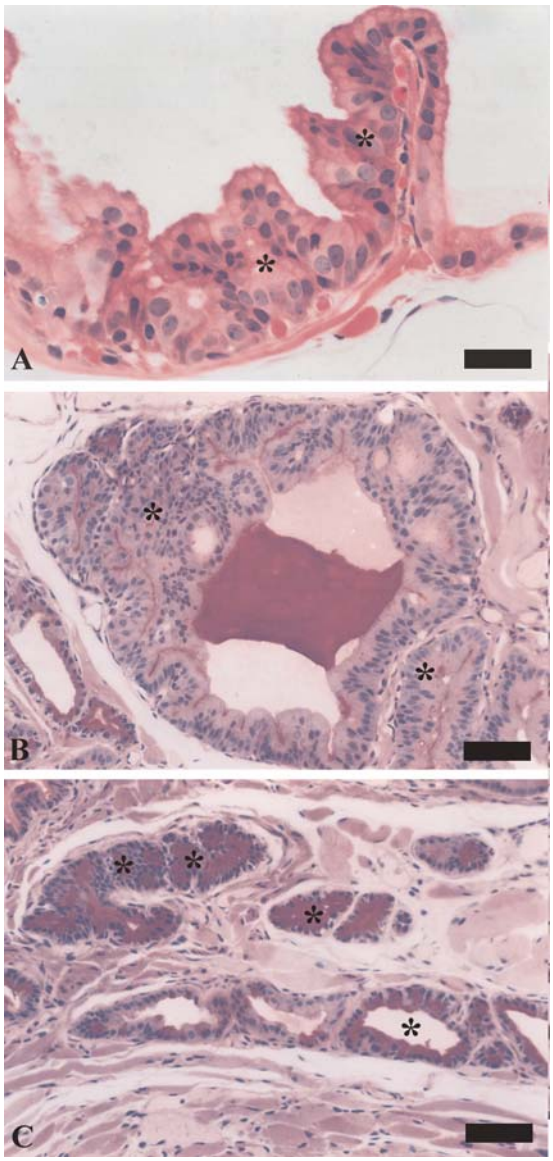

FIG. 6. Dysplastic growth of the epithelium in the prostate of testosterone-treated female gerbils. **A**) Area of prostatic intraepithelial neoplasia (PIN) (asterisks). **B**) Area of atypical hyperplasia (asterisks). **C**) Areas with small acinar structures characteristic of mucinous adenocarcinomas (asterisks). Bars = 25 μm (**A**) and 50 μm (**B** and **C**).

correlation between testosterone levels and estradiol levels in the intermediate concentration range of the former. At the highest testosterone concentration achieved, other mechanisms, such as increased E2 catabolism, seem to be activated.

On the third day of treatment, there was a marked increase in the number of proliferating cells in the prostatic epithelium. The pattern of proliferation was characterized by wide variability, as demonstrated by statistical analysis, which may be attributed to localized cell divisions. As a matter of fact, cell divisions were more frequent in the small, apparently growing acini or buds. The increased proliferation resulted in epithelial hyperplasia, accompanied by a significant increase in the number of acini and the presence of epithelial infoldings and vesicles. The intraepithelial vesicles frequently observed in the epithelium of prostates treated with testosterone for 3, 7, and 14 days are similar to the pseudocribriform pattern of intraepithelial neoplasia found in the gerbil male prostate [29, 30]. In human prostatic neoplasias, this epithelial organization may lead to the development of invasive adenocarcinoma. However, in prostates treated for 21 days, these figures were not as frequent as during earlier periods, suggesting that they represented a transient organization of the epithelial layer.

The epithelial cells became taller and presented a large chromophobic region in the supranuclear cytoplasm on Days 7 and 14 of treatment. This chromophobic area corresponds to the region occupied by the Golgi complex and its vesicular system, and is also seen in the normal male prostate of adult gerbils [1] and other rodents [6, 7]. These aspects were confirmed by transmission electron microscopy (unpublished results). The transition of the prostatic epithelium from small cuboidal or prismatic to tall prismatic or pseudostratified columnar revealed an intense enlargement of the epithelial cells and their engagement in secretory activity, which was maintained up to the 14th day of treatment. Accordingly, statistical analysis revealed a significant increase in the volume density of the epithelial compartment. In contrast to this epithelial development, the relative volume of the lumen was reduced to less than a half during this period.

A second cell type observed at high frequency in the secretory epithelium treated for 3, 7, and 14 days was the basal cell. These cells have been suggested to be responsible for the maintenance of the epithelial cell population in the female prostate [10]. The number of basal cells was relatively constant across testosterone treatments, with a proportion of 1 basal cell ?18 to about 12 luminal secretory cells. This aspect more closely resembles the situation found in the rat ventral prostate, and differs from the human male prostate, in which a one-to-one proportion is observed [31]. Immunocytochemical studies on

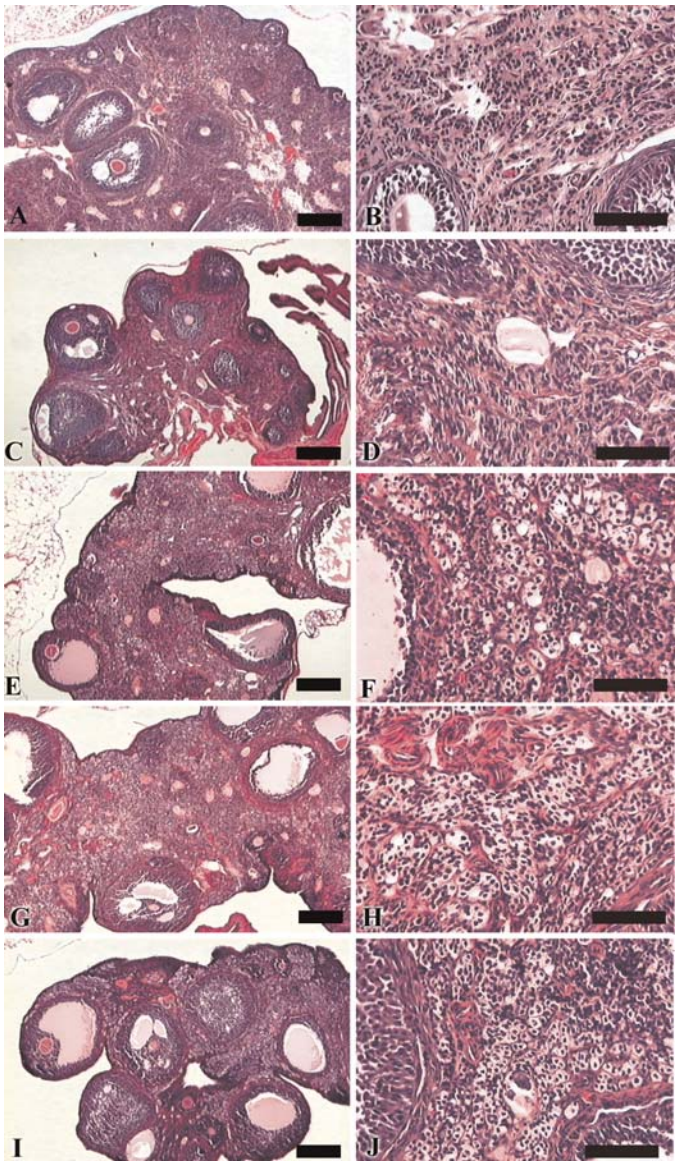

FIG. 7. Histological aspects of the ovary of control and testosterone-treated female gerbils. General views (**A**, **C**, **E**, **G**, and **I**) showing a progressive development of the stroma and acquisition of a polycystic condition with time after the beginning of testosterone treatment. Details of the ovarian stroma (**B**, **D**, **F**, **H**, and **J**) showing progressive hyperplasia of stromal cells, which are characterized by a dense cell nucleus, clear cytoplasm, and a chord-like arrangement. **A** and **B**, control; **C** and **D**, 3 days; **E** and **F**, 7 days; **G** and **H**, 14 days; and **I** and **J**, 21 days of testosterone treatment. Bars = 175 μm (**A**, **C**, **E**, **G**, and **I**) and 50 μm (**B**, **D**, **F**, **H**, and **J**).

the human male prostate revealed the existence of androgen receptors in these cells [32], a fact that might allow these cells to proliferate in response to testosterone. This was confirmed for the gerbil female prostate. However, we have also observed that luminal cells undergo mitosis when treated with testosterone (data not shown), indicating that proliferation does not exclusively depend on basal cells.

Clear cells, which expressed and accumulated a secretory material mainly consisting of neutral carbohydrates, were rare in the epithelium of the normal female prostate [1], but became gradually more frequent with testosterone treatment, increasing from 1:60 to 1:13 epithelial cells after 21 days of testosterone treatment (see Table 2).

?19

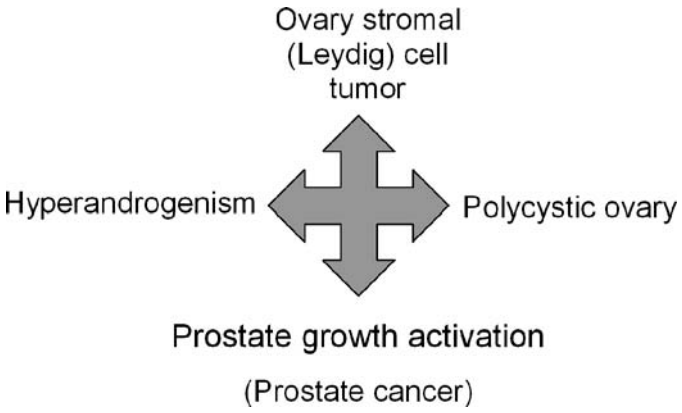

FIG. 8. Possible interactions between high testosterone circulating levels, a hormonal condition observed in hyperandrogenism and ovary and prostate diseases. The present series of results obtained for the female gerbil suggest that these four conditions might be correlated and result in serious complications.

Both morphometric and stereologic analyses revealed a decrease in the total number of acini and an inversion in the relative volume of the epithelial and luminal compartments. This increase in luminal content was more evident when the sectional area of the lumen was taken into account. This is associated with smaller epithelial cells that still showed a developed Golgi complex and numerous secretory vesicles. Taken together, these results demonstrate that the gland entered a synthetic phase, resulting in the accumulation of secretion in the lumen. These epithelial dynamics led to an enlarged gland after 21 days of treatment, as confirmed by 3-D reconstruction.

?20

?21

On the basis of these results, it is possible to conclude that the experimental administration of testosterone promoted the growth and a greater secretory activity of the female prostate. It is worth mentioning that the dynamics of the tissue compartments analyzed here reproduces in detail the prostate development of male mice [33] and Wistar rats (Vilamaior et al., unpublished data).

We conclude that the lack of androgenic stimuli can contribute to the underdevelopment of the normal adult gerbil female prostate. New questions related to the physiological processes that maintain the active state of the prostate in the female organism can be raised, as there are indications that other hormones, such as estrogen and prolactin, are involved in male prostate homeostasis [6, 13, 17, 18, 34]. Furthermore, the presence of enzymatic complexes, such as 5α-reductase (producing dihydrotestosterone from testosterone) [32] and aromatase (which converts testosterone, but not dihydrotestosterone, into estrogen) [35–38], must be investigated in this system.

The transient decrease in circulating PSA concentration seems to represent a temporary recruitment of epithelial cells for proliferation and differentiation, occurring soon after the beginning of treatment. Surprisingly, there was a strong negative correlation between the decrease in PSA levels and the increase in estrogen levels. At this point, we cannot distinguish a negative effect of the increased estrogen levels on prostatic secretory activity from the recruitment of epithelial cells for proliferation. However, this aspect should be analyzed in the future. It also remains to be determined whether this species expresses PSA or a member of the kallikrein family, which showed cross-reactivity with the antibodies employed in this work, because it is well known that rats and mice do not express PSA [39].

As mentioned previously here, it was very common to find characteristics related to the pseudocribriform structure of the epithelium immediately after the proliferating phase. It was also mentioned that most of these characteristics disappeared after longer testosterone treatment. This pseudocribriform arrangement is indicative of high proliferation, and is usually associated with the development of prostatic dysplasias. Although this pattern was evidently associated with the growth of the epithelium in testosterone-treated females, it may have anticipated a dysplastic growth of the organ. As a matter of fact, in the present study, each prostate analyzed after 21 days of testosterone treatment presented signs of dysplastic growth. Histological aspects of prostatic intraepithelial neoplasia, atypical hyperplasia, and mucinous adenocarcinomas were identified among the epithelial lesions. Although the duration of the experiment was relatively short, we may assume that longer testosterone administration will result in prostate cancer.

Finally, we also suggest that hyperandrogenism or exogenous testosterone intake might result in a complex series of effects (Fig. 8) threatening the health of women, resulting in increased prostatic activity with signs of epithelial dysplasia, a thickened urethral wall, ovarian stromal hyperplasia, and polycystic ovaries. The simple assumption that hyperandrogenism results in polycystic ovaries [40] should be reconsidered, taking into account other organs with a potential to respond to androgens.

ACKNOWLEDGMENTS

The authors are indebted to Dr. M. Zaviačič for providing the bibliographic material. The authors express their gratitude to Mr. L.R. Falleiros, Jr. for technical assistance, to Manuel Garcia-Florez for helping with the measurements of the luminal area, and to Rejane M. Góes and Maria Cristina C.G. Marcondes for helpful discussions.

REFERENCES

1. Santos FCA, Góes RM, Carvalho HF, Taboga SR. Structure, histochemistry and ultrastructure of the epithelium and stroma in the gerbil (*Meriones unguiculatus*) female prostate. Tissue Cell 2003; 35:447–457.
2. Custódio AMG, Góes RM, Taboga SR. Acid phosphatase activity in gerbil (*Meriones unguiculatus*) prostate: comparative study in male and female glands during postnatal development. Cell Biol Int 2004; 28:335–344.
3. Shehata R. Urethral glands in the wall of the female urethra of rats, mice and closely related rodents. Acta Anat (Basel) 1974; 90:381–387.
4. Shehata R. Female prostate in *Arvicanthis niloticus* and *Meriones libycus*. Acta Anat (Basel) 1975; 92:513–523.
5. Shehata R. Female prostate and urethral glands in the home rat, *Rattus norvegicus*. Acta Anat 1980; 107:286–288.
6. Smith AF, Landon GV, Ghanadian R, Chisholm GD. The ultrastructure of the male and female prostate of *Praomys (Mastomys) natalensis*. Cell Tissue Res 1978; 190:539–552.
7. Gross SA, Didio LJA. Comparative morphology of the prostate in adult male and female *Praomys* (*Mastomys*) *natalensis* studied with electron microscopy. J Submicrosc Cytol 1987; 19:77–84.
8. Flamini AM, Barbieto CG, Gimeno EJ, Portiansky EL. Morphological characterization of the female prostate (Skene's gland or paraurethral gland) of *Lagostomus maximus maximus*. Ann Anat 2002; 184:341–345.
9. Zaviačič M. The female prostate: from vestigial Skene's paraurethral glands and ducts to woman's functional prostate. Bratislava, Slovakia: Slovak Academic Press; 1999.
10. Zaviačič M, Jakubovská V, Belošovič M, Breza J. Ultrastructure of the normal adult human female prostate gland (Skene's gland). Anat Embryol (Berl) 2000; 201:51–61.
11. Skene AJC. The anatomy and pathology of two important glands of the female urethra. Am J Obstet Dis Women Child 1880; 13:265–270.
12. Wernet N, Albrecht M, Sesterhenn I, Goebbels R, Bonkhoff H, Seitz G, Inniger R, Remberger K. The "female prostate": location, morphology, immunohistochemical characteristics and significance. Eur Urol 1992; 22: 64–69.
13. Isaacs JT. Role of androgens in prostatic cancer. Vitam Horm 1994; 49: 433–502.
14. Marker PC, Donjacour AA, Dahiya R, Cunha GR. Hormonal, cellular, and molecular control of prostatic development. Dev Biol 2003; 253:165–174.
15. Merk FB, Leav I, Kwan PW, Ofner P. Effects of estrogen and androgen on the ultrastructure of secretory granules and intercellular junctions in regressed canine prostate. Anat Rec 1980; 197:111–132.
16. Wernet N, Gerdes J, Loy V, Seitz G, Scherr O, Dhom G. Investigations of the estrogen (ER-ICA-test) and progesterone receptor in the prostate and prostatic carcinoma on immunohistochemical basis. Virchows Arch A Pathol Anat Histopathol 1988; 412:387–391.
17. Nevalainen MT, Valve EM, Anhonen T, Yagi A. Androgen-dependent expression of prolactin in rat prostate epithelium in vivo and organ culture. FASEB J 1997; 11:1297–1307.
18. Timms BG, Petersen SL, Von Saal FS. Prostate gland growth during development is stimulated in both male and female rat fetuses by intrauterine proximity to female fetuses. J Urol 1999; 161:1694–1701.
19. Staub NL, Beer MD. The role of androgens in female vertebrates. Gen Comp Endocrinol 1997; 108:1–24.
20. Moore E, Wisniewski A, Dobs A. Endocrine treatment of transsexual people: a review of treatment regimens, outcomes, and adverse effects. J Clin Endocrinol Metab 2003; 88:3467–3473.
21. Tobin VA, Canny BJ. The regulation of gonadotropin-releasing hormone-induced calcium signals in male rat gonadotrophs by testosterone is mediated by dihydrotestosterone. Endocrinology 1998; 139:1038–1045.
22. Behmer AO, Tolosa EMC, Neto AGF. Manual de práticas para histologia normal e patológica. São Paulo, Brazil: Edart-Edusp; 1976.
23. Weibel ER. Principles and methods for the morphometric study of the lung and other organs. Lab Invest 1978; 12:131–155.
24. Huttunen E, Romppanen T, Helminen HJ. A histoquantitative study on the effects of castration on the rat ventral prostate lobe. J Anat 1981; 3:357–370.
25. Garcia-Florez M, Oliveira CA, Carvalho HF. Early effects of estrogen on the rat ventral prostate. Braz J Med Biol Res 2005; 38:487–497.
26. Carvalho HF, Line SRP. Basement membrane associated changes in the rat ventral prostate following castration. Cell Biol Int 1996; 20:809–198.
27. Vilamaior PSL, Taboga SR, Carvalho HF. Modulation of smooth muscle cell function: morphological evidence for a contractile to synthetic transition in the rat ventral prostate. Cell Biol Int 2005; 29:809–816.
28. Carvalho KP, Monteiro-Leal LH. The caudal complex of *Giardia lamblia* and its relation to motility. Exp Parasitol 2004; 108:154–162.
29. Vicent AL, Ash LR. Further observations on spontaneous neoplasms in the Mongolian gerbil, *Meriones unguiculatus*. Lab Anim Sci 1978; 28: 297–300.
30. Vicent AL, Gary ER, William AS. The pathology of the Mongolian gerbil (*Meriones unguiculatus*): a review. Lab Anim Sci 1979; 29:645–651.
31. El-Alfy M, Pelletier G, Hermo LS, Labrie F. Unique features of the basal cells of human prostate epithelium. Microsc Res Tech 2000; 51:436–446.
32. Steers WD. 5α-reductase activity in the prostate. Urology 2001; 58:17–24.
33. Singh J, Zhu Q, Handelsman DJ. Stereological evaluation of mouse prostate development. J Androl 1999; 20:251–258.
34. Reiter E, Hennuy B, Bruyninx M, Cornet A, Klug M, McNamara M, Closset J, Hennen G. Effects of pituitary hormones on the prostate. Prostate 1999; 38:159–165.
35. Andó S, Sirianni R, Forastieri P, Casaburi I, Lanzino M, Rago V, Giordano F, Giordano C, Carpino A, Pezzi V. Aromatase expression in prepuberal Sertoli cells: effect of thyroid hormone. Mol Cell Endocrinol 2001; 178:11–21.
36. Bulun SE, Yang S, Fang Z, Gurates B, Tamura M, Zhou J, Sebastián S. Role of aromatase in endometrial disease. J Steroid Biochem Mol Biol 2001; 79:19–25.
37. Lephart ED, Lund TD, Horvarth TL. Brain androgen and progesterone metabolizing enzymes: biosynthesis, distribution and function. Brain Res 2001; 37:25–37.
38. Kamat A, Hinshelwood MM, Murry BA, Mendelson CR. Mechanisms in tissue-specific regulation of estrogen biosynthesis in humans. Trends Endocrinol Metab 2002; 13:122–128.
39. Olsson AY, Lilja H, Lundwall A. Taxon-specific evolution of glandular kallikrein genes and identification of a progenitor of prostate-specific antigen. Genomics 2004; 84:147–156.
40. Spinder T, Spijkstrat J, van den Tweel J, Burger C, van Kessel H, Hompes P, Gooren L. The effects of long-term testosterone administration on pulsatile luteinizing hormone secretion and on ovarian histology in eugonadal female-to-male transsexual subjects. J Clin Endocrinol Metab 1989; 69:151–157.

Artigo: Anti-estrogênicos letrozol e tamoxifeno afetam a manutenção da homeostase tecidual da próstata feminina do gerbilo (*Meriones unguiculatus*). Este trabalho será vertido para língua inglesa e submetido ao periódico *The Prostate*.

Anti-estrogênicos letrozol e tamoxifeno afetam a manutenção da homeostase tecidual da próstata feminina do gerbilo (*Meriones unguiculatus)*

F. C. A. Santos[1] e S. R. Taboga[2]*

[1]*Departamento de Biologia Celular, Universidade Estadual de Campinas, Campinas, SP, Brasil.*

[2]*Departamento de Biologia, IBILCE, Universidade Estadual Paulista, São José do Rio Preto, SP, Brasil.*

***Endereço para correspondência:**

Sebastião R. Taboga, Departamento de Biologia – IBILCE/UNESP

E-mail: taboga@ibilce.unesp.br

Tel +55-17-32212386; Fax: +55-17-32212390

Resumo

A próstata feminina do gerbilo é um órgão maduro e funcional, cuja atividade secretória é regulada por hormônios esteróides. Estudos populacionais indicam que há uma significativa ocorrência de lesões prostáticas espontâneas tanto em mulheres como em fêmeas de roedores, sendo que estas alterações têm sido associadas a perturbações do equilíbrio hormonal interno, seja por fatores intrínsecos ao organismo ou pela ação de agentes endócrinos exógenos. A proposta deste trabalho é avaliar a resposta da próstata de fêmeas adultas do gerbilo a um curto período de exposição a agentes anti-estrogênicos, observando de que modo as alterações do balanço hormonal interno podem interferir com a fisiologia normal da próstata feminina. Para isso, fêmeas adultas receberam doses orais diárias de letrozol (1mg/kg/dia), ou doses subcutâneas de tamoxifeno (1mg/kg/) a cada 48 horas, durante 21 dias. Os níveis séricos de testosterona e estradiol foram monitorados, e as próstatas e ovários foram coletados para análises estruturais, ultra-estruturais e imunocitoquímicas. O tratamento com letrozol resultou em aumento dos níveis séricos de testosterona, hiperplasia glandular, incremento da atividade secretória e crescimento displásico, simulando os efeitos causados por andrógenos exógenos. Os efeitos causados pelo tamoxifeno indicam que este agente endócrino atuou como agonista estrogênico na próstata, causando hipertrofia glandular, diminuição da atividade secretória e desenvolvimento de lesões prostáticas. Deste modo, pode-se concluir que as terapias com letrozol e tamoxifeno resultam em uma série de efeitos complexos que comprometem a fisiologia de órgãos hormônio-dependentes, como a próstata feminina e os ovários. O desequilíbrio hormonal provocado pela administração destas drogas resulta em profundas

alterações na morfologia prostática, de maneira muito similar ao que ocorre durante o desenvolvimento de lesões espontâneas em mulheres no período pós-menopausa. Assim, a opção por estas terapias deve ser tomada com cautela, visto que longos períodos de tratamento podem resultar em lesões malignas da próstata feminina.

Palavras-chave: próstata feminina, morfologia, imunocitoquímica, andrógenos, anti-estrógenos.

Introdução

A próstata feminina é uma glândula madura e diferenciada, cuja função é produzir um fluído rico em frutose e zinco, de constituição química muito semelhante ao líquido prostático produzido pela próstata masculina (Zaviačič, 1993; 1999).

A glândula prostática de fêmeas do gerbilo (Santos et al., 2003; Custódio et al., 2004) apresenta grande homologia com a próstata ventral de roedores machos (Gross e Didio, 1987; Corradi et al., 2004) e com a próstata feminina humana (Zaviačič et al., 2000). Embora existam vários trabalhos que descrevam a estrutura histológica desta glândula, pouco é conhecido até hoje sobre os fatores que regulam sua função.

O tratamento de fêmeas adultas do gerbilo com testosterona revelou que as células epiteliais e estromais da próstata feminina expressam receptores androgênicos e que o estímulo hormonal causa aumento da atividade secretória e crescimento displásico da glândula. Assim, por se tratar de uma glândula regulada por esteróides, alterações nos níveis hormonais séricos podem interferir com a estrutura e fisiologia da próstata feminina (Santos et al., 2006).

Atualmente, têm sido crescentes os relatos de desenvolvimento de lesões prostáticas de mulheres senis (Sloboda et al., 1998). O surgimento destas lesões está associado ao desequilíbrio hormonal que ocorre no organismo da mulher, devido à falha dos ovários em produzir esteróides no período pós-menopausa (Zaviačič, 1999).

Com o aumento da incidência de cânceres de mama positivos ao receptor estrogênico, diversas terapias anti-estrogênicas foram desenvolvidas com a finalidade de impedir a progressão tumoral (Green e Furr, 1999; Miller, 2003). Dentre os agentes

terapêuticos mais indicados destacam-se o tratamento com letrozol (Berstein et al., 2002; Haynes et al., 2003; Smith, 2003) e o tamoxifeno (Cabot et al., 1996), ou a combinação de ambos (Dixon et al., 2003; Ingle e Suman, 2003; Miller et al., 2003). Estas drogas também estão sendo apontadas como benéficas na supressão do câncer prostático masculino, cujas células tornam-se altamente proliferativas pela ação combinada de andrógenos e estrógenos (Block et al., 1996).

O letrozol é um inibidor não-esteroidal da enzima aromatase capaz de evitar até 99% da conversão periférica de testosterona em estrógeno (Haynes et al., 2003). O tamoxifeno é um trifeniletileno não-esteroidal que exerce ação antagonista sobre o estrógeno, por ligar-se competitivamente ao receptor estrogênico (Cabot et al., 1996). O uso de ambas as drogas levam a drásticas alterações hormonais que podem influenciar a fisiologia de todos os órgãos reprodutivos regulados por hormônios. Como a próstata feminina do gerbilo se mostra sensível às alterações dos níveis de hormônios esteróides, torna-se relevante observar o efeito destes agentes endócrinos sobre a manutenção da homeostase glandular.

Assim, o objetivo deste estudo é avaliar a resposta da próstata de fêmeas adultas do gerbilo a um curto período de exposição a agentes anti-estrogênicos, observando de que modo as alterações do balanço hormonal interno podem interferir com a fisiologia normal da próstata feminina.

Material e Métodos

Animais e delineamento experimental

Para este estudo foram utilizadas 90 fêmeas adultas (90 dias de idade) do gerbilo (*Meriones unguiculatus*, Gerbillinae: Muridae). Dez animais receberam injeções intradérmicas contendo apenas o veículo de diluição e foram utilizados como controle do experimento. Os demais animais foram subdivididos em dois grupos. No grupo 1, 40 animais receberam doses orais diárias de 1mg/kg de letrozol (LET - Femara/Novartis) diluído em 0,2 mL de óleo de milho, segundo adaptação do método de Tobin & Canny (1998). No grupo 2, 40 animais receberam injeções intradérmicas de tamoxifeno [TAM - 1mg/kg de citrato de tamoxifeno (Sigma) diluído e 0,2 mL de óleo de milho] a cada 48 horas, segundo modificação do método de Fitts et al., (2004). Ambas as drogas foram administradas por um período de 21 dias, sendo que 10 animais de cada grupo experimental foram sacrificados com 3, 7, 14 e 21 dias de tratamento. Após anestesia por inalação de CO_2, os animais foram pesados e imediatamente decapitados para a coleta de amostras de sangue, do complexo prostático (uretra e tecidos associados) e dos ovários. Os ovários e os complexos prostáticos foram pesados e fixados de acordo com diferentes protocolos que serão descritos a seguir. O tratamento dos animais foi realizado de acordo com as diretrizes éticas da Universidade Estadual de Campinas (UNICAMP), descritas no guia para cuidados e uso de animais de laboratório.

Níveis plasmáticos de testosterona total, estradiol e PSA

Os níveis plasmáticos de testosterona, estradiol (E2) e antígeno específico prostático (PSA) foram determinados por métodos imunoquímicos. Cinco amostras de cada grupo experimental foram centrifugadas a 3000rpm e armazenadas a -20ºC para posteriores análises. As medidas foram realizadas em aparelho automatizado Vitros ECi-Johnson & Johnson para análise quimioluminescente ultra-sensível. A sensibilidade do método foi de 0,1-150 ng/mL para testosterona, 0,1-3.814,0 pg/mL para estradiol e 0,1-100 ng/mL para PSA humano.

Análise morfológica

O complexo prostático e os ovários foram fixados por imersão em solução de Karnovsky (paraformaldeído 5% e glutaraldeído 2,5% em tampão fosfato 0,1M, pH 7,2) ou em paraformaldeído 4% em tampão fosfato por 24 horas. Depois da fixação, os tecidos foram lavados em água, desidratados em etanol, clarificados em xilol, embebidos em paraplast (Histosec, Merck, Darmstadt, Germany) ou em resina de glicol metacrilato (Historesin embedding kit, Leica, Nussloch, Germany), e seccionados a 3µm em micrótomo rotatório automático (Leica RM2155, Nussloch, Germany). Os cortes histológicos da próstata feminina e dos ovários foram corados pela hematoxilina eosina (H&E,Behmer et al., 1976). As fibras reticulares do estroma foram identificadas pelo método da reticulina de Gömöri (Behmer et al., 1976) e as fibras do sistema elástico foram evidenciadas pela técnica da resorcina-fucsina de Weigert (Santos et al., 2004). Os tecidos foram analisados e fotografados em fotomicroscópio de luz Zeiss Jenaval (Zeiss-Jenaval, Jena, Germany) ou Olympus (Olympus, hamburg, Germany).

Imunocitoquímica

Os cortes histológicos das próstatas femininas fixadas em paraformol 4% foram submetidos a reações imunocitoquímicas para a detecção dos receptores de andrógeno (AR) e estrógeno alfa (ERα), segundo adaptação de protocolos já aplicados à próstata (Vilamaior et al., 2005; Santos et al., 2006). Os anticorpos primários para AR (rabbit polyclonal IgG, N-20) e ERα (rabbit polyclonal IgG, MC-20) (Santa Cruz Biotechnology, Santa cruz, CA, USA) foram aplicados em uma diluição de 1:100 e 1:50, respectivamente. Anticorpos específicos conjugados à peroxidade (Sigma Chemical Co., Saint Louis, MO, USA) foram utilizados como anticorpos secundários e a 3,3'-diaminobenzidina como substrato da peroxidase. Os cortes foram contracorados com a hematoxilina de Harris.

Análises morfométrica e estereológica

As análises morfométricas e estereológicas foram realizadas a partir de lâminas coradas pela técnica da hematoxilina eosina e em Sistema Analisador de Imagens, com o programa Image–Pro-Plus (Média Cybernetics). O volume relativo dos compartimentos teciduais da próstata feminina foi determinado de acordo com o sistema de teste de multipontos M168 proposto por Weibel (1978) e aplicado à próstata por Huttunen et al. (1981). Para isso, foram capturados 30 campos aleatórios de cada grupo experimental (6 campos por animal). A densidade de volume foi calculada depois da contagem do número de pontos que coincidiram com cada um dos compartimentos teciduais da glândula (epitélio, lúmen, estroma muscular e estroma não muscular). Os volumes absolutos não puderam ser determinados por não ser possível separar a próstata feminina dos tecidos aderentes para determinar o seu peso exato.

Para quantificar a freqüência de tipos de células epiteliais, 30 alvéolos prostáticos foram selecionados aleatoriamente. O número de células epiteliais secretoras, secretoras claras e basais por alvéolo foi contado e a contribuição individual de cada tipo celular foi expressa em porcentagem. Para as análises morfométricas, foram realizadas 200 medidas de altura das células epiteliais (µm), espessura da camada muscular lisa (µm) e espessura da camada de fibras de colágeno (µm). As análises cariométricas compreenderam 200 medidas de razão área núcleo/citoplasma, área nuclear (μm^2), perímetro nuclear (µm) e fator forma nuclear [4π.área nuclear/(perímetro nuclear)^2].

Análise ultra-estrutural

Os fragmentos do complexo prostático foram fixados durante 24 horas pelo glutaraldeído a 3% em tampão Millonig pH 7,3, acrescido de ácido tânico a 0,25% e glicose a 0,54%. Em seguida, eles foram lavados em tampão, pós-fixados em solução de tetróxido de ósmio a 1% por 2 horas, desidratados em acetona e incluídos em araldite, segundo Cotta-Pereira (1976). Os cortes ultra-finos foram obtidos em navalha de diamante e contrastados com acetato de uranila a 2% (Watson, 1958) e com citrato de chumbo a 2% por 10 minutos (Venable e Coggeshall, 1965). As observações e obtenção dos negativos micrográficos foram realizadas com o microscópio eletrônico de transmissão Zeiss (EM 910).

Análise estatística

Os dados obtidos foram analisados no softwere Statistica 6.0 (Copyright©StarSoft, Inc. 1984-1996, Tulsa, OK, USA). Os testes de hipóteses utilizados para comprovar a significância dos resultados foram a análise de variância (ANOVA) e o teste de Tukey para comparações múltiplas, com nível de significância de 5% ($p \leq 0,05$).

Resultados

Peso corpóreo, ovariano e do complexo prostático

A tabela I demonstra a variação do peso corpóreo, ovariano e prostático durante as fases de tratamento com LET e TAM. No tratamento com LET pode-se observar um aumento significativo do peso prostático e corpóreo a partir de 14 e 21 dias de tratamento, respectivamente. No entanto, os ovários apresentaram um acréscimo em sua massa desde o 3º dia de administração da droga.

Nos grupos tratados com TAM não houve alterações significativas do peso corpóreo e ovariano. Contudo, alterações significativas de peso prostático foram observadas a partir do 14º dia de tratamento.

Para representar o comportamento do complexo prostático e dos ovários com relação ao peso corpóreo, foram realizadas medidas de peso relativo, as quais estão descritas na tabela I. Com relação ao complexo prostático, pode-se observar que ambos os tratamentos provocaram um acréscimo no peso relativo glandular, embora este aumento tenha sido mais pronunciado na terapia com TAM (LET +45%, TAM +80%). Nos ovários, pode-se constatar que estas drogas apresentaram efeitos opostos. Enquanto o LET causou

um acréscimo de até 36% no peso relativo ovariano, o TAM diminuiu este peso em até 26%.

Níveis sorológicos de hormônios esteróides de antígeno PSA-reativo

Os níveis sorológicos de testosterona, estradiol e de antígeno reativo ao PSA humano durante os tratamentos com LET e TAM estão representados na tabela I.

Na terapia com LET pode-se constatar um gradual acréscimo nos níveis séricos de testosterona, sendo que este hormônio chegou a 6,1 ± 1,5 ng/ml aos 21 dias de tratamento. Esta variação foi significativa e é cerca de 4 vezes mais elevada que os níveis séricos encontrados em fêmeas adultas não-tratadas. O tratamento com LET não causou alterações significativas nos níveis séricos de estradiol e de antígeno reativo ao PSA. No entanto, o teste de correlação de Pearson revelou uma considerável relação negativa entre os níveis séricos de testosterona e estradiol (r = -0,62). Os níveis de antígeno reativo ao PSA humano não demonstraram correlação com os níveis séricos de testosterona e estradiol.

O TAM causou uma significativa diminuição nos níveis séricos de testosterona aos 3 e 7 dias de tratamento. Na primeira semana de tratamento, os níveis deste hormônio chegaram a um terço (0,5 ± 0,04 ng/ml) do observado nas fêmeas controle (1,6 ± 0,5 ng/ml). Porém esta variação foi transitória, sendo que os níveis de testosterona retornaram a níveis normais aos 21 dias de tratamento (1,8 ± 0,1 ng/ml). Os níveis de estradiol e de antígeno reativo ao PSA sofreram oscilações não significativas durante todo o tratamento com TAM. Os testes estatísticos não apontaram correlação entre os níveis de testosterona e estradiol, ou entre testosterona e antígeno reativo ao PSA. No entanto, um significativo

coeficiente de correlação negativo foi observado entre os níveis de estradiol e PSA (r = -0,71).

Características morfológicas e imunocitoquímicas das glândulas prostáticas tratadas com LET e TAM

A próstata de fêmeas adultas do gerbilo é constituída por um grupo de ductos e alvéolos inseridos em um estroma fibro-muscular, que estabelece íntimo contato com a parede da uretra, em suas porções mediana e distal. Os alvéolos são revestidos por um epitélio que varia de cúbico a prismático simples, e apresentam um volumoso lúmen que armazena os produtos de secreção (Figs. 1a,b). Dois tipos principais de células epiteliais podem ser observados: as células basais e as secretoras. As células basais são pequenas, com forma irregular, e encontram-se apoiadas sobre a membrana basal (Fig. 1b). As células secretoras são mais numerosas, estão em contato com o lúmen glandular e são caracterizadas por apresentar núcleo volumoso e citoplasma acidófilo (Fig. 1b). Entre estas células secretoras, eventualmente podem ser encontradas células com citoplasma cromofóbico e núcleo elíptico, que são denominadas células secretoras claras (dado não demonstrado).

O estroma da próstata feminina é muito denso, sendo constituído principalmente por fibras e células musculares lisas e estriadas esqueléticas (Fig. 1c). Fibras reticulares são encontradas na porção basal do epitélio e em contato com as células musculares (Fig. 1d). As fibras de colágeno se distribuem ao redor dos alvéolos e as escassas fibras do sistema elástico são observadas na região parabasal do epitélio (Fig. 1e).

Testes imunocitoquímicos demonstraram reação positiva para AR no núcleo das células epiteliais secretoras e dos fibroblastos adjacentes ao epitélio (Figs. 1f,g,h).

Marcações positivas para ERα foram observadas no núcleo das células epiteliais secretoras e das células estromais (Figs. 1i).

Ultra-estruturalmente, as células epiteliais prostáticas de fêmeas adultas normais exibem um citoplasma elétron-denso, rico em mitocôndrias, retículo endoplasmático rugoso e complexo de Golgi (Fig. 2a). Inúmeras vesículas de secreção polimórficas são observadas na região supra-nuclear (Fig. 2b). O núcleo das destas células é volumoso e com cromatina descondensada (Figs. 2a,b). O compartimento estromal é composto principalmente por células musculares lisas e fibroblastos (Fig. 2a). As células musculares lisas exibem poucas organelas e são circundadas por feixes de fibras de colágeno (Fig. 2c).

Os dados morfológicos indicam que o LET causou importantes alterações no arranjo tecidual da próstata feminina do gerbilo, entre as quais um evidente desenvolvimento glandular e secretório. Nas fases iniciais do tratamento (3 e 7 dias), o compartimento epitelial tornou-se mais desenvolvido, assumindo um padrão pseudoestratificado colunar e formando várias dobras direcionadas para o compartimento luminal (Figs. 3a,b,c). Vesículas intraepiteliais foram observadas em vários alvéolos. As células epiteliais tornaram-se mais volumosas e apresentaram uma vasta área cromofóbica supranuclear e um núcleo alongado (Fig. 3d). O compartimento luminal sofreu uma aparente redução (Figs. 3a,c). No entanto, aos 14 dias de tratamento pode-se observar uma regressão do epitélio glandular, que foi acompanhada de uma ampliação do lúmen (Fig. 3e). As células epiteliais tornaram-se mais baixas, porém com núcleo volumoso (Fig. 3f). Na última fase de tratamento com LET (21 dias), o compartimento epitelial voltou a exibir as mesmas características observadas na primeira semana de tratamento (Fig 3g,h).

O TAM também causou alterações na arquitetura glandular da próstata feminina do gerbilo. Durante todo o tratamento ocorreu uma gradual dilatação do lúmen, que foi acompanhada por uma regressão do compartimento epitelial (Figs. 3i-p). As células epiteliais secretoras tornaram-se muito baixas. Muitas células de secreção apócrina foram observadas principalmente aos 14 dias de tratamento (Fig. 3n). Em quase todas as glândulas analisadas foi muito comum a ocorrência de espaços intercelulares no compartimento epitelial (Figs. 3l,p). Vesículas intraepiteliais foram observadas a partir do 14º dia de tratamento (Figs. 3m,o) e tornaram-se uma característica típica da próstata feminina na fase final de tratamento com TAM (Fig. 3o).

O compartimento estromal das glândulas prostáticas tratadas com LET tornou-se mais denso, apresentando maior quantidade de fibras de colágenos principalmente aos 7 dias de tratamento (Fig. 4a). As fibras reticulares localizadas na base do epitélio apresentaram-se mais espessas e sinuosas (Figs. 4b,c). Grande quantidade de fibras do sistema elástico pôde ser observada em todas as etapas do tratamento com LET (Fig. 4d). No tratamento com TAM houve um considerável aumento das fibras de colágeno localizadas nas proximidades do epitélio (Fig. 4e). As fibras reticulares mostraram-se mais numerosas, formando várias camadas dispostas na base do epitélio (Figs. 4f,g). O TAM também provocou um acréscimo das fibras do sistema elástico, sendo que essas fibras foram observadas formando redes complexas nas proximidades dos ductos (Fig. 4h).

O comportamento dos receptores androgênicos e estrogênicos nos tratamentos com LET e TAM pode ser observado na figura 5. O LET causou uma maior expressão do AR em todas as fases do tratamento (Fig. 5a). Essa maior expressão pode ser constatada pelo aumento no número de células epiteliais e estromais positivas ao AR e pela maior

intensidade das marcações (Fig. 5b). Por outro lado, glândulas tratadas com LET apresentaram uma menor marcação para ERα, sendo que marcações leves foram observadas apenas no núcleo de células epiteliais e de células estromais próximas ao epitélio (Fig. 5d). No tratamento com TAM o padrão de expressão de AR foi semelhante ao do controle (Fig. 5e). Com este tratamento, os núcleos de fibroblastos e células epiteliais secretoras mostraram-se positivos ao receptor androgênico (Fig. 5f). No entanto, as marcações para ERα foram mais intensas e numerosas (Fig. 5g), abrangendo o núcleo das células epiteliais secretoras e o núcleo e citoplasma dos fibroblastos (Fig. 5h).

Estereologia

A densidade de volume das próstatas normais e tratadas com LET e TAM está apresentada na tabela II. Na próstata de fêmeas controle, o epitélio, o lúmen e o estroma não-muscular ocupam volumes equivalentes (26-29%), e o estroma muscular representa em torno de 18% do volume glandular. Os resultados demonstram que o LET provocou um aumento significativo na proporção do compartimento epitelial em todas as fases do tratamento, com exceção do 14º dia (14,1%), onde observa-se um declínio significativo deste componente tecidual. O compartimento luminal apresentou uma oscilação significativa durante a terapia com LET, mas manteve-se mais desenvolvido aos 14 e 21 dias de tratamento (66,5% e 36,8%, respectivamente). A densidade de volume do estroma muscular foi mais alta aos 3 (26%) e 7 (23,2%) dias de tratamento, porém sofreu uma significativa diminuição aos 14 (11%) e 21 dias (14%). O estroma não-muscular apresentou um decréscimo significativo em sua densidade de volume em todas as fases do tratamento com LET.

Nas glândulas tratadas com TAM pode-se constatar que o compartimento epitelial sofreu um gradual decréscimo em sua densidade de volume a partir do 7º dia de tratamento, alcançando 22,3% aos 21 dias de administração da droga. Inversamente, o compartimento luminal tornou-se mais volumoso a partir do 7º dia de tratamento com TAM, chegando a ocupar 47,6% do volume relativo da glândula prostática. O estroma muscular tornou-se menos freqüente (14,5%) aos 21 dias de tratamento, enquanto que o estroma não-muscular sofreu reduções significativas a partir do 14º dia de tratamento (20% aos 14 dias e 15,6% aos 21 dias). A aplicação do teste paramétrico de Tukey demonstrou que todas as alterações de densidade de volume ocorridas nos tratamentos com LET e TAM foram estatisticamente significativas ($p \leq 0,05$).

Morfometria e cariometria

Na tabela II constam os dados referentes às análises morfométricas e cariométricas dos grupos tratados pelo LET e TAM. A análise da freqüência de células epiteliais demonstrou que o tratamento com LET causou um significativo acréscimo na proporção de células secretoras claras (controle = 1,6 ± 0,2%), que passaram a representar 3,8 ± 0,2% da população epitelial prostática. Por outro lado, ocorreu uma redução proporcional na freqüência de células secretoras típicas, que passaram de 90,4 ± 0,3% (controle) para 88,4 ± 0,3% aos 21 dias de tratamento. As células basais não sofreram alterações significativas em sua proporção, perfazendo em média de 7,7 a 8,1% do total de células epiteliais. O tratamento com TAM não alterou significativamente a freqüência dos tipos celulares analisados.

O tratamento com LET também causou alterações significativas na altura das células epiteliais secretoras, que tornaram-se mais altas em todas as fases do tratamento (controle = 14,4 ± 0,3 µm; 3 LET = 16,7 ± 0,2 µm; 7 LET = 23,1 ± 0,3 µm e 21 LET = 18 ± 0,2 µm), exceto aos 14 dias, onde observou-se uma significativa redução da altura epitelial (8,9 ± 0,1 µm). A camada sub-epitelial de células musculares (controle = 9,6 ± 0,1 µm) tornou-se mais espessa aos 3 dias de tratamento (14,3 ± 0,2 µm), porém sofreu um gradual declínio a partir do 7º dia, alcançando os valores mínimos de 5,3 ± 0,1 e 7,5 ± 0,1 µm aos 14 e 21 dias de experimento, respectivamente. A espessura da camada sub-epitelial de fibras de colágeno (controle = 2,4 ± 0,05 µm) atingiu valores máximos aos 7 dias de tratamentos (7,2 ± 0,3 µm), sendo reduzida a 3,3 ± 0,2 µm aos 21 dias de tratamento.

O tratamento com TAM induziu uma gradual diminuição da espessura do epitélio secretor (controle = 14,4 ± 0,3 µm; 21 dias TAM = 11 ± 0,2 µm) e da camada de células musculares (controle = 9,6 ± 0,1 µm; 21 dias TAM = 7,2 ± 0,1 µm). Inversamente, a camada sub-epitelial de fibras de colágeno (controle = 2,4 ± 0,05 µm) tornou-se sucessivamente mais espessa, atingindo o valor máximo de 3,8 ± 0,1 µm aos 21 dias de tratamento. Estas alterações foram estatisticamente significativas ($p \leq 0,05$).

A análise dos parâmetros cariométricos indicou que o tratamento com LET causou um gradual incremento da razão área núcleo/citoplasma (controle = 0,24 ± 0,01; 21 dias LET = 0,31 ± 0,01). Acréscimo semelhante também pode ser observado para a área (controle = 23 ± 0,4 μm^2; 21 dias LET = 28,1 ± 0,4 μm^2), perímetro (controle = 19,5 ± 0,2 µm; 21 dias LET = 20,8 ± 0,2 µm) e fator forma nucleares (controle = 0,76 ± 0,01; 21 dias LET = 0,81 ± 0,01), sendo todas estas alterações estatisticamente significativas, com $p \leq$

0,05. No tratamento com TAM a razão área núcleo/citoplasma não se alterou significativamente durante o tratamento com TAM. Além disso, embora os valores médios da área e do perímetro nucleares tenham sofrido oscilações significativas durante a terapia, ao fim do tratamento estes valores (21 dias TAM: área = 24,5 ± 0,4 μm^2; perímetro = 19,3 ± 0,1 μm) foram semelhantes aos observados nos órgãos controle (área = 23 ± 0,4μm^2; perímetro = 19,5 ± 0,2 μm). Um aumento significativo do fator forma nuclear (controle = 0,76 ± 0,01) ocorreu a partir dos 3 dias de terapia com TAM (0,82 ± 0,01), valor que se manteve constante até o fim do tratamento.

Anti-estrógenos e displasia prostática

Ambas as terapias anti-estrogênicas causaram importantes alterações displásicas no epitélio e estroma da próstata feminina do gerbilo adulto. A figura 6 demonstra as principais alterações morfológicas observadas na próstata de fêmeas tratadas pelo LET por 21 dias. As lesões mais comuns compreendem neoplasia intraepitelial prostática (Figs. 6a,b,e,f), prostatites severas (Fig. 6c), hiperplasia epitelial e estromal (Figs. 6a,b,h, i) e focos de adenocarcinoma (Figs. 6c,d). Estes arranjos teciduais anormais passaram a ser detectados a partir do 3º dia de tratamento com LET e abrangeram 100% das glândulas analisadas ao final do tratamento.

No tratamento com TAM todas as glândulas analisadas com 14 e 21 dias de tratamento apresentaram crescimento displásico. A figura 7 representa as principais alterações observadas aos 21 dias de tratamento. Nesta etapa as lesões mais comuns foram neoplasia intraepitelial prostática, hiperplasia e adenocarcinoma de células mucinosas

(Figs. 7a-c,f). A formação de microalvéolos com diferenciação neuroendócrina foi constatada na maioria das glândulas analisadas (Figs. 7d,e). Outra característica marcante foi a formação de extensos espaços intercelulares no epitélio secretor (Fig. 7g). O estroma subjacente às regiões de lesão epitelial apresentou grande quantidade de fibras de colágeno e fibras do sistema elástico (Figs. 7h-j). As células musculares apresentaram um fenótipo espinhoso e grande quantidade de organelas (Fig. 7i).

Estrutura ovariana

A figura 8 representa as características histológicas dos ovários das fêmeas controle (Figs. 8a-c) e tratadas com LET (Figs. 8d-f) e TAM (Figs. 8g-h). Como não foram observadas diferenças histológicas importantes entre as fases de cada tratamento, todos os dados demonstrados para os experimentos em questão correspondem à mesma fase (21 dias). No tratamento com LET (Figs. 8d-f) as células da granulosa sofreram intensa proliferação e passaram a ocupar toda a cavidade antral. A partir dos 14 dias de tratamento nenhum folículo apresentou ovócito e muitas células da granulosa entraram em apoptose. Além disso, uma marcante hiperplasia de células estromais foi observada em todas as fases do tratamento com LET.

No tratamento com TAM (Figs. 8g-i), a maioria dos folículos entraram em atresia. Folículos não-atrésicos apresentaram uma proliferação atípica das células da granulosa e as células estromais sofreram uma intensa hiperplasia.

Discussão

Este trabalho demonstra que as terapias endócrinas com LET e TAM causam importantes alterações na próstata feminina do gerbilo. Embora essas drogas tenham exercido efeitos diferenciados sobre a fisiologia e a manutenção da atividade secretória da glândula, ambas induziram crescimento displásico e a instalação de desordens pré-malignas e malignas na próstata feminina.

Durante o tratamento das fêmeas do gerbilo com LET, os níveis séricos de testosterona tornaram-se gradualmente mais elevados e atingiram valores até 4 vezes maiores do que os observados em fêmeas não tratadas. Experimentos com camundongos machos deficientes na expressão de aromatase (McPherson et al., 2001) e com ratos machos submetidos à inibição da mesma enzima (Haynes et al., 2003) demonstraram que estes animais também sofreram um aumento nos níveis séricos de testosterona, além de uma significativa redução nos níveis de estradiol. Esta alteração hormonal ocorre por que a deficiência ou inibição da enzima aromatase impede a conversão periférica de testosterona em estrógeno, fato que ocasiona o acúmulo de testosterona e a diminuição gradual dos níveis de E2 (Roseli e Resko, 2001; Kamat el al., 2002; Santen, 2003).

Estudos *in vivo* demonstraram que ratas adultas tratadas diariamente com LET por 14 dias apresentaram interrupção da ciclicidade ovariana, elevação dos níveis de testosterona e diminuição dos níveis séricos de E2 a taxas similares às observadas em animais ovariectomizados (Sinha et al., 1998). Efeito semelhante também foi observado em mulheres que utilizaram o LET com terapia endócrina para o tratamento do câncer de mama, onde constatou-se que esta droga suprimiu totalmente os níveis de E2 nos primeiros

14 dias de tratamento (Haynes et al., 2003). No entanto, os resultados obtidos com as fêmeas do gerbilo demonstram que o LET não alterou significativamente os níveis séricos de E2 durante o período de 21 dias de tratamento, embora tenha-se observado uma relação negativa entre os níveis de testosterona e estradiol.

O aumento dos níveis séricos de testosterona durante o tratamento com LET induziu alterações glandulares semelhantes às observadas em fêmeas adultas do gerbilo tratadas com testosterona (Santos et al., 2006). Estas alterações compreendem principalmente hiperplasia epitelial e estromal, modificação na expressão de receptores hormonais, acréscimo do peso prostático e aumento da atividade secretora.

Os dados morfológicos e morfométrico-estereológicos demonstram que o compartimento epitelial tornou-se mais desenvolvido aos 3 e 7 dias de tratamento, apresentando nestas fases um comportamento hiperplásico, com a formação de várias dobras epiteliais direcionadas para o lúmen e uma grande quantidade de vesículas intraepiteliais. Aos 14 dias, com a dilatação luminal, o epitélio se distendeu e as dobras desapareceram, embora a ocorrência de vesículas intraepiteliais tenha aumentado. Estas vesículas também foram encontradas em todas as fases do tratamento com TAM e são semelhantes ao padrão pseudocribiforme de neoplasia intraepitelial observado em fêmeas de gerbilo tratadas com testosterona (Santos et al., 2006) e em gerbilos machos (Vicent et al., 1979). De modo semelhante ao que ocorre em neoplasias prostáticas humanas e de roedores (Shappell et al., 2004), o surgimento deste tipo de neoplasia nos tratamentos com LET e TAM parece preceder as alterações malignas observadas nestes experimentos.

Aos 21 dias de tratamento, novo crescimento hiperplásico foi observado no epitélio, ocasionando uma redução no volume relativo do compartimento luminal e estromal. Este

padrão de comportamento dos componentes glandulares durante a terapia com LET demonstra que o desenvolvimento glandular foi dado por pulsos alternados de proliferação epitelial e ampliação luminal, que ocasionaram num intenso desenvolvimento prostático.

O tratamento com LET também alterou a proporção dos tipos celulares epiteliais da próstata feminina do gerbilo. As células claras, que são raras em fêmeas normais, tornaram-se duas vezes mais freqüentes, enquanto que as secretoras típicas sofreram uma diminuição proporcional em sua freqüência. Fêmeas de gerbilo sob o efeito de andrógenos exógenos apresentaram até cinco vezes mais células claras do que fêmeas não-tratadas. Nestes animais, os níveis sorológicos de testosterona foram até 12 vezes maiores do que os observados em fêmeas controle (Santos et al., 2006). No tratamento com TAM, onde os níveis séricos de testosterona não se alteraram, não foram observadas modificação na freqüência da população epitelial. Assim, estes resultados permitem concluir que a expressão de células claras é influenciada por andrógenos e dependente da concentração hormonal alcançada.

A hiperplasia de células estromais prostáticas observada durante o tratamento com LET foi acompanhada de uma maior atividade secretora das células musculares lisas e fibroblastos, fato que ocasionou um considerável acréscimo na quantidade de fibras de colágeno e elásticas. Assim, a redução do volume relativo do compartimento estromal e da camada de células musculares lisas e de fibras de colágeno apontada pelas análises morfométrico-estereológicas são decorrentes de um processo de remodelação do estroma durante o desenvolvimento glandular.

As intensas reações imunocitoquímicas observadas para AR indicam que o aumento dos níveis séricos de testosterona provocaram uma maior expressão deste receptor, fato que

pode ser associado ao maior desenvolvimento prostático e ao acréscimo da atividade secretora ocorrido durante o tratamento com LET. Por outro lado, pode-se constatar uma diminuição no número e intensidade das marcações para ERα. Diversos trabalhos têm demonstrado que a próstata masculina humana e de roedores expressa a enzima aromatase tanto em condições normais, quanto durante o desenvolvimento de lesões (Kaburagi et al., 1987; Hiramatsu et al., 1997; Negri-Cesi et al., 1998; Simpson et al., 1999; Risbridger et al., 2003). Na próstata, o bloqueio desta enzima pelo LET causa uma diminuição na disponibilidade tecidual de E2, dificultando a ligação deste hormônio ao seu receptor (Smith et al., 2002). Deste modo, é provável que a menor expressão de ERα seja decorrente da diminuição dos níveis intra-prostáticos de E2.

A ocorrência de crescimento displásico e de adenocarcionoma prostático foi muito elevada durante os 21 dias de tratamento com LET. Alterações de mesma natureza também foram encontradas em fêmeas adultas do gerbilo tratadas com testosterona, porém neste tipo de tratamento as lesões foram menos severas e freqüentes (Santos et al., 2006). Em mulheres, o desenvolvimento de lesões prostáticas espontâneas está associado ao desequilíbrio hormonal que ocorre no organismo feminino durante a senescência (Zaviačič et al., 2000; Islam et al., 2001; Sharifi-Aghdas e Ghaderian, 2004; Kato et al., 2005).

Os resultados obtidos com este trabalho demonstram que o aumento nos níveis séricos de testosterona endógena, provocado pelo tratamento com LET, reproduz em detalhes a condição de hiperandrogenismo causada pela administração de andrógenos. Contudo, o LET apresentou um maior potencial para desenvolver lesões na próstata feminina do gerbilo durante o curto período de tratamento experimental. A inibição da enzima aromatase afeta o balanço hormonal sistêmico por causar o aumento dos níveis

séricos de testosterona e a diminuição gradativa dos níveis séricos de E2 (Miller, 2003; Howell e Cuzick, 2005). Embora a análise sorológica realizada neste experimento não tenha detectado alterações importantes nos níveis sorológicos de E2, acredita-se que o bloqueio da aromatase tenha diminuído a disponibilidade tecidual deste hormônio. Estudos com camundongos machos deficientes na expressão de aromatase demonstram que o equilíbrio entre andrógenos e estrógenos é fundamental para a manutenção da fisiologia normal da próstata (McPherson et al., 2001; Risbridger et al., 2003). Assim, o desequilíbrio hormonal provocado pela administração de LET pode ter sido o evento chave para o desenvolvimento das lesões prostáticas observadas neste experimento.

As análises morfológicas e morfométrico-estereológicas das próstatas femininas tratadas com TAM demonstram que esta droga promoveu hiperplasia e hipertrofia glandular, eventos que ocasionaram um aumento de até 80% do peso relativo prostático. O compartimento epitelial sofreu um processo de atrofia, enquanto que o lúmen apresentou uma intensa dilatação. A análise ultra-estrutural confirma que a atrofia sofrida pelo epitélio foi decorrente de uma diminuição na quantidade de organelas e de vesículas de secreção, fato que está diretamente relacionado com a redução da capacidade secretora da glândula.

O compartimento estromal tornou-se mais denso, exibindo uma maior quantidade de células e fibras de colágeno e elásticas. As fibras de colágeno sofreram um processo de remodelamento, de modo a acompanhar a expansão sofrida pelos alvéolos prostáticos, enquanto que as fibras do sistema elástico concentraram-se na região periductal.

A análise imunocitoquímica demonstrou que o tratamento com TAM não afetou a expressão de AR na próstata feminina. No entanto, as marcações para ERα foram mais freqüentes e intensas nas células epiteliais e nas células mais profundas do estroma

prostático. Nas fêmeas tratadas com TAM os níveis sorológicos de E2 e de antígeno reativo ao PSA não se alteraram, porém os níveis de testosterona reduziram-se para menos da metade aos 3 e 7 dias de tratamento.

O TAM é um agente esteroidal amplamente utilizado no tratamento do câncer de mama por atuar como antagonista estrogênico, impedindo a ligação de E2 a ambos os receptores ERα e ERβ (Cabot et al., 1996; White, 1999; Dixon et al., 2003; Smith, 2003). No entanto, estudos que avaliaram o impacto do TAM sobre os órgãos reprodutivos de roedores demonstraram que esta droga exibe função mista agonista/antagonista, de acordo com a espécie e o órgão analisado (Taguchi, 1987; Fitts et al., 2004; Zhang et al., 2005). Na próstata ventral de camundongos machos, o TAM atua como agonista parcial do ERα, desencadeando efeitos similares aos observados em animais estrogenizados (Singh e Handelsman, 1999).

O crescimento displásico e as modificações teciduais observadas nas glândulas prostáticas femininas tratadas com TAM são muito semelhantes às alterações observadas nas próstatas de roedores machos estrogenizados no período intra-embrionário ou neonatal (Prins et al., 2001; Omoto et al., 2005; Risbridger et al., 2005; Zhang et al., 2005). Além disso, a diminuição inicial dos níveis séricos de testosterona é outro fator indicativo da atividade agonista do TAM na próstata feminina do gerbilo, visto que os estrógenos interferem indiretamente na síntese de andrógenos, via ação sobre o hipotálamo (McPherson et al., 2001; Härkönen e Mäkelä, 2004). Por outro lado, a hiperplasia estromal e a atresia folicular observadas nos ovários destes animais indicam que o TAM atuou como antagonista estrogênico nestes órgãos. Assim, pode-se concluir que o TAM atuou como

um agonista estrogênico na próstata feminina do gerbilo, embora tenha exercido uma aparente ação antagonista sobre a fisiologia ovariana.

Deste modo, pode-se concluir que as terapias anti-estrogênicas com LET e TAM, que são amplamente utilizadas como primeira linha de tratamento contra a progressão do câncer de mama ER-positivo (Green e Furr, 1999; Ingle e Suman, 2003; Miller, 2003; Santen, 2003), promovem uma série de efeitos complexos que comprometem a fisiologia de outros órgãos hormônio-dependentes, como a próstata feminina e os ovários. O desequilíbrio hormonal provocado pela administração destas drogas causa profundas alterações na morfologia prostática, de maneira muito similar ao que ocorre durante o desenvolvimento de lesões espontâneas em mulheres no período pós-menopausa. Assim, estas terapias devem ser utilizadas com cautela, visto que longos períodos de tratamento podem resultar em lesões malignas da próstata feminina.

Agradecimentos

Este trabalho foi financiado pela FAPESP (Fundação de amparo à pesquisa de São Paulo, processo 00/11648-1 e 03/08653-1) e teve bolsa de estudos CAPES para F.C.A. Santos. Os autores agradecem a L.R. Falleiros-Jr. e R. S. Souza pela assistência técnica e a R.M. Góes e H.F. Carvalho pelas contribuições na elaboração deste trabalho.

Referências

Behmer AO, Tolosa EMC, Neto AGF. 1976. **Manual de práticas para histologia normal e patológica.** EDART-EDUSP, SP.329p.

Berstein L, Maximov S, Gershfeld E, Meshkova I, Gamajunova V, Tsyrlina E, Larionov A, Kovalevskij A, Vasilyev D. 2002. Neoadjuvant therapy of endometrial cancer with the aromatase inhibitor letrozole: endocrine and clinical effects. ***Obstetrics & Gynecology***, 105:161-165.

Block, J.L.; Block, N.L.; Lokeshwar, B.L. 1996. Inhibition of aromatase activity and growth suppression by –methoxy-4-androstene-3,7-dione in an androgen sensitive human prostatic carcinoma cell line. **Cancer Letters,** 101: 143-148.

Cabot MC, Giuliano AE, Volner A, Han TY. 1996. Tamoxifen retards glycosphingolipid metabolism in human cancer cells. **FEBS Letters**, 394: 129-131.

Corradi LS, Gpoes RM, Carvalho HF, Taboga SR. 2004. Inhibition of 5-aplha-reductase activity induces stromal remodeling and smooth muscle differentiation in adult gerbil ventral prostate. **Differentiation**, 72(5): 198-208.

Cotta-Pereira G, Rodrigo FG, David-Ferreira JF. 1976. The use of tannic acid-glutaraldehyde in the study of elastic related fibers. **Stain Technol,** 51: 7-11.

Custódio AMG, Góes RM, Taboga SR. 2004. Acid phosphatase activity in gerbil prostate: comparative study in male and female during postnatal development. **Cell Biology International**, 28: 335-344.

Dixon JM, Jackson J, Renshaw L, Miller WR. 2003. **J Steroid Biochem Mol Biol,** 86: 295-299.

Fitts JM, Klein RM, Powers CA. 2004. Comparison of tamoxifen and testosterone propionate in male rats: differential prevention of orchidectomy effects on sex organs, bone mass, growth, and the growth hormone – IGF-I axis. **J Androl**, 25(4): 523-534.

Green S and Furr B. 1999. Prospects for the treatment of endocrine-responsive tumours. **Endocrine-Related Cancer**, 6: 349-371.

Gross SA, Didio LJA. 1987 Comparative morphology of the prostate in adult male and female of Praomys (mastomys) natalensis studies with electron microscopy. **J Submicros Cytol**, 19 (1): 77-84.

Härkönen PL, Mäkelä SI. 2004. Role of estrogens in development of prostate cancer. **J Steroid Biochem Mol Biol**,,92: 297-305.

Haynes BP, Dowsett M, Miller WR, Dixon JM, Bhatnagar AS. 2003. The pharmacology of letrozole. **J Steroid Biochem Mol Biol**, 87: 35-45.

Hiramatsu M, Maehara I, Ozaki M, Harada N, Orikasa S, Sasano H. 1997. Aromatase in hyperplasia and carcinoma of the human prostate. **Prostate**, 31: 118-124.

Howell A, Cuzick J. 2005. Vascular effects of aromatase inhibitors: data from clinical trials. **J Steroid Biochem Mol Biol,** 95: 10-43-149.

Huttunen E, Romppanen T, Helminen HJ, 1981. A histoquantitative study on the effects of castration on the rat ventral prostate lobe. **J Anatomy,** 3: 357-370.

Ingle JN, Suman VJ 2003. Aromatase inhibitors versus tamoxifen for management of postmenopausal breast cancer in the advanced disease and neoadjuvant settings. **J Steroid Biochem Mol Biol,** 86: 313-319.

Islam AHMM, Kato H, Hayama M, Kobayashi S, Ota H, Nishizawa O. 2001. Adenocarcinoma of female paraurethral duct showing neuroendocrine differentiation. **Urology**, 58(6): 1058iv-vi.

Kaburagi YK, Marino MB, Kirdani RY, Greco JP, Karr JP, Sandberg AA. 1986. The possibility of aromatization of androgen in human prostate. **J Steroid Biochem,** 26(6): 739-742.

Kamat A, Hinshelwood MM, Murry BA, Mendelson CR. 2002. Mechanisms in tissue-specific regulation of estrogen biosynthesis in humans. **TRENDS in Endocrinology & Metabolism**, 13(3): 122-128.

Kato H, Kobayashi S, Islam AM, Nishizawa O. 2005. Female para-urethral adenocarcinoma: histological and immunohistochemical study. **Int J Urol**, 12:117-119.

McPherson SJ, Wang H, Jones ME, Pedersen J, Iismaa TP, Wreford N, Simpson ER, Risbridger GP. 2001. Elevated androgens and prolactin in aromatase-deficient mice cause enlargement, but not malignancy, of the prostate gland. **Endocrinology**, 142: 2458-2467.

Miller WR, Dixon JM, Macfarlane L, Cameron D, Anderson TJ. 2003. Pathological features of breast cancer response following neoadjuvant treatment with either letrozole or tamoxifen. **Eur J Cancer,** 39: 462-468.

Negri-Cesi P, Poletti A, Colciago A, Magni P, Martini P, Motta M. 1998. Presence of 5α-reductase isozymes and aromatase in human prostate cancer cells and in benign prostate hyperplastic tissue. **Prostate**, 34: 238-291.

Omoto Y, Imamov O, Warner M, Gustafsson JA. 2005. Estrogen receptor alpha and imprinting of the neonatal mouse ventral prostate by estrogen. **Proc Natl acad Sci USA**, 102(5): 1484-1489.

Prins GS, Birch L, Habermann H, Chang WY, Tebeau C, Putz O, Bieberich C. 2001. Influence of neonatal estrogens on rat prostate development. **Reprod Fertil Dev**, 13: 241-252.

Risbridger GP, Almahbobi GA, Taylor RA. 2005. Early prostate development and its association with late-life prostate disease. **Cell Tissue Res**, 322: 173-181.

Risbridger GP, Bianco JJ, Ellem SJ, McPherson SJ. 2003. Oestrogens and prostate cancer. **Endocrine-Related Cancer**, 10: 187-191.

Roselli CE, Resko JA. 2001. Cytochrome P450 aromatase (CYP19) in the non-human primate brain: distribution, regulation, and functional significance. **J Steroid Biochem Mol Biol,** 79: 247-253.

Santen RJ. 2003. Inhibition of aromatase: insights from recent studies. **Steroids,** 68: 559-567.

Santos FCA, Carvalho HF, Góes RM, Taboga SR. 2003. Structure, histochemistry and ultrastructure of the epithelium and stroma in the gerbil (*Meriones unguiculatus*) female prostate. **Tissue & Cell**, 35: 447-457.

Santos FCA, Corradi LS, Leite RP, Góes RM, Taboga SR. 2004. A modified method for the selective staining of elastic system fibers in methacrylate tissue sections. **Braz J Morphol Sci,** 21(3): 135-138.

Santos FCA, Leite RP, Custódio AMG, Carvalho KP, Monteiro-Leal LH, Santos AB, Góes RM, Carvalho HF, Taboga SR. 2006. Testosterone stimulates growth and secretory activity of the adult female prostate of the gerbil (*Meriones unguiculatus*). **Biol Reprod**, 75(3): 370-379.

Shappell SB, Thomas GV, Roberts RL, Herbert R, Ittmann MM, Rubin MA, Humphrey PA, Sundberg JP, Rozengurt N, Barrios R, Ward JM, Cardiff RD. 2004. Prostate pathology of genetically engineered mice: definitions and classification. The consensus report from the bar harbor meeting of the mouse models of human cancer consortium prostate pathology committee. **Cancer Research**, 64: 2270-2305.

Sharifi-Aghdas F, Ghaderian N. 2004. Female paraurethral cysts: experience of 25 cases. **BJU International**, 93: 353-356.

Simpson E, Rubin G, Clyne C, Robertson K, O'Donnell L, Davis S, Jones M. 1999. Local estrogen biosyntesis in males and females. **Endocrine-Related Cancer**, 6: 131-137.

Singh J and Handelsman DJ. 1999. Imprinting by neonatal sex steroids on the structure and function of the mature mouse prostate. **Biol Reprod,** 61: 200-208.

Sinha S, Kaseta J, Santner SJ, Demers LM, Bremmer WJ, Santen RJ. 1998. Effect of CGS 20267 on ovarian aromatase and gonadotropin levels in the rat. **Breast Cancer Res Treat**, 48: 45-51.

Sloboda J, Zaviačič M, Jakubovský J, Hammar E, Johnsen J. 1998. Metastasizing adenocarcinoma of the female prostate (Skene´s paraurethrl galnds). Histological and immunohistochemical prostate markers studies and first ultrastructural observation. **Pathol Res Pract**, 194: 129-136.

Smith MR, Kaufman D, George D, Oh WK, Kazanis M, Manola J, Kantoff PW. 2002. Selective aromatase inhibition for patients with androgen-independent prostate carcinoma. **Cancer**, 95(9): 1864-1868.

Smith IE. 2003. Letrozole versus tamoxifeno in the treatment of advanced breast cancer and as neoadjuvant therapy. **J Steroid Biochem Mol Biol**, 86: 289-293.

Taguchi O. 1987. Reproductive tract lesions in male mice treated neonatally with tamoxifen. **Biol Reprod**, 37: 133-116.

Tobin VA, Canny BJ. 1998. The regulation of gonadotropin-releasing hormone-induced calcium signals in male rat gonadotrophs by testosterone is mediated by dihydrotestosterone. **Endocrinology,** 139: 1038-1045.

Venable JH, Coggeshall R. 1965. A simplified lead citrate stain for use in elctron microscopy. **J Cell Biol,** 25: 407-408.

Vicent AL, Gary ER, Willian AS. 1979. The pathology of the Mongolian gerbil (*Meriones unguiculatus*): A review. **Lab Animal Sci**, 29: 645-651.

Vilamaior PSL, Taboga SR, Carvalho HF. 2005. Modulation of smooth muscle cell function: Morphological evidence for a contractile to synthetic transition in the rat ventral prostate. **Cell Biol Int**, 29: 809-816.

Watson ML. 1958. Staining tissue sections of electron microscopy with heavy metals**. J Biophys Biochem Cytol,** 4: 475-478.

Weibel ER. 1978. Principles and methods for the morphometric study of the lung and other organs. **Lab Invest,** 12: 131-155.

White INH. 1999. The tamoxifen dilemma. **Carcinogenesis**, 20(7): 1153-1160.

Zaviačič M. 1993. Update on the female prostate and the phenomenon of female ejaculation. **The Journal of Sex Research,** 30(2): 148-151.

Zaviačič M. 1999. **The Female Prostate: From vestigial Skene's parauretral glands and ducts to woman's functional prostate.** 1.ed. Bratislava, Slovakia: Slovack Academic Press, 171p.

Zaviačič M, Jakubovská V, Belošovič J, Breza J. 2000. Ultrastrucuture of the normal adult human female prostate gland (Skene's gland). **Anat Embriol** *(Berl)*, 201(1): 51-61.

Zhang H, McElrath T, Tong W, Pollard JW. 2005. The molecular basis of tamoxifen induction of mouse uterine epithelial cell proliferation. **J Endocrinol**, 184: 129-140.

Legendas

Tabela I. [1]Peso corpóreo, prostático e ovariano de fêmeas controle e tratadas com letrozol (LET) e tamoxifeno (TAM) (*n* = 10 animais por grupo). O peso relativo prostático e ovariano corresponde a razão entre o peso destes órgãos e o peso corpóreo. A sua variação é demonstrada com relação ao controle, que é referido como 100%. [2]Níveis séricos de testosterona, estrógeno e proteína reativa ao antígeno específico da próstata (PSA) em fêmeas controle e tratadas com LET e TAM (*n* = 5 amostras por grupo). Os valores mencionados correspondem à média e ao erro padrão, respectivamente. Os asteriscos indicam diferenças estatisticamente significativas (*$p \leq 0,05$) entre o grupo controle e os tratamentos. Letras sobrescritas (^{a,b,c,d,e}) representam diferenças significativas entre os períodos de tratamento.

Tabela II. Dados da estatística descritiva referentes à estereologia, freqüência de células epiteliais, morfometria e cariometria da próstata feminina adulta do gerbilo durante as fases de tratamento pelo letrozol (LET) e o tamoxifeno (TAM). Os valores mencionados correspondem à média e ao erro padrão, respectivamente. Asteriscos indicam diferenças estatisticamente significativas (*$p \leq 0,05$) entre o grupo controle e os grupos de tratamento. Letras sobrescritas (^{a,b,c,d,e}) representam diferenças significativas entre os períodos de tratamento; [1]*n* = 30 campos em 5 animais por grupo; [2]*n* = 30 alvéolos por grupo; [3]*n* = 200 medidas em 5 animais por grupo.

Figura 1. Histologia, histoquímica e imunocitoquímica da próstata adulta normal do gerbilo. **1a.** Visão geral da próstata feminina corada pelo método H&E. Epitélio (Ep), estroma (s), secreção (*). **1b.** Detalhe do epitélio destacando as células basais (b) e secretoras (sc). **1c-d.** Cortes histológicos corados pela reticulina de Gömöri para evidenciar as fibras reticulares (setas) e de colágeno (co). **1e.** Fibras elásticas escassas (setas) na porção basal do epitélio. **1f-h.** Expressão de AR nas células epiteliais (setas) e estromais (cabeça de seta) da próstata feminina. **1i.** Células epiteliais (setas) e estromais (cabeça de seta) positivas ao ERα.

Figura 2. Ultra-estrutura da próstata feminina adulta normal do gerbilo. **2a.** Células secretoras (S) com citoplasma elétron-denso e núcleo volumoso (N) com cromatina fina. Lâmina basal (LB), fibroblasto (Fb). Barra: 3,4 µm. **2b.** Detalhe do citoplasma apical de uma célula secretora evidenciando a riqueza em vesículas de secreção (V). Barra: 1,7 µm **2c.** Estroma prostático com células musculares lisas (SMC) entremeadas às fibras de colágeno (CO). Barra: 1,2 µm.

Figura 3. Aspectos morfológicos das próstatas femininas tratadas com LET **(a-h)** e TAM **(i-p)** por 3, 7, 14 e 21 dias. Coloração: H&E. Aos 3 e 7 dias de terapia com LET **(a-d)** ocorreu a formação de vesículas (setas) e dobras intraepitelias (cabeça de seta). Aos 14 dias **(e-f)** a dilatação luminal (*) promoveu a distensão do epitélio (Ep). Ao final da terapia **(g-h)**, novo crescimento epitelial foi observado. Mitose (seta). Vesículas intraepiteliais (setas) foram observadas em todas as fases de tratamento com TAM (m,o). Ampliação luminal e atrofia do epitélio secretor foram constatadas a partir do sétimo dia de tratamento

(k-p). Observe a formação de espaços intercelulares no epitélio (cabeça de seta). Células secretoras claras (c).

Figura 4. Distribuição das fibras estromais nas próstatas femininas tratadas com LET **(a-d)** e TAM **(e-h)** por 7, 14 e 21 dias. Coloração: reticulina de Gömöri (a, b, c, e, f, g) e resorcina-fucsina de Weigert (d, h). No tratamento com LET **(a-c)** as fibras reticulares (setas) foram observadas entre as células musculares lisas (smc) que circundavam os alvéolos prostáticos. As fibras de colágeno (co) foram observadas nas proximidades da membrana basal e em regiões mais profundas do estroma. As fibras do sistema elástico (el) tornaram-se muito desenvolvidas na base do epitélio **(d)**. No tratamento com TAM **(e-g)** as fibras reticulares sofreram um intenso desenvolvimento (setas). Camadas espessas de fibras de colágeno (co) foram observadas logo abaixo do epitélio. **(h)** Redes complexas de fibras elásticas (el) se formaram ao redor dos ductos prostáticos (d).

Figura 5. Reações imunocitoquímicas das próstatas femininas tratadas com LET **(a-d)** e TAM **(e-g)** por 14 dias. Contracoloração: hematoxilina. No tratamento com LET as marcações epiteliais e estromais para AR **(a-b)** foram mais freqüentes e intensas (setas). **5c.** Controle negativo da reação. Por outro lado, as marcações para ERα **(d)** foram mais suaves (setas), abrangendo as células epiteliais e algumas células estromais dispostas na base do epitélio (Ep). No tratamento com TAM não foram observadas alterações na expressão de AR **(e-f)**. No entanto, células ERα-positivas **(g-h)** foram observadas nas células epiteliais e nos fibroblastos (setas).

Figura 6. Alterações morfológicas causadas pelo LET aos 21 dias de tratamento. **6a-b.** Neoplasia intraepitelial com padrão pseudocribiforme de arranjo (setas). **6c.** Infiltrados inflamatórios luminais e estromais (setas). **6d.** Foco de adenocarcinoma invasivo. **6e-f.** Ultra-estrutura de parte de um alvéolo com neoplasia intraepitelial prostática (NIP). As células neoplásicas apresentaram grande quantidade de retículo endoplasmático rugoso (RER) e liso (REL), e nucléolos bem desenvolvidos (setas). Barra e: 5,4 µm; f: 2,7 µm. **6g.** Pontos de interrupção da lâmina basal (LB - setas). Barra: 800 nm. **6h-i.** Detalhe das células musculares lisas (SMC) e fibroblastos (Fb) que exibiram um fenótipo mais sintético. Barra h: 1,6 µm; i: 1,3 µm.

Figura 7. Alterações teciduais induzidas pelo TAM aos 21 dias de tratamento. **7a-c.** Neoplasia intraepitelial prostática com padrão pseudocribiforme de arranjo (setas) e intensa proliferação de células típicas de adenocarcinoma de células mucinosas (cabeça de seta). **7d.** Visão geral onde pode-se observar a hiperplasia das células estromais (S) e a formação de microalvéolos (setas). Epitélio (Ep). Barra: 7 µm. **7e.** Detalhe de um microalvéolo com diferenciação neuroendócrina. Grânulos (g). Barra: 2 µm. **7f.** Ultra-estrutura de uma vesícula intraepitelial. Observe a presença de uma lâmina basal no interior da vesícula (seta). Barra: 1,6 µm. **7g.** Formação de espaços intraepiteliais entre as células basais (B) e secretoras (Sc). Barra: 900 nm. **7h-j.** Estroma prostático apresentando grande quantidade de fibras de colágeno (CO) na base do epitélio (Ep) e fibras elásticas (setas) associadas às células musculares lisas. As células musculares lisas (SMC) exibem um fenótipo altamente sintético e espinhoso. Barra h: 2,3 µm; i: 900 nm; j: 560 nm.

Figura 8. Características histológicas dos ovários controle **(a-c)** e tratados por LET **(d-f)** e TAM **(g-i)** por 14 dias. Coloração: H&E. No tratamento com LET as células da granulosa (g) sofreram intensa proliferação e passaram a ocupar toda a cavidade antral. Inúmeras apoptoses foram observadas entre as células foliculares (setas). Na terapia com TAM a maioria dos folículos sofreu atresia (setas). Folículos não atrésicos (F) apresentaram uma proliferação atípica das células da granulosa (g). Em ambos os tratamentos as células estromais (s) tornaram-se hiperplásicas, exibindo um núcleo volumoso e citoplasma cromofóbico.

Tabela I		Controle (veículo)	Dias de tratamento			
			3	7	14	21
Dados Biométricos[1]						
Peso corpóreo (g)	LET*	61,5[a] ± 1,6	68,8[a] ± 1,6	63,1[a] ± 2,6	61,1[a] ± 3,1	74,4[b] ± 2,3
	TAM	61,5 ± 1,6	60,7 ± 1,9	60,7 ± 3,0	69,4 ± 1,9	69,2 ± 1,5
Peso complexo prostático (g)	LET*	0,1[a] ± 0,005	0,12[a] ± 0,003	0,12[a] ± 0,007	0,13[b] ± 0,007	0,17[c] ± 0,009
	TAM*	0,1[a] ± 0,005	0,1[a] ± 0,003	0,11[a] ± 0,002	0,15[b] ± 0,01	0,20[c] ± 0,007
Peso ovariano (g)	LET*	0,04[a]±0,003	0,05[b] ±0,002	0,05[b] ±0,001	0,05[b] ±0,001	0,06[b] ± 0,002
	TAM	0,04 ± 0,003	0,04 ± 0,001	0,03 ± 0,001	0,03 ± 0,001	0,03 ± 0,001
Peso relativo prostático (%)	LET*	--	+6,7[a]	+17,0[a]	+32,5[b]	+45,9[b]
	TAM*	--	+5,7[a]	+15,1[a]	+33,9[b]	+79,2[c]
Peso relativo ovariano (%)	LET*	--	+25,9[a]	+38,8[b]	+37,3[b]	+36,1[b]
	TAM*	--	+7,9[a]	-2,9[a]	-25,8[b]	-26,6[b]
Dados sorológicos[2]						
Testosterona (ng/ml)	LET*	1,6[a] ± 0,5	2,5[a] ± 0,9	3,0[a] ± 1,1	3,4[a] ± 1,0	6,1[b] ± 1,5
	TAM*	1,6[a] ± 0,5	0,5[b] ± 0,04	0,7[b] ± 0,1	1,5[a] ± 0,3	1,8[a] ± 0,1
Estrógeno (pg/ml)	LET	22,9 ± 2,6	24,0 ± 3,8	23,0 ± 3,3	26,2 ± 2,8	23,4 ± 3,9
	TAM	22,9 ± 2,6	31,3 ± 3,1	20,0 ± 2,6	30,5 ± 0,7	26,9 ± 2,1
PSA (ng/ml)	LET	0,16 ± 0,05	0,14 ± 0,05	0,20 ± 0,05	0,23 ± 0,02	0,25 ± 0,02
	TAM	0,16 ± 0,05	0,04 ± 0,01	0,23 ± 0,09	0,09 ± 0,03	0,15 ± 0,02

Tabela II		Controle (veículo)	Dias de tratamento			
			3	7	14	21
Dados estereológicos[1]						
Epitélio (%)	LET*	$26,7^{a} \pm 0,9$	$38,8^{b} \pm 1,0$	$42,7^{c} \pm 1,0$	$14,1^{d} \pm 0,8$	$32,6^{e} \pm 0,6$
	TAM*	$26,7^{a} \pm 0,9$	$26,4^{a} \pm 0,7$	$20,6^{b} \pm 0,6$	$21,4^{b} \pm 0,6$	$22,3^{b} \pm 0,4$
Lúmen (%)	LET*	$27,0^{a} \pm 0,9$	$17,7^{b} \pm 1,4$	$21,3^{b} \pm 0,9$	$66,5^{c} \pm 1,1$	$36,8^{d} \pm 0,7$
	TAM*	$27,0^{a} \pm 0,9$	$25,4^{a} \pm 0,8$	$35,3^{b} \pm 0,6$	$40,0^{c} \pm 1,0$	$47,6^{d} \pm 1,1$
Estroma muscular (%)	LET*	$17,8^{a} \pm 0,5$	$26,0^{b} \pm 1,0$	$23,2^{c} \pm 0,7$	$10,9^{d} \pm 0,5$	$14,0^{e} \pm 0,4$
	TAM*	$17,8^{a} \pm 0,5$	$18,0^{a} \pm 0,4$	$17,9^{a} \pm 0,5$	$18,5^{a} \pm 0,5$	$14,5^{b} \pm 0,6$
Estroma não-muscular (%)	LET*	$28,5^{a} \pm 1,0$	$17,4^{b} \pm 1,1$	$12,8^{c} \pm 0,6$	$8,5^{d} \pm 0,5$	$16,6^{c} \pm 0,6$
	TAM*	$28,5^{a} \pm 1,0$	$27,2^{a} \pm 0,9$	$26,2^{a} \pm 0,7$	$20,0^{b} \pm 1,0$	$15,6^{c} \pm 0,8$
Freqüência dos tipos de células epiteliais[2]						
Células secretoras (%)	LET*	$90,4^{a} \pm 0,3$	$90,3^{a} \pm 0,2$	$90,6^{a} \pm 0,2$	$88,3^{b} \pm 0,3$	$88,4^{b} \pm 0,3$
	TAM	$90,4 \pm 0,3$	$89,9 \pm 0,3$	$90,3 \pm 0,2$	$90,2 \pm 0,2$	$90,9 \pm 0,2$
Células secretoras claras (%)	LET*	$1,6^{a} \pm 0,2$	$1,5^{a} \pm 0,1$	$1,7^{a} \pm 0,1$	$3,8^{b} \pm 0,2$	$3,8^{b} \pm 0,2$
	TAM	$1,6 \pm 0,2$	$1,6 \pm 0,1$	$1,4 \pm 0,1$	$1,4 \pm 0,1$	$1,4 \pm 0,1$
Células basais (%)	LET	$8,0 \pm 0,2$	$8,1 \pm 0,2$	$7,7 \pm 0,2$	$7,9 \pm 0,2$	$7,9 \pm 0,2$
	TAM	$8,0 \pm 0,2$	$8,5 \pm 0,2$	$8,3 \pm 0,1$	$8,4 \pm 0,2$	$7,7 \pm 0,2$
Dados morfométricos[3]						
Altura das células secretoras (µm)	LET*	$14,4^{a} \pm 0,3$	$16,7^{b} \pm 0,2$	$23,1^{c} \pm 0,3$	$8,9^{d} \pm 0,1$	$18,0^{e} \pm 0,2$
	TAM*	$14,4^{a} \pm 0,3$	$14,1^{a} \pm 0,2$	$11,4^{b} \pm 0,2$	$12,3^{c} \pm 0,2$	$11,0^{b} \pm 0,2$
Espessura da camada muscular lisa (µm)	LET*	$9,6^{a} \pm 0,1$	$14,3^{b} \pm 0,2$	$10,5^{c} \pm 0,1$	$5,3^{d} \pm 0,1$	$7,5^{e} \pm 0,1$
	TAM*	$9,6^{a} \pm 0,1$	$9,3^{a} \pm 0,1$	$9,4^{a} \pm 0,1$	$9,5^{a} \pm 0,1$	$7,2^{b} \pm 0,1$
Espessura da camada de fibras de colágeno (µm)	LET*	$2,4^{a} \pm 0,05$	$5,5^{b} \pm 0,3$	$7,2^{c} \pm 0,3$	$2,5^{a} \pm 0,1$	$3,3^{a} \pm 0,2$
	TAM*	$2,4^{a} \pm 0,05$	$3,0^{b} \pm 0,1$	$3,4^{c} \pm 0,1$	$3,1^{b} \pm 0,1$	$3,8^{d} \pm 0,1$
Dados cariométricos[3]						
Razão área núcleo/citoplasma	LET*	$0,24^{a} \pm 0,01$	$0,26^{a} \pm 0,01$	$0,27^{a} \pm 0,01$	$0,30^{b} \pm 0,01$	$0,31^{b} \pm 0,01$
	TAM	$0,24 \pm 0,01$	$0,27 \pm 0,01$	$0,24 \pm 0,01$	$0,27 \pm 0,01$	$0,27 \pm 0,01$
Área nuclear (µm²)	LET*	$23,0^{a} \pm 0,4$	$29,1^{a} \pm 0,5$	$34,7^{c} \pm 0,5$	$34,1^{c} \pm 0,5$	$28,1^{b} \pm 0,4$
	TAM*	$23,0^{a} \pm 0,4$	$34,4^{b} \pm 0,5$	$29,4^{c} \pm 0,5$	$27,2^{d} \pm 0,4$	$24,5^{a} \pm 0,4$
Perímetro nuclear (µm)	LET*	$19,5^{a} \pm 0,2$	$22,6^{b} \pm 0,2$	$23,2^{b} \pm 0,2$	$22,9^{b} \pm 0,1$	$20,8^{c} \pm 0,2$
	TAM*	$19,5^{a} \pm 0,2$	$22,8^{b} \pm 0,2$	$21,2^{c} \pm 0,2$	$20,2^{d} \pm 0,1$	$19,3^{a} \pm 0,1$
Fator forma nuclear	LET*	$0,76^{a} \pm 0,01$	$0,71^{b} \pm 0,01$	$0,81^{c} \pm 0,01$	$0,81^{c} \pm 0,01$	$0,81^{c} \pm 0,01$
	TAM*	$0,76^{a} \pm 0,01$	$0,82^{b} \pm 0,01$	$0,81^{b} \pm 0,01$	$0,83^{b} \pm 0,01$	$0,81^{b} \pm 0,01$

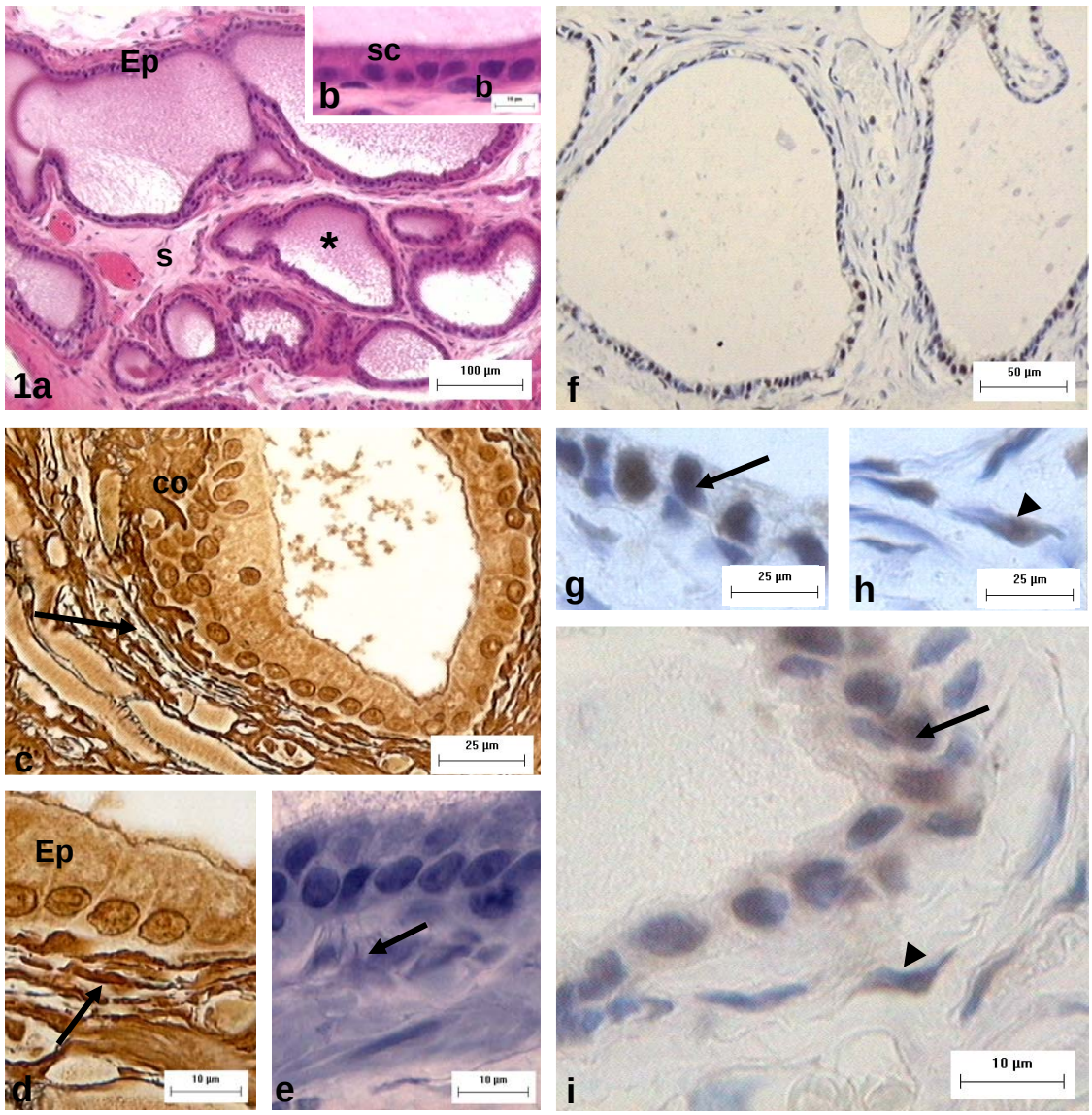
Ep
sc
b
b
s
*
100 µm
1a
50 µm
f
co
25 µm
c
25 µm
g
25 µm
h
Ep
10 µm
d
10 µm
e
10 µm
i

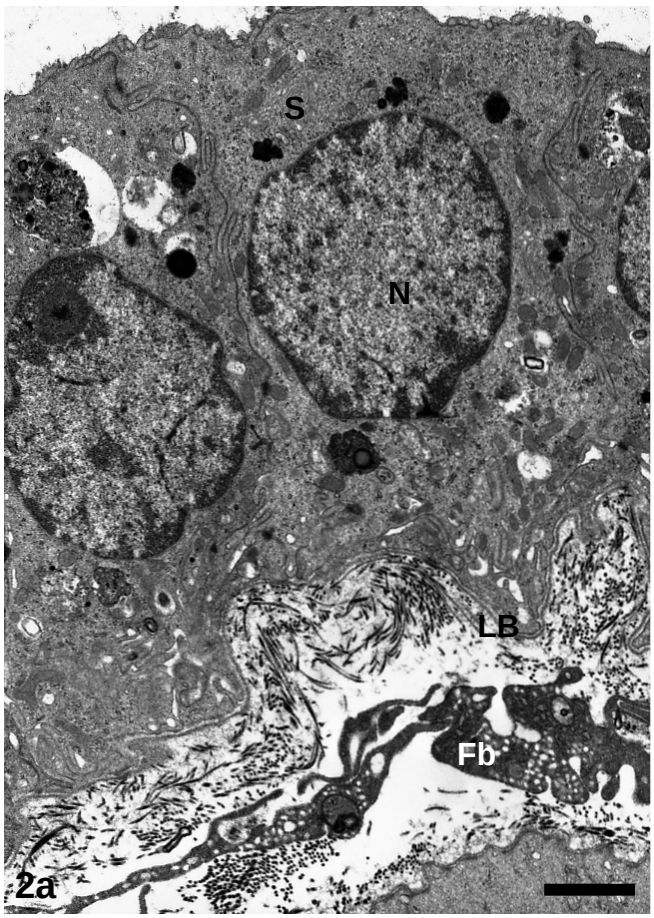
S
N
LB
Fb
2a

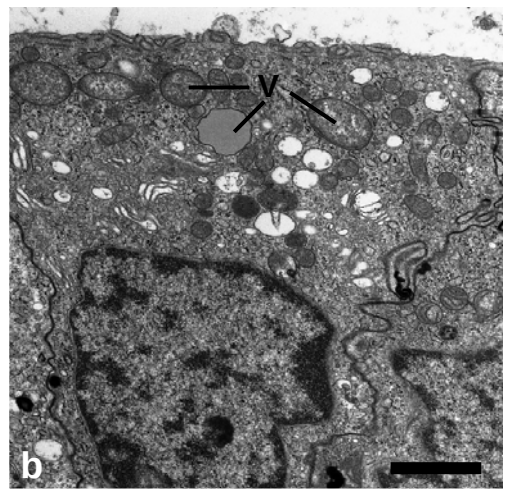
V
b

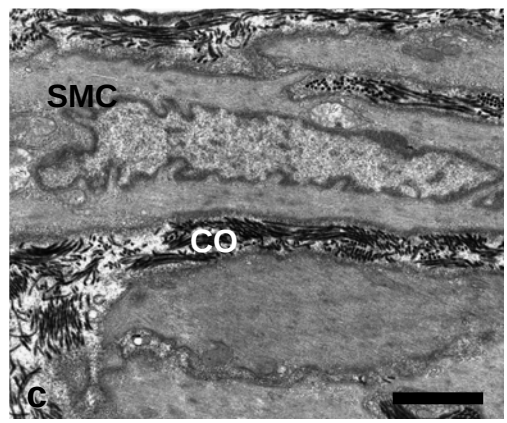
SMC
CO
c

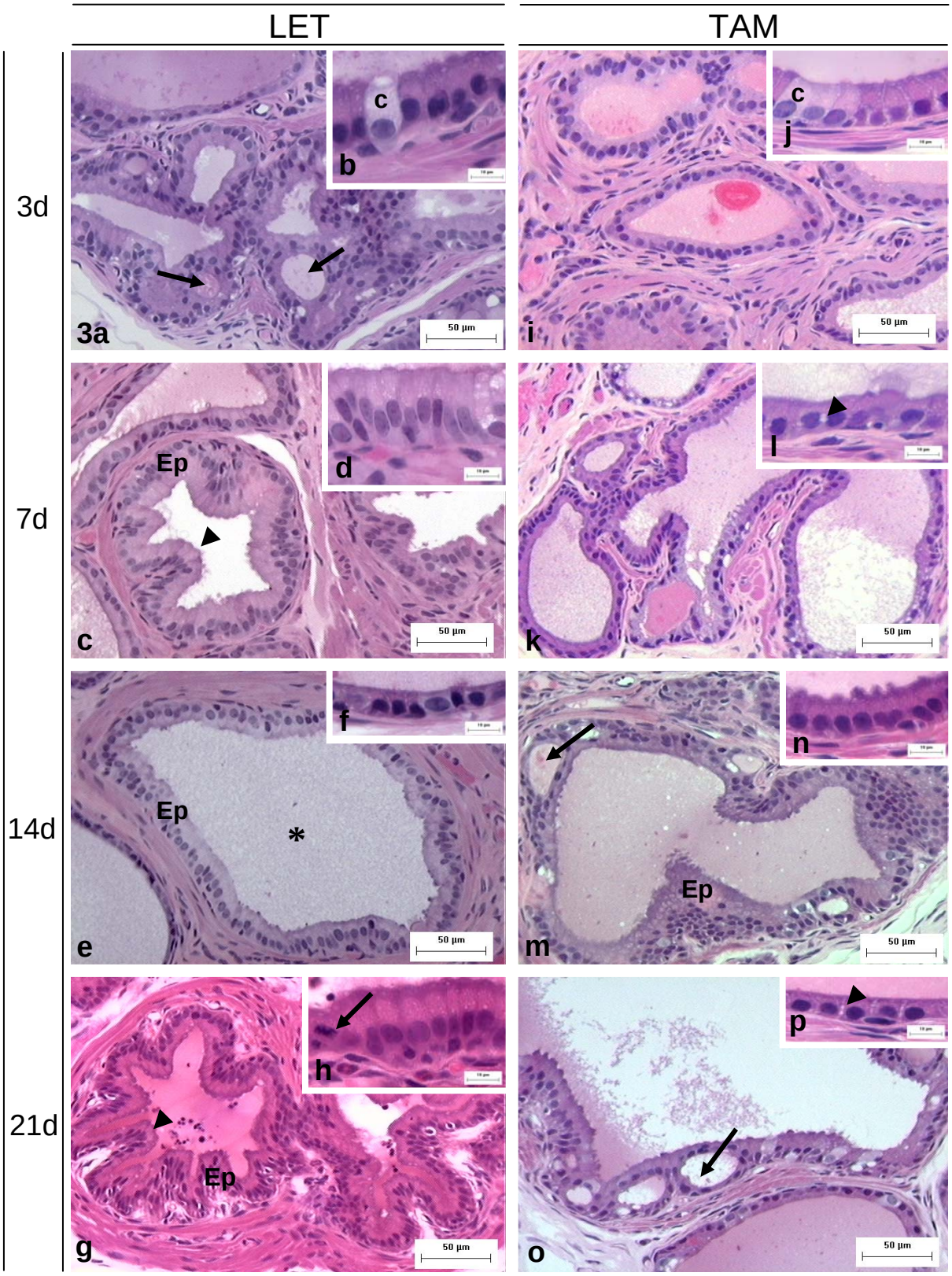
LET
TAM
3d
7d
14d
21d
3a
b
c
i
j
c
d
Ep
k
l
e
f
Ep
*
m
n
Ep
g
h
Ep
o
p
50 µm

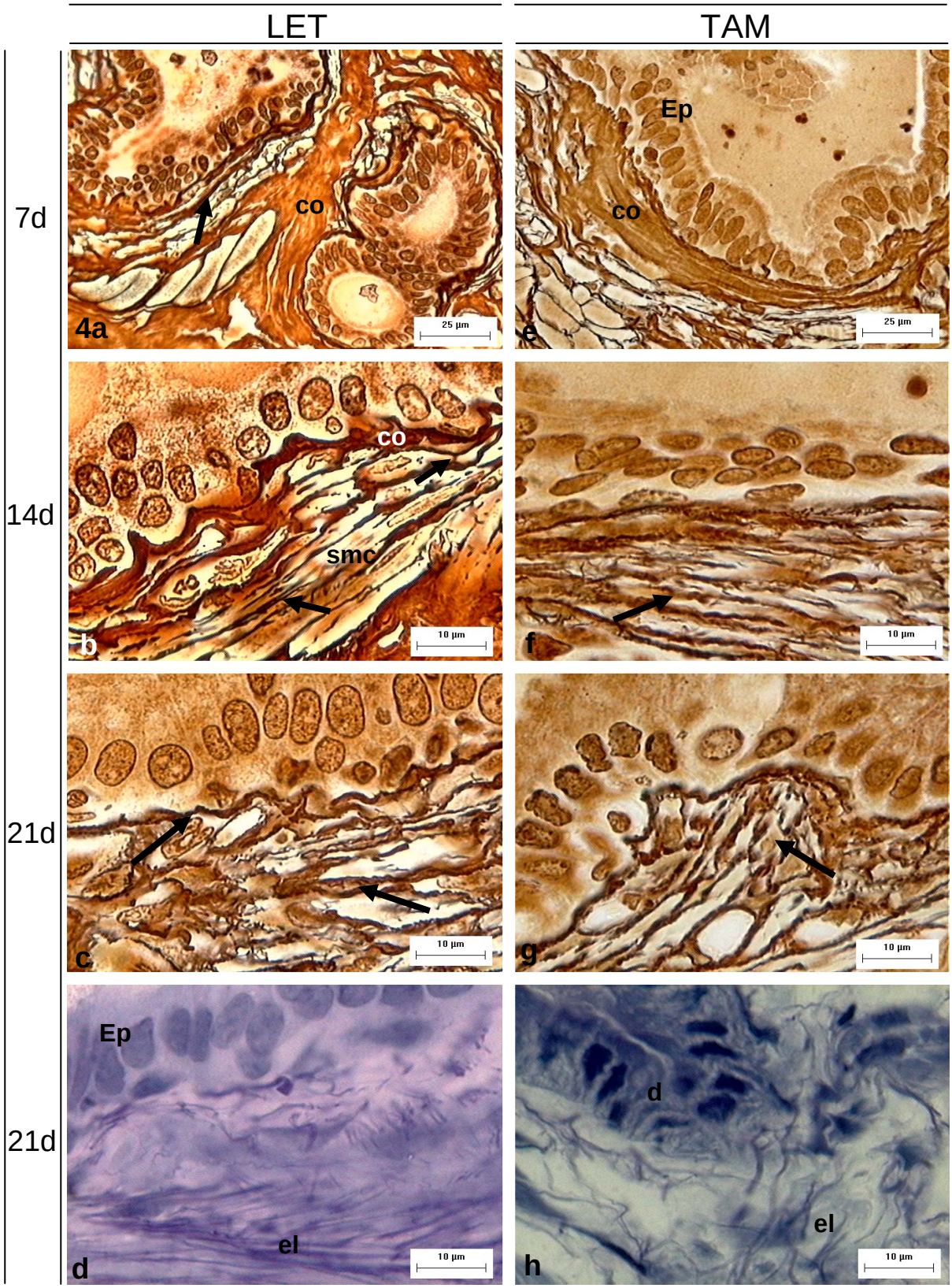
LET
TAM
7d
14d
21d
21d
co
Ep
co
4a
e
25 µm
co
smc
b
f
10 µm
c
g
10 µm
Ep
el
d
d
el
h
10 µm

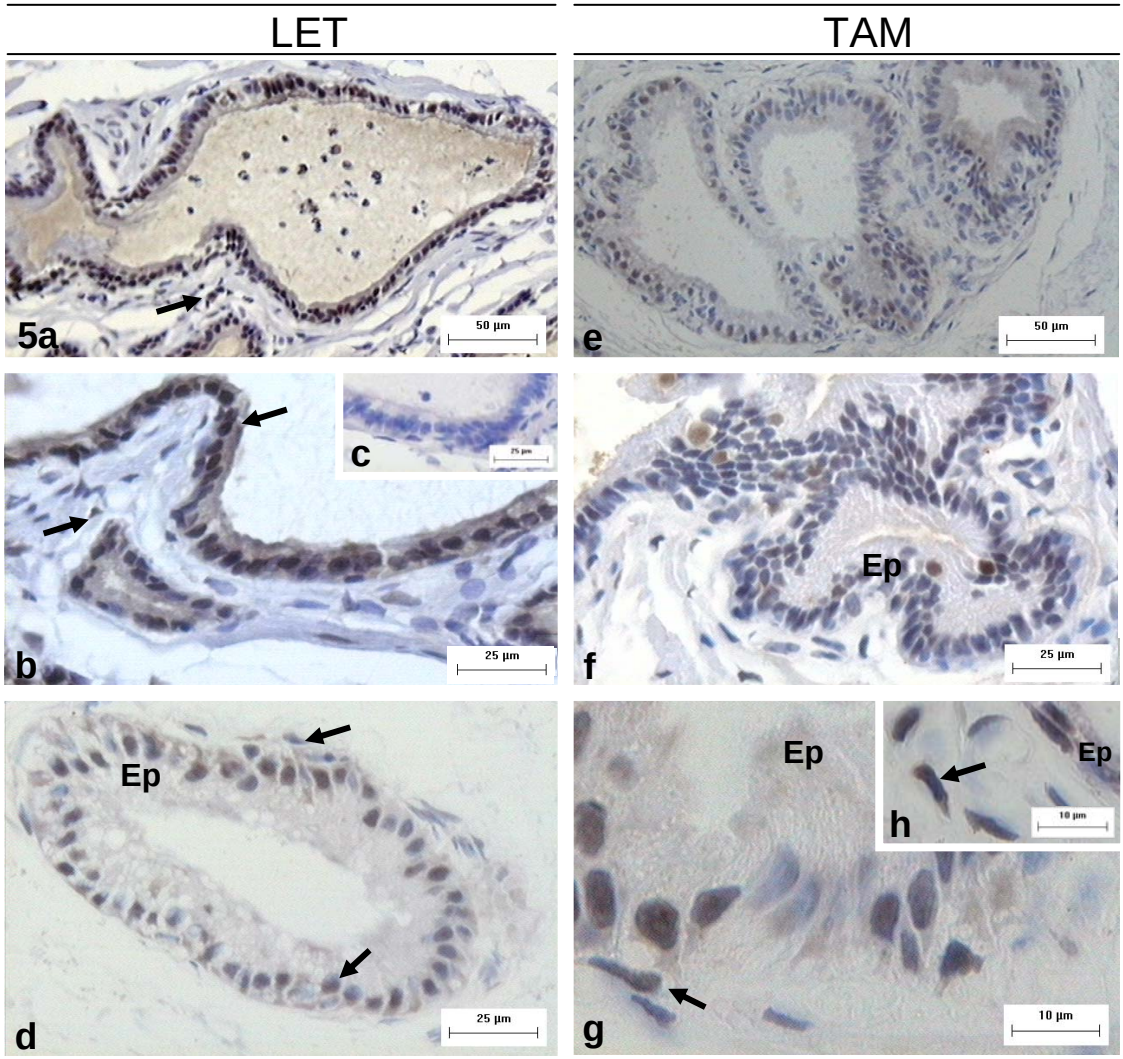
LET
TAM
5a
50 µm
e
50 µm
c
25 µm
b
25 µm
Ep
f
25 µm
Ep
d
25 µm
Ep
Ep
h
10 µm
g
10 µm

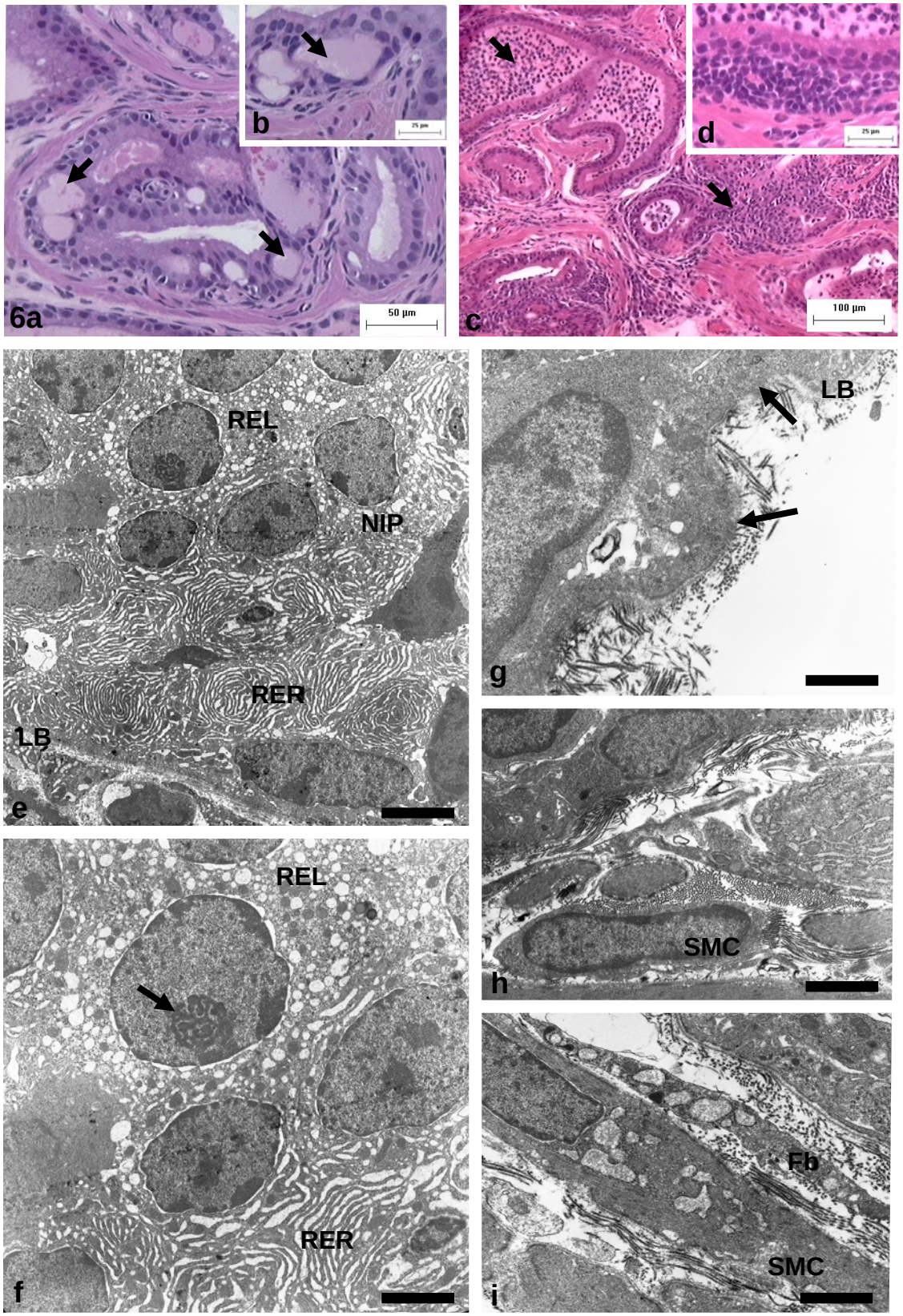
6a
50 µm
b
25 µm
c
100 µm
d
25 µm
REL
NIP
RER
LB
e
LB
g
REL
RER
f
SMC
h
Fb
SMC
i

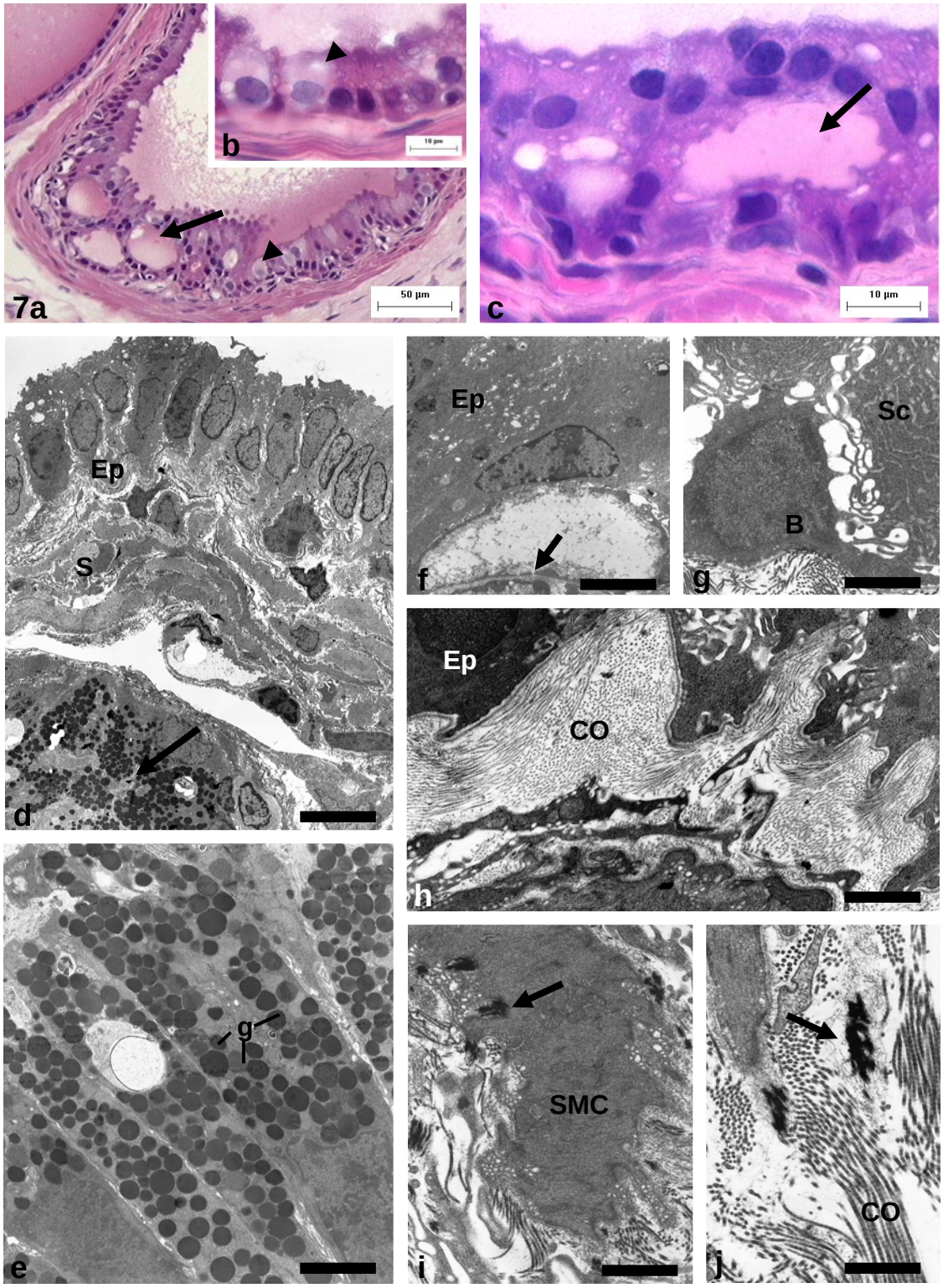
7a
50 µm
b
10 µm
c
10 µm
Ep
S
d
Ep
f
Sc
B
g
Ep
CO
h
g
e
SMC
i
CO
j

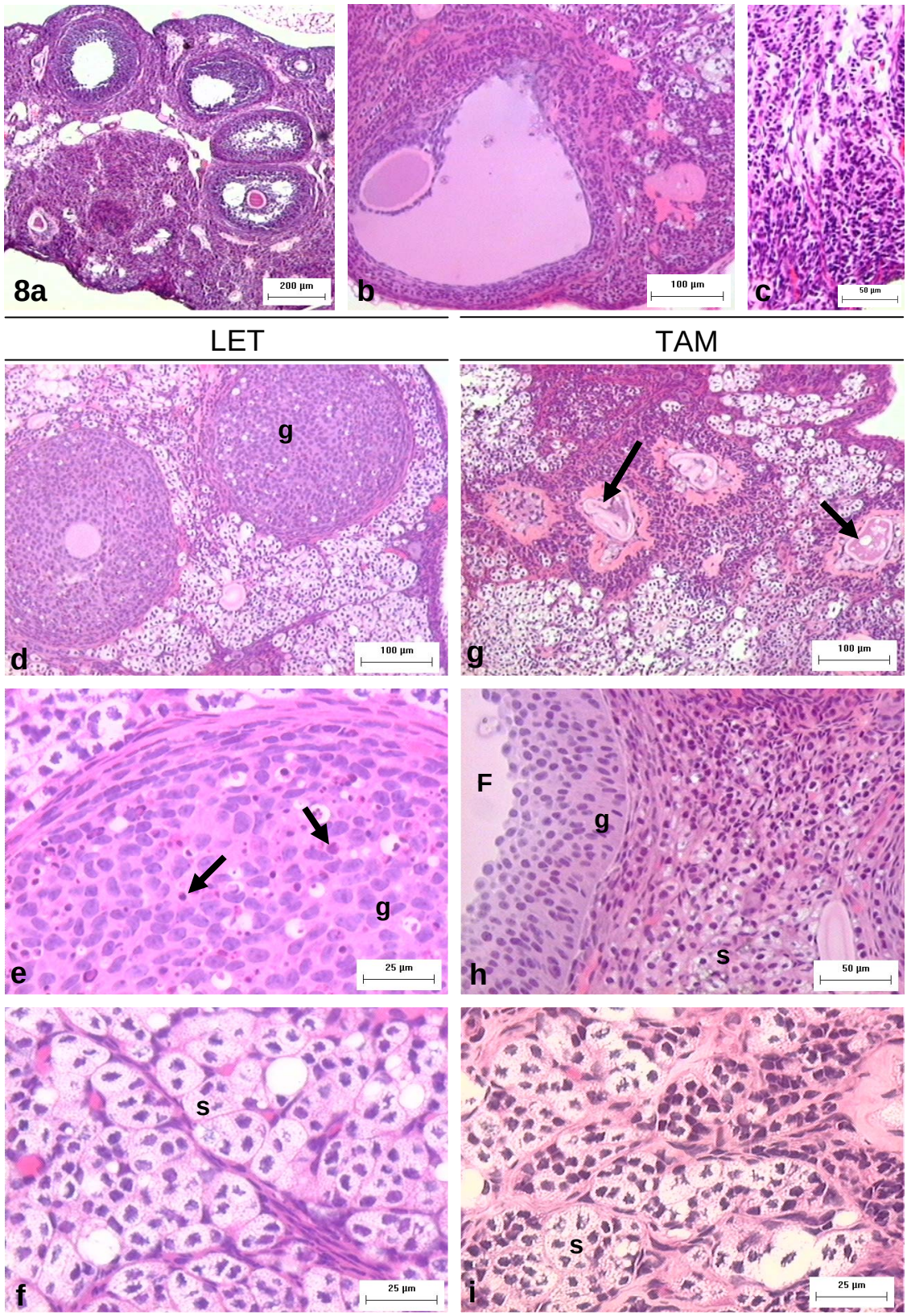
controle
8a
200 µm
b
100 µm
c
50 µm
LET
TAM
g
d
100 µm
g
100 µm
e
g
25 µm
F
g
s
h
50 µm
s
f
25 µm
s
i
25 µm

Artigo: Female prostate: a review of the biological repercussions of this gland in humans and rodents. Este trabalho foi aceito no periódico *Animal Reproduction* e será publicado no próximo volume da revista.

Anim. Reprod., v.3, n.1, p.3-18, Jan./Mar. 2006

Female prostate: a review about the biological repercussions of this gland in humans and rodents

F.C.A. Santos[1], S.R. Taboga[2,3]

[1]Department of Cell Biology, State University of Campinas - UNICAMP, Campinas, SP, Brazil.
[2]São Paulo State University, IBILCE/UNESP, Department of Biology, São José do Rio Preto, SP, Brazil.

Abstract

The prostate is not a gland exclusive to the male reproductive system since it is also found in females of several mammals, including humans and rodents. In males, prostatic morphogenesis is an event controlled by androgens, which act indirectly via paracrine factors secreted by the mesenchyme. In females, prostatic embryological development occurs in an environment without steroid hormones, but the presence of these hormones in an adult organism induces the differentiation and secretory activity of prostatic cells. The increasing interest in female prostate studies comes from its biological role in the production of prostatic fluid, which participates in the nutrition and maintenance processes of spermatozoa that are introduced into the female reproductive system and has the potential to cause benign and malignant lesions. In recent decades, the occurrences of prostatitis (Skeneitis), benign prostatic hyperplasia, and urethral adenocarcinoma in post-menopausal women have been common. The installation of these disorders in aged women seems to be associated with the hormonal imbalance caused by the failure of the ovaries to produce steroids. Experiments involving testosterone and anti-estrogen administration in female rodents have shown that the morphology and physiology of the female prostate are regulated by androgens and estrogens. While androgens induce the differentiation, development, and secretory activity of the gland, the estrogens appear to modulate the androgenic effects, maintaining the normal physiology and growth of the prostate. Long-term exposure to synthetic hormones (contraceptives and hormonal replacement drugs), which interferes with women's hormonal balance, can cause important changes in the female prostate morphophysiology. Thus, it is necessary to frequently monitor the female prostate in order to prevent prostatic disorders that can endanger the quality of life of women.

Keywords: female prostate, prostate morphogenesis, rodents, androgens, estrogens.

Introduction

Development of the female prostate in mammals has been reported since the seventeenth century (de Graaf, 1672). Studies in humans have shown that the female prostate plays an important role in the reproductive process and in sexual behavior (Zaviačič, 1999). Besides, frequent reports of urogenital system disorders, whose origin is the prostate, have increased the care and attention directed to this gland (Sharifi-Aghdas and Ghaderian, 2004; Kato *et al.*, 2005; McCluggage *et al.*, 2006). Although there are several works that describe the histological structure of the female human (Zaviačič, 1999) and rodent (Shehata, 1974; 1975; 1980; Gross and Didio, 1987; Flamini *et al.*, 2002) prostate, issues related to the function and physiology of this gland have been discussed only recently (Zaviačič *et al.*, 2000a; b; Santos *et al*., 2003a; Custódio *et al.*, 2004; Santos *et al.*, 2006). The objective of this work is to review the main studies on the female prostate, emphasizing the events that cause its embryological development as well as factors that control its function, physiology, and pathology during adult life.

Embryological development of the urogenital system

The developing urogenital tract contains epithelial structures of mesodermal (mesonephric or Wolffian duct and paramesonephric or Müllerian duct) and endodermal origin (urogenital sinus- UGS) that are associated with undifferentiated embryonic connective tissue known as the mesenchyme (Cunha *et al.*, 2002; Marker *et al.*, 2003; Staack *et al.*, 2003). The initial stages of gonadal development are identical in male and female embryos, and this phase is called the indifferent or ambisexual stage of sex differentiation. In mice, the male and female gonads become morphologically distinguishable only on Day 13 of gestation (Staack *et al.*, 2003). In male mice, after Day 13, the mesenchymal cells of the gonadal rudiment aggregate and condense into epithelial cords that become seminiferous tubules. After Day 14 of gestation, the Leydig cells of fetal testes differentiate and start to secrete testosterone (Pointis *et al.*, 1980). Testosterone prevents programmed cell death of mesonephric ducts and stimulates their development to form the epididymis, vas deferens, seminal vesicles, and efferent ducts. Meanwhile, the Sertoli cells initiate production of Müllerian inhibiting substance (MIS), which elicits regression of the paramesonephric ducts. In females, the fetal ovaries are relatively inactive endocrinologically

[3]Corresponding author: taboga@ibilce.unesp.br
Tel: +55 (17) 3221-2386; Fax: +55 (17) 3221-2390
Received: May 26, 2006
Accepted: August 8, 2006

and are not required for the development of the female urogenital system. When there is no androgenic stimulus, the mesonephric duct recedes, and in the absence of MIS, the paramesophrenic duct develops giving rise to the oviducts, uterine horns, cervical canal, and the upper portion of the vagina (Staack *et al.*, 2003).

The prostate develops from the UGS, which is an endodermal tube derived from the hindgut and ends in the cloaca. The urorectal septum subdivides the cloaca into the UGS ventrally and the rectum and anal canal dorsally. The cloaca subdivides in such a manner that the mesonephric and paramesonephric ducts terminate in the UGS. The UGS is further subdivided into the bladder and the definitive UGS. In mice, the two elements derived from the UGS are clearly distinguished on Day 13-14 of gestation (Staack *et al.*, 2003).

The UGS is composed of an epithelial layer (urogenital sinus epithelium; UGE), which is derived from the endoderm and surrounded by a mesenchymal layer (urogenital sinus mesenchyme; UGM) originated from the mesoderm. This structure is found in the neck of the developing bladder and it arises in both male and female mice and rats 13 days post conception and after 7 weeks of gestation in humans. The urogenital sinus is morphologically indistinguishable between males and females until about Day 17-18 of gestation in mice and not until Week 10-12 in humans. After that, prostatic morphogenesis, a process that is both initiated by and dependent on circulating androgens produced by the fetal testes, begins (Marker *et al.*, 2003).

In males, the initial event in prostatic morphogenesis is the outgrowth of solid epithelial buds from the UGE into the surrounding UGM. In rodents, most of the prostatic ducts are unbranched at birth. However in the neonate, as these ducts elongate within the UGM, they begin to bifurcate and emit lateral branches and give rise to three different prostatic lobes: the ventral prostate, dorsolateral prostate, and anterior prostate or coagulating gland (Marker *et al.*, 2003). The process of ductal branching morphogenesis occurs simultaneously with ductal canalization (lumen formation) and epithelial and stromal cytodifferentiation (Wang *et al.*, 2001).

Prostatic morphogenesis is dependent on steroid hormones. Androgens are necessary to initiate prostatic development, to continue embryonic and neonatal growth, and then to start prostatic secretory activity during puberty (Isaacs *et al.*, 1994). However, the androgenic action is not exerted directly on the epithelial cells. Under the influence of androgens, the mesenchymal cells produce and secrete specific paracrine factors that control growth and prostatic gland differentiation. Hence, with epithelial cell differentiation, the levels of androgenic receptors (AR) increase, and the expression of epithelial estrogenic receptors (ERβ) and stromal estrogenic receptors (ERα) is induced.

Mesenchymal-epithelial interactions play a key role in directing the growth and development of the prostate because the mesenchymal paracrine signaling to the epithelium is essential to prostatic embryogenesis. Thus, androgen action on the mesenchymal cells results in specific paracrine factors that act on the epithelial cells inducing their proliferation (Thomson *et al.*, 2001). On the other hand, there is also a paracrine signal from the epithelium to the mesenchyme. This signal regulates the differentiation of the mesenchyme that surrounds the growing buds in a stroma composed of smooth muscle cells and fibroblasts (Hayward *et al.*, 1996). Hence, during prostatic morphogenesis, the AR is necessary to the mesenchyme but not to the epithelium since its expression precedes prostatic bud development. In the epithelial cells, AR function is limited to the regulation of secretory proteins and perhaps cellular differentiation (Donjacour and Cunha, 1993).

Among the paracrine factors that interfere with prostatic morphogenesis, it is relevant to mention the family of homeobox transcription factors NKx3.1, Hoxa-13, Hoxb-13 and Hoxd-13, fibroblast growth factors FGF-7 and -10 (Huang *et al.*, 2004), the glycoprotein Sonic hedgehog (Shh), the Shh receptor, patch (ptc), transcription factors of the family Gli, and BMP-4 (Pu *et al.*, 2004). The NKx3.1 gene is expressed in the urogenital sinus epithelium (UGE) before the beginning of prostatic budding and it seems to play a role in epithelial differentiation and in prostatic development, mainly during the epithelial cell determination process in this gland (Bieberich *et al.*, 1996). Hoxa-13, Hoxb-13, and Hoxd-13 are expressed in the urogenital sinus mesenchyme (UGM), and they are involved in prostatic development. These factors are expressed at high levels during fetal life, but their levels decline postnatally. FGF-10 and FGF-7 are produced by the UGM cells and interact with a unique receptor, FGFR2iiib, which is expressed by the UGE cells. Together, these factors play a critical role in the expansion and branching of the prostatic buds (Huang *et al.*, 2004). Shh glycoprotein is secreted by the UGE cells in the mesenchymal interface of the developing prostate, activating its receptor patch (ptc), which is expressed in the mesenchymal cells. The Shh-ptc complex triggers a cascade of molecular signals that increase the levels of the *gli* transcription factors, which mediate the Shh effects. In vertebrates, there are three types of *gli* transcripts (*gli*-1, -2, -3) that are redundant and share one function. It is believed that the Shh gene participates in budding initiation and prostatic expansion. Furthermore, Shh seems to regulate many other genes involved in prostatic development, including Hoxa-13, Hoxd-13, and NKx3.1 (Pu *et al.*, 2004). The bone morphogenetic proteins (BMP-4) are members of the transforming growth factor-β (TGF-β) family, and in general, act as inhibitors of proliferation during prostate development. In the mouse prostate, BMP-4 mRNA is localized in the mesenchyme, and its levels decline postnatally. In Fig. 1, a model is proposed in which these paracrine factors act to direct rodent prostatic morphogenesis during the postnatal period (Huang *et al.*, 2004).

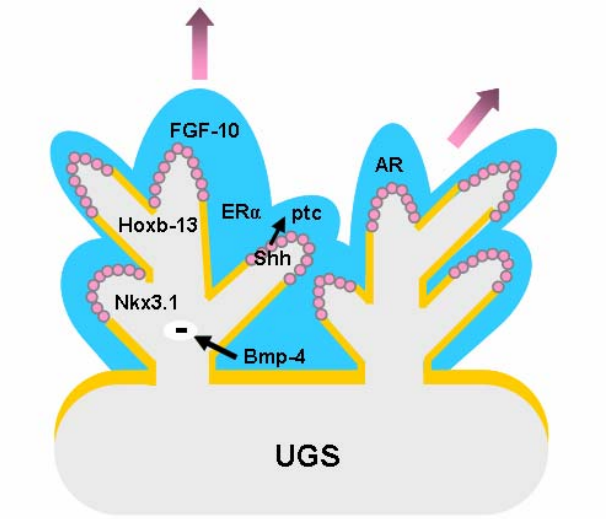

Figure 1. In a normal male prostate, androgen receptor AR and estrogen alpha receptor ERα expression occurs in the stromal cells (blue) located near the outgrowing prostatic buds (grey). Bmp-4 expression, which is high before prostate budding, declines rapidly after birth, releases its inhibitory effects on ductal outgrowth. Shh is secreted by distal tip epithelial cells (pink), activates ptc receptors on adjacent stromal cells, and participates in ductal outgrowth and prostatic differentiation. Fibroblast growth factor (FGF)-10 is expressed by distal mesenchymal cells and stimulates ductal outgrowth and branching. NKx3.1 is expressed early by undifferentiated epithelial cells and is involved in initiation of prostate development and epithelial differentiation. Hoxb-13 is expressed in epithelial cells and is involved in maintaining a differentiated phenotype. The smooth muscle layer is shown in yellow (adapted from Huang *et al.*, 2004).

In female human and rat embryos, the absence of testosterone induces the UGS to give rise to the lower vagina and the urethra (Shapiro *et al.*, 2004). The UGM starts to surround the urethral epithelium and is subdivided into three areas: the periurethral mesenchyme, the mesenchymal zone that undergoes smooth muscle differentiation, and the mesenchymal zone that contains the ventral mesenchymal pad (VMP). The latter structure has a localization analogous to the male ventral prostate and represents the UGM without the invasion of the UGE (Thomson *et al.*, 2002). The differentiation of a part of the UGM in smooth muscle is crucial to prostatic morphogenesis in both males and females since this event regulates paracrine signaling between the epithelium and the mesenchyme (Thomson *et al.*, 2002).

During mesenchyme differentiation, androgens regulate the thickness and continuity of the smooth muscle layer in such a way that the absence of androgens in female embryos causes the formation of a continuous, thick muscle layer. This layer separates the VMP from the urethral epithelium, preventing the prostatic epithelial buds that are arising in the urethra from making direct contact with the VMP. Hence, the dense layer of smooth muscle prevents the interaction of VMP with the growing prostatic buds, blocking the paracrine communication between the epithelium and mesenchyme (Thomson *et al.*, 2002). In males, with the presence of androgens, the formation of smooth muscles is inhibited or delayed, and the prostatic buds emerge out of the urethra and can penetrate the VMP. Henceforth, the mesenchyme-epithelial paracrine interaction is established and causes branching and outgrowth of the ventral prostate. The illustrative model of prostatic induction in males and females was proposed by Thomson and co-workers and is shown in Fig. 2.

The formation of prostatic buds is a constitutive process in males and females, but the branching and outgrowth of these buds is regulated by androgens. In females, the separation between the VMP and the urethral epithelium, which is caused by the smooth muscle layer, prevents the formation of a fully-developed and lobulated prostatic gland. Then, the reduced prostatic tissue observed in females of several species is formed from the UGS, which has not suffered any androgenic stimulus. Although the adult female prostate is smaller than the male prostate (about 15% - 25% of the size of a ventral male prostate), it has a differentiated and functional secretory epithelium (Zaviačič *et al.*, 2000a; Santos *et al.*, 2003a; Custódio *et al.*, 2004). As the female prostate grows and develops in an environment with low levels of androgens (only 5% of the total androgenic precursors produced in the male organism), it is believed that factors other than these hormones can act in the development and maintenance of this gland in adults (Timms *et al.*, 1999).

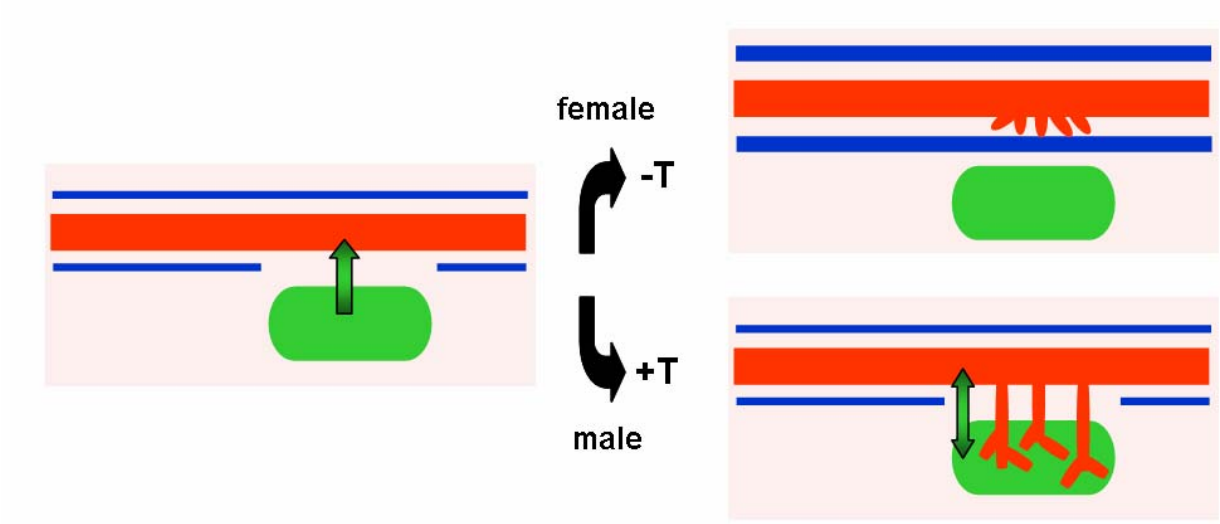

Figure 2. Descriptive model of ventral prostatic development in female and male rat embryos. On the left side, the ventral mesenchymal pad (VMP; green) is shown during the initial phases of prostatic induction (Days 17-18 of gestation). Observe that the smooth muscle layer (blue) is discontinuous and it allows signaling between the VMP and the urethral epithelium (red). On the right side, prostatic morphogenesis is shown in males and females (after Day 21.5 of gestation). In females, the absence of testosterone allows the smooth muscle to form a thick and continuous layer, preventing paracrine signaling between the outgrowing prostatic buds (red) and the VMP. In males, testosterone induces the formation of a thin and discontinuous muscle layer that allows the epithelial-mesenchymal interaction. Emerging urethral-epithelial buds (red) penetrate the VMP. In the neonate, these buds undergo side branching inside the VMP, giving rise to the ventral prostate (adapted from Thomson *et al*., 2002).

The developmental frequency of a functional prostate gland in females is very high. In humans, about 90% of women develop mature prostatic tissue that is active in secretory processes (Zaviačič *et al.*, 2000b). In rodent females, prostatic morphogenesis seems to be influenced by the intrauterine position of the animals during gestation (Clark *et al.*, 1991; Timms *et al.*, 1999). Thus, in the female rat fetus, the development of prostatic buds is more frequent when gestation occurs with twin female fetuses (67%) but rarely occurs between two males (29%). This occurs because animals bearing two female or two male fetuses have natural differences in testosterone (T) and estrogen (E) levels. Females bearing two female fetuses have higher levels of E, which is the hormone responsible for modulating the effects of androgens on the developing prostate and induces larger growth of prostatic buds during glandular morphogenesis (Timms *et al.*, 1999).

Female prostate: new concepts and change of paradigms

The first report of the "female prostate" occurred in 1672 when Reinier de Graaf used this term to describe a set of glands located around the urethra, which according to him, had considerable homology with the male prostate (de Graaf, 1672). Two centuries later, Alexander Skene described the female prostate as being formed by two paraurethral ducts that open into orifices on both sides of the urethra and as having limited underprovided secretory function (Skene, 1880). Since then, this set of glands has been called "Skene's paraurethral glands." For a long time, this gland was considered a vestigial organ without any biological importance to the female organism (Zaviačič and Ablin, 2000). However, since 1950, new studies have discussed the female prostate, mainly in relation to the biological role that this organ could have in woman (Huffman, 1948; 1951; McCrea, 1952; Tepper *et al.*, 1984; Wernet et *al.*, 1992; Zaviačič, 1993; Zaviačič *et al.*, 1993; 1997a; b; 2000a; b). One of the main works about the female prostate, which describes the human female prostate and investigates its structural and functional aspects as well as its sexological implications, is the research developed by Zaviačič *et al.* (1999).

Zaviačič presents the human female prostate as a paraurethral set of numerous glands and ducts that are inserted into a fibromuscular stroma (Zaviačič *et al.*, 2000a). The glands are lined by differentiated and mature epithelium that has two main cell types: the basal cells, which are stem cells responsible for the maintenance of the prostatic cell population; and the secretory or luminal cells that continually produce the prostatic fluid (Zaviačič *et al.*, 2000b). The luminal cells are the most numerous ones and express the prostate-specific antigen (PSA) and the prostate specific acid phosphatase (PSAP), two important prostate markers (Zaviačič *et al.*, 1993).

Together with the studies of the human female

prostate, many studies have demonstrated the occurrence of a prostate in females of several rodents species such as *Praomys natalensis* (Smith *et al.*, 1978; Gross and Didio, 1987), *Rattus novergicus* (Shehata, 1980; Vilamaior *et al.*, 2005), *Lagostomus maximus maximus* (Flamini *et al.*, 2002), *Meriones libycus* (Shehata, 1974; 1975), and *Meriones unguiculatus* (Santos *et al.*, 2003a; Custódio *et al.*, 2004). Furthermore, the morphological characteristics presented by these works indicate that the prostate of the females of these species is equivalent to the male ventral prostate and that its epithelial cells show a functional phenotype.

Until now, the biological role of prostate development in the female organism has not been clear. Biochemical studies demonstrated that prostatic fluid released during female ejaculation has the same chemical composition as male prostatic fluid. The more abundant components of the human female ejaculate are PSA, PSAP, zinc, and fructose (Zaviačič, 1993; 1999). Evidence indicates that the fructose produced by this gland flows in a small amount from the urethra to the vagina and plays an important role in reproduction. Thus, since fructose is the main source of energy for spermatozoa, female prostatic fluid also contributes to the success of fertilization. Recent studies have detected levels of PSA in the serum and in the urine of women (Zaviačič and Ablin, 2000; Schmidt *et al.*, 2001). These works have indicated that the prostate is the main producer of PSA in females although there are other extraprostatic sources (Diamandis and Yu, 1997; Yu and Berkel, 1999; Galadari *et al.*, 2004; Kocak, 2004; Sauter *et al.*, 2004).

Another area of exploration for the possible functions of the female prostate is its importance to female sexual ~~behavior manifestation~~ sensitization?? (Zaviačič, 1993). A few reports have associated the female prostate with the Gräfenberg spot (G-spot), emphasizing the relevance of stimulus of this spot in order to produce the phenomenon of female ejaculation (Schubach, 2002). According to Gräfenberg, the G-spot refers to an "area" or "zone" richly innervated in the upper-anterior wall of the vagina through which the female prostate can be accessed (Gräfenberg, 1950). However, controversial articles have maintained that the female prostate and the G-spot are the same structure (Addiego *et al.*, 1981; Hines, 2001).

In addition to the biological and behavioral implications mentioned above, the main focus of interest about the female prostate comes from its capacity of developing severe lesions during aging. Recent works have described the occurrence of cancers of the urethra, whose origin is the female prostate (Dodson *et al.*, 1994, 1995; Ali *et al.*, 1995; Ebisuno *et al.*, 1995; Sloboda *et al.*, 1998; Islam *et al.*, 2001; Sharifi-Aghdas and Ghaderian, 2004; Kato *et al.*, 2005; McCluggage *et al.*, 2006). Furthermore, there is evidence that other prostatic pathologies, such as prostatitis and benign prostatic hyperplasia, can occur in the female prostate with the same level of severity observed in the male prostate (Zaviačič, 1999). Acute cystitis is the most common form of infection of the female urinary system, and the incidence of this lesion in young women in the USA is from 0.5-0.7 episodes per person per year. Currently, it is known that the origin of this cystitis is the female prostate. When the inflammation of the prostate occurs (prostatitis or Skeneitis) it disseminates throughout the entire female reproductive system resulting in urethro-prostato-cystitis (Zaviačič, 1999). This phenomenon occurs due to communication of the system of prostatic glands with the urethra and the anterior wall of the vagina.

Based on the information stated above, it is impossible to consider the female prostate an insignificant vestigial organ, and thus, the definition of Skene must be reassessed. In spite of the fact that the female prostate has smaller dimensions compared to the male prostate, it is active in secretory processes and requires the same attention as any other organ in the female organism because alterations in its physiology can endanger the health and quality of life of women. Hence, studies that elucidate the processes that maintain homeostasis of this gland are necessary because little is known about the physiological events that preserve the functionality of the female prostate in normal as well as in pathological conditions.

Female prostate: experiments with rodents

The morphology and function of the human female prostate has been described by many researchers in collaboration with Dr. Milan Zaviačič (Zaviačič, 1993; Zaviačič *et al.*, 1993; Zaviačič *et al.*, 1997a; b Zaviačič, 1999; Zaviačič and Ablin, 2000; Zaviačič *et al.*, 2000a; b). In the rodent, the female prostate has been described by many researchers (Shehata, 1974; 1975; 1980; Gross and Didio, 1987; Flamini *et al.*, 2002); however, none of these works has investigated the mechanisms that control the function of the female prostate gland. The experiments with human female prostatic tissue are very limited because the female prostate can only be obtained through necropsies of women who suffered cerebral death (Zaviačič, 2000a). Hence, it is necessary to adopt experimental models that use a prostatic gland similar to the human female prostate in order to extrapolate the data to the human species.

Our research group has adopted the Mongolian gerbil (*Meriones unguiculatus*, Gerbilinae, Muridae) as an experimental model because the female prostate of this rodent has great homology with the human female prostate and the male gerbil ventral prostate (Taboga *et al.*, 2001). In addition, the occurrence of prostates in females of these animals is very common since we can find a fully developed gland in 80% of the adult females studied.

Anatomically, the female gerbil prostate is composed of a cluster of glands and ducts that are

concentrated in both sides of the median urethra (Fig. 3A-C). The ducts insert into the urethra musculature and open into various areas of the urethral lumen. The secretory portion of the adult female prostate of the gerbil is lined with an epithelium that varies from simple cubic to columnar pseudostratified (Fig. 4A). The epithelial cells consist of two types: the basal cells, which form a discontinuous layer of stem cells for the maintenance of prostatic growth (Fig. 4A); and the secretory cells, which have a cytoplasm rich in organelles involved in the process of synthesis and secretion of glycoproteins (Fig. 4A, D, E). The secretory cells express proteins reactive to human anti-PSA antibodies in their apical portion (Fig. 4B) and strong immunostaining to PSAP througout the cytoplasm (Fig. 4C). Levels of PSA-like protein can also be detected in the serum of these animals (levels of PSA serum in adult females: 0.1-1.3 ng/ml; Santos *et al.*, 2006) and have values close to the ones observed in adult women (0.1-0.9 ng/ml; Zaviačič and Ablin, 2000; Schmidt *et al.*, 2001).

Immunocytochemical studies have shown that the female gerbil prostate expresses receptors for two important steroid hormones, estrogen and testosterone. The secretory epithelial cells (Fig. 5A, B) and fibroblasts (Fig. 5A, C) test positive for androgen receptors (AR). The estrogen alpha receptor (ERα), which is often expressed in stromal cells of human and rodent males (Prins *et al.*, 2001; Rovuele *et al.*, 2001; Omoto *et al.*, 2005), has also been detected in the epithelial secretory cells (Fig. 5D-F). The occurrence of ER α-positive epithelial cells seems to be associated with the development of prostatic hyperplasia and metaplasia. It has also been described in the human prostatic epithelium (Härkönen and Mäkelä, 2004).

The prostatic glands and ducts are associated with a fibromuscular stroma, which is rich in cells, fibers, and blood vessels (Santos *et al.*, 2001). Reticular fibers and collagen fibers are observed in the basal epithelium, always in association with the smooth muscle cells (Fig. 6A, B). Ultrastructurally, smooth muscle cells have a large nucleus, around which there is a considerable cluster of organelles (Fig. 6C). Bundles of collagen fibers are abundant and observed near the smooth muscle cells while elastic fibers are very scarce (Fig. 6C).

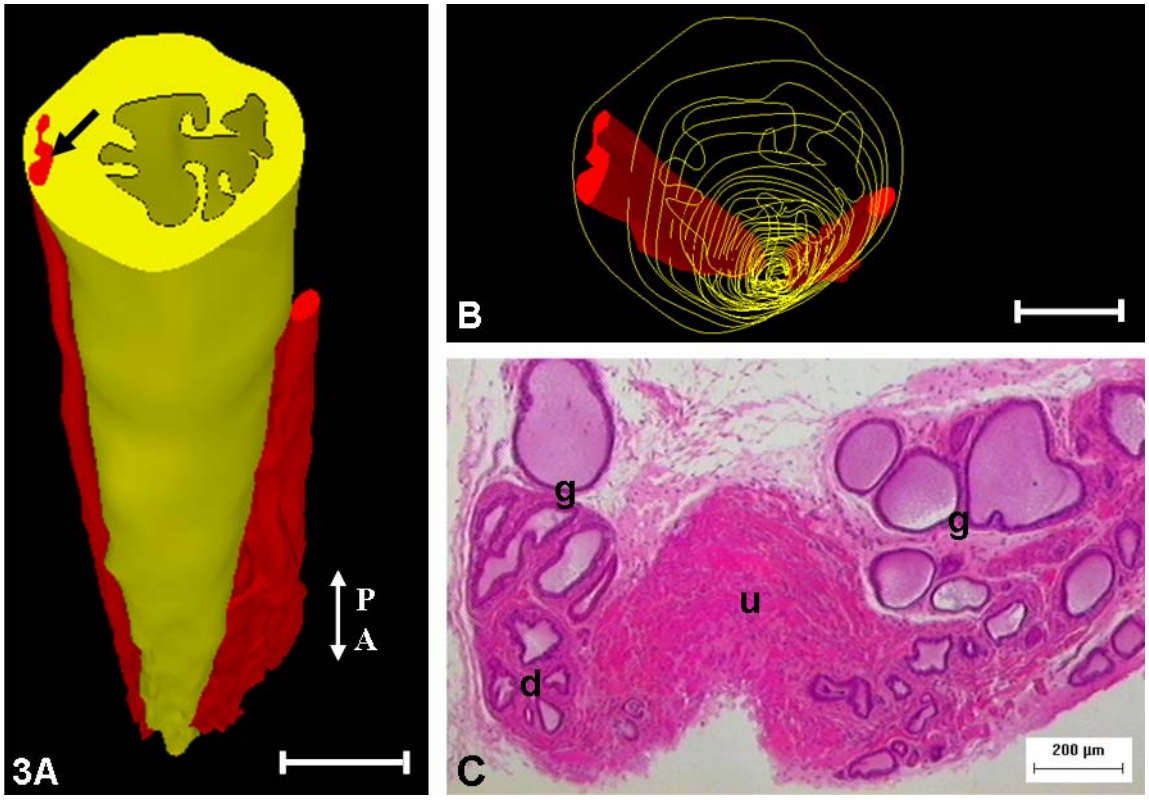

Figura 3. Three-dimensional reconstruction of the adult female gerbil prostate (*Meriones unguiculatus*) in longitudinal (**A**) and transversal (**B**) views. The prostatic urethra (yellow), prostate ducts, and alveoli (red) are shown. The double arrow indicates the gland orientation relative to the anterior (A) and posterior (P) urethra. Ducts that insert into the urethral musculature (arrows) are also shown. **C**: histological sections of the female prostate are shown in addition to the ducts (d) and prostatic alveoli (g) orientation relative to the prostatic urethra (u). (Bar = a: 25 µm, b: 20 µm).

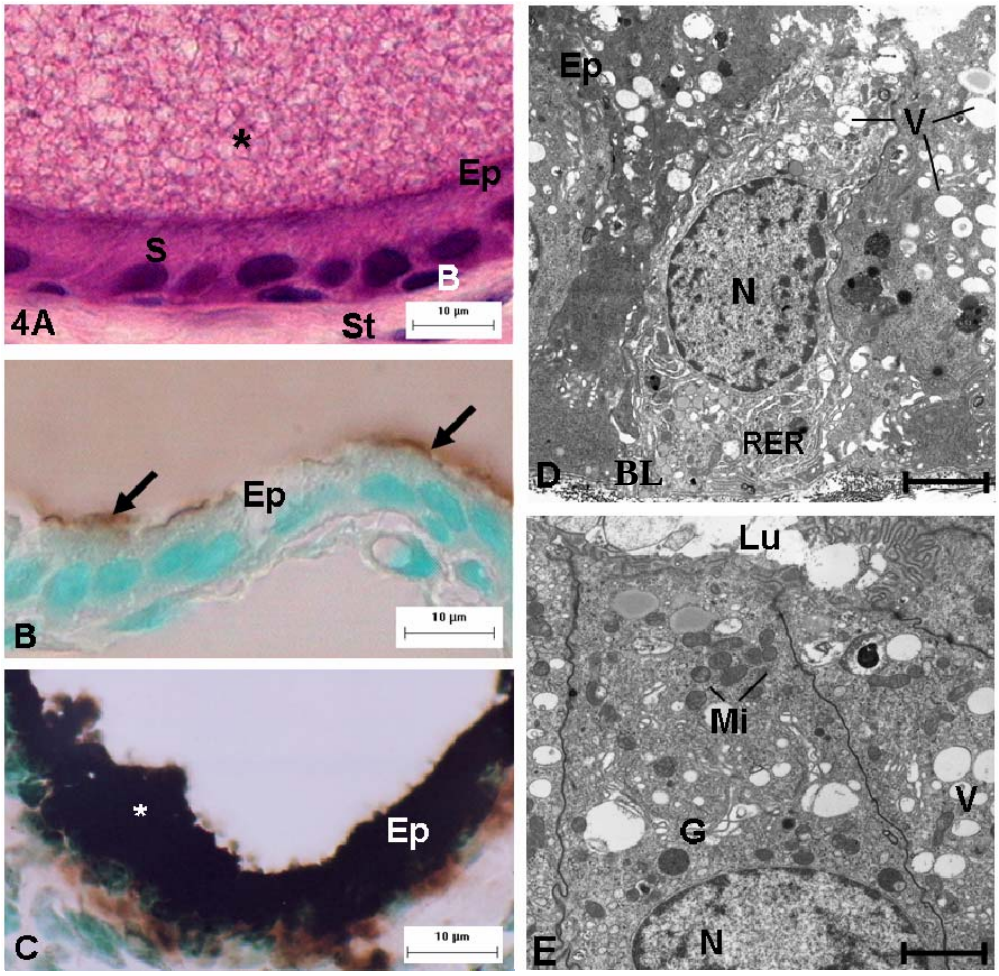

Figure 4. **A**: detail of the secretory epithelium (Ep) stained using the hematoxylin-eosin method. Secretory cells (S), basal cells (B), stroma (St), and secretion (*) are shown. **B**: prostate specific antigen (PSA) expression in apical portion (arrows) of secretory epithelium (Ep) counterstained with Methyl-Green. **C**: cryosection of the adult female prostate showing a positive reaction for prostate specific acid phosphatase (PSAP) counterstained with Methyl-Green (*). **D**: epithelial ultrastructure (Ep) showing the secretory cells with large nuclei (N) and cytoplasm with a fully-developed rough endoplasmatic reticulum (RER) and secretory vesicles (V). (basement lamina, BL; Bar = 2 µm) **E**: detail of the apical portion of a secretory cell where it is possible to observe mitochondria (Mi), the Golgi complex (G), and secretory vesicles (V). (lumen, Lu; nuclei, N; Bar = 1.4 µm).

Recently in our laboratory, we conducted preliminary studies on the female prostate of *Wistar* rats (*Rattus novegicus;* Vilamaior *et al.*, 2005). The first results showed that the prostate of adult female rats have morphology similar to the ventral prostate lobe of young male rats (Fig. 7A-C). In these females, the gland is characterized by alveoli with an underdeveloped lumen and stroma full of smooth muscle cells, fibroblasts, and fibrous elements of that extracellular matrix. The epithelium is lined by cells that vary from cubic to columnar and sometimes have some buds. In the luminal compartment, a small development can be present with scarce secretion in its interior (Fig. 7B). These results refute several data from the current literature that suggest that in rat and mouse females, total involution of the mesenchymal and endodermic tissues, which would give rise to the gland during prostatic morphogenesis, occurs (Thomson, 2001; Thomson et al., 2002; Marker et al., 2003). These reports evidence that testosterone is a key component of prostatic morphogenesis, and its absence during female embryonic development results in the formation of vestiges insufficient for any functional role. However, according to our observations, one can infer that this gland possesses moderate secretory capacity although it does not show a level of development as accentuated as that of the female gerbil prostate (Santos *et al.*, 2005).

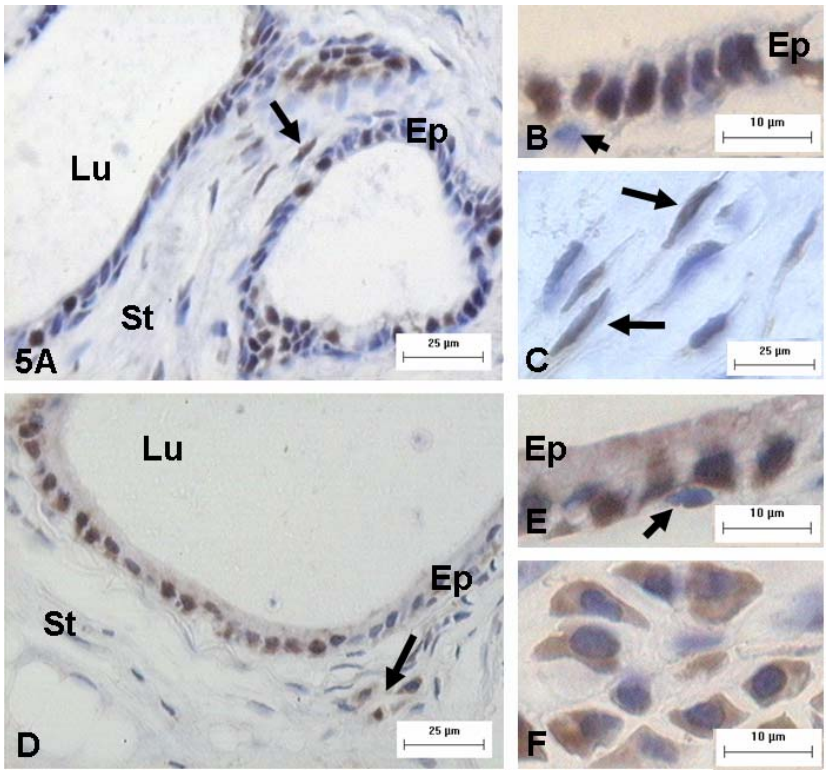

Figure 5. Immunocytochemical identification of the androgen receptor (AR**; A-C**) and estrogen receptor alpha (ERα**; D-F**) in a control female prostate counterstained with Harris's hematoxylin. **A**: strong staining is observed in the secretory epithelial cell nuclei (Ep) and in fibroblasts (arrows). (stroma, St; lumen, Lu). **B**: epithelial basal cells (Ep) are AR-negative (arrow). **C**: detail of fibroblasts with an AR-positive stain. **D**: ERα-positive stain is observed in epithelial secretory cells (Ep) and in the nucleus and cytoplasm of stromal cells (arrows). **E**: detail of the secretory epithelium (Ep) showing that basal cells (arrows) do not express ERα. **F**: a cluster of stromal cells showing intense cytoplasmatic and nuclear ERα staining.

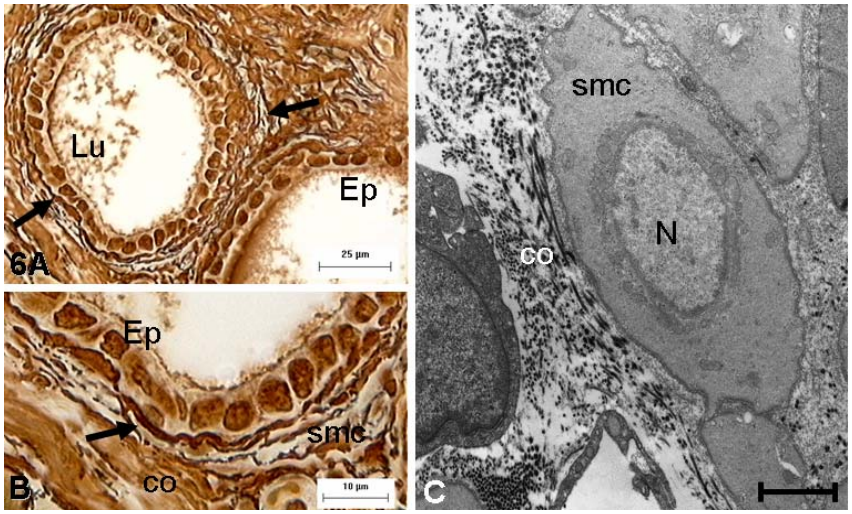

Figure 6. **A** and **B**: histological sections of the female gerbil prostate stained with Gömöri's reticulin. The reticular fiber network is stained in brown (arrows). Epithelium (Ep), lumen (Lu), collagen (co), and smooth muscle cells (smc). **C**: ultrastruture of the prostatic stroma showing smooth muscle cells (smc) and their association with collagen fibers (co). (nucleus, N; Bar = 1.4 µm).

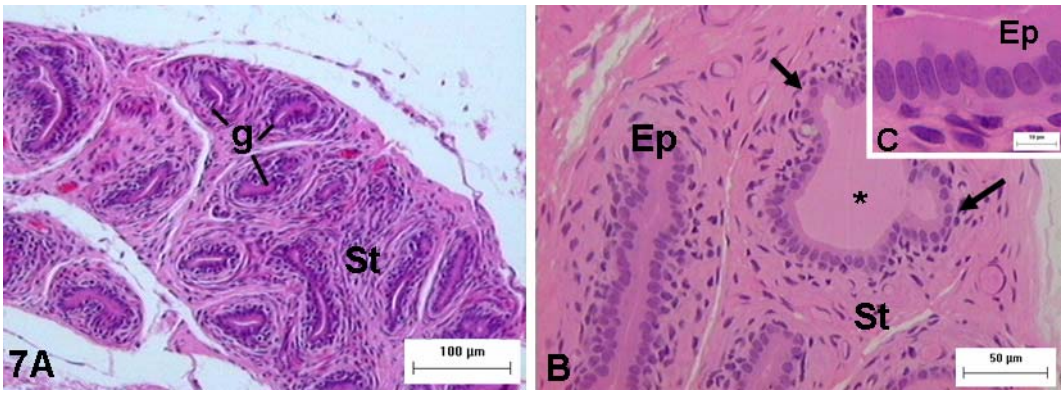

Figure 7. Histological sections of the adult female prostate of a *Wistar* rat (*Rattus novergicus*) stained with hematoxylin-eosin. **A**: the secretory portion of the gland is underdeveloped (g) and lines a reduced lumen. The stroma (St) is dense with a large amount of cells. **B**: prostatic alveoli with epithelial branching (arrows) and the reduced glandular lumen full of secretion (*). Stromal cells are displayed near the alveoli (St). **C**: simple columnar epithelium showing secretory cells with a large nucleus and cytoplasm.

The morphofunctional characteristics of the adult female prostate of gerbils and *Wistar* rats indicate that the growth and the activity of this gland are maintained in an environment with low androgen levels (serum testosterone levels in adult female gerbil: 0.4 – 2.7 ng/ml; Santos *et al.*, 2006). Thus, it is believed that other factors such as estrogen, for example, play an important role in physiological regulation of the prostate. Hence, it is fundamental to understand the elements that regulate the differentiation, growth, and secretion of female prostate because alterations in these events can cause lesions. That is the reason why we have developed additional experiments related to hormonal treatment of gerbil and rat female prostates, and the results obtained are outlined briefly in the following section.

Hormonal regulation of rodent female prostate

Androgenic effects on the gerbil and rat adult female prostate

Although the gerbil and *Wistar* rat adult female prostates present different levels of glandular development, both respond in a similar way to treatment with androgens. Experimental treatment of adult female gerbils with testosterone cypionate (T) for 21 days (Santos *et al.*, 2003b; Leite *et al.*, 2004) showed that this steroid hormone exercises a biphasic effect on prostatic regulation (Santos *et al.*, 2006). Initially, there was copious cellular proliferation that caused glandular growth (Fig. 8A-B). After the first 7 days of treatment, the prostatic gland showed great secretory activity that caused an increment in the luminal area. Neoplastic intraepithelial foci with pseudocribiform architecture were also observed, thus indicating that T administration can cause important tissue disruptions in the female gerbil prostate. Serologic data from this experiment showed that serum testosterone levels in the treated females increased in some cases to 12 times greater than the levels observed in untreated females (1.6 ng/ml in control females and up to 18.9 ng/ml in T-treated females); however, the serum estrogen levels were not altered significantly during the treatment (Santos *et al.*, 2006).

Initial results obtained in experiments with *Wistar* rat females (Vilamaior *et al.*, 2005) indicate that the pattern of prostatic response to treatment with T is similar to that in female gerbils. Nevertheless, because the prostate of untreated female rats is underdeveloped compared to female gerbils, the glandular alterations became evident during the first 3 days of hormonal treatment (Fig. 8C-D). The more noticeable alterations during this initial phase of treatment were intense cellular proliferation and enlargement of the luminal compartment, which had a large amount of PAS-positive secretion (Fig. 8C-D). These experiments showed that testosterone administration promotes growth and greater secretory activity in the female prostate of the rodents studied. These effects reproduce in detail the events that occur during prostatic development in male mice and Wistar rats (Vilamaior *et al.*, 2006). Thus, it is possible to conclude that the lack of androgens contributes to reduced female prostate development (Santos *et al.*, 2006) and that the secretory activity observed in the prostates of untreated females (Santos *et al.*, 2003a; b) is maintained by the small amount of testosterone present in the serum of these animals.

In the male organism, the androgens are related to the differentiation, growth, and maintenance of prostate secretory activity (Hayward *et al.*, 1996; Steers, 2001; Thomson, 2001). Thus, the data obtained by the testosterone treatment suggest that androgens play a similar role in the female prostate, which is related primarily to the differentiation of secretory epithelium and regulation of secretory activity.

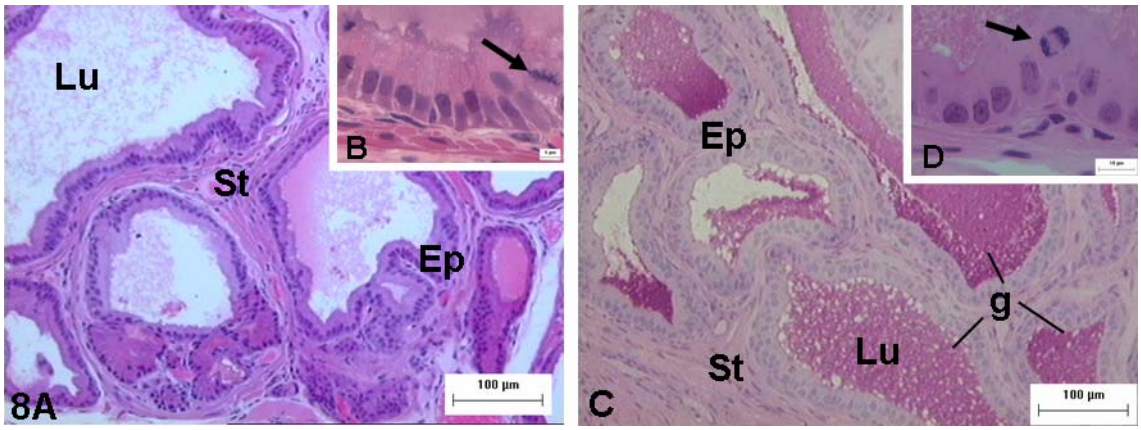

Figure 8. **A** and **B:** histological sections of adult female gerbil prostate after testosterone (T) treatment and stained with hematoxylin-eosin. Note the intense development that occurred in the epithelium (Ep), lumen (Lu), and stroma (St). Cellular proliferation is observed in the secretory epithelium (arrow). **C** and **D**: histological sections of a female rat prostate after 3 days of T treatment and stained using the periodic acid & Schiff method (PAS). The prostatic gland undergoes intense development, presenting many alveoli (g) and spreading of the luminal compartment (Lu) in which there is a large amount PAS-positive secretion. Note the presence of cell division (arrow) in the prostatic epithelium (Ep).

Anti-estrogenic effects on the adult gerbil female prostate

Although the tissue of the prostate is androgen dependent, its physiology and pathology are also influenced by estrogens (García-Flórez *et al.*, 2005). Besides modulating androgen effects, estrogens appear to increase tissue sensitivity to other hormones by increasing the number of their receptors (Timms *et al.*, 1999). As the estrogen serum levels are elevated in the female organism, it is believed that this hormone can act directly in the maintenance and physiology of the female prostate.

Studies involving the male rodent prostate indicate that control of hormonal development and prostatic function is complex and dependent on the balance among steroid hormones (Risbridger *et al.*, 2003; García-Flórez *et al.*, 2004). In male rats, the increasing of the estrogen:androgen ratio, which occurs with aging, precedes or coincides with an increase incidence of prostate cancer (Härkönen and Mäkela, 2004). In post-menopausal women, when the ovaries fail to produce estrogens, there is a greater probability of pre-malignant and malignant prostatic lesion development (Sloboda *et al.*, 1998).

Initial studies involving the senile gerbil prostate suggest that the occurrence of spontaneous prostatic lesions is more frequent and precocious in females than in males (unpublished data). These data indicate that estrogens play an important role in prostatic physiological maintenance and that the androgen:estrogen imbalance is the key factor in the installation of prostatic disorders. Based on this, our research group has developed preliminary evaluations of the effect of estrogen suppression on the female gerbil prostate. To evaluate the effects of estrogen suppression on the female prostate, two anti-estrogen drugs, letrozole and tamoxifen, were used. These two estrogenic inhibitors were developed for the treatment of estrogen-positive breast cancer as an attempt to interrupt breast cancer cell progression (Cabot *et al.*, 1996; Berstein *et al.*, 2002; Dixon *et al.*, 2003; Haynes *et al.*, 2003; Smith, 2003). Letrozole is a non-steroidal inhibitor of the aromataze enzyme capable of preventing 99% of peripheral estrogen conversion (Haynes *et al.*, 2003). Tamoxifen is a non-steroidal triphenylethylene that exercises an antagonistic action on estrogen by binding competitively to the estrogen receptor (Cabot *et al.*, 1996). The initial results obtained so far show that both drugs cause important alterations in prostate physiology of female gerbils (Santos *et al.*, 2004; 2005).

With letrozole treatment, it is possible to observe accentuated glandular hyperplasia, characterized by increases in epithelial and stromal cells as well as an increase in the total number of ducts and alveoli (Fig. 9A). Furthermore, intra-epithelial neoplastic foci in a pseudocribiform arrangement (Fig. 9B) were very frequent, evolving in some cases into more severe tissue disorders (Santos *et al.*, 2004). These morphological data observed using letrozole treatment reproduce, in part, the morphological alterations observed with androgen treatment. In fact, the hormonal alterations caused by the letrozole treatment are similar in some aspects to the serum hormonal modifications caused by the T treatment. Evaluation of serologic data showed that the letrozole treatment increases serum testosterone levels by six times without substantially altering estradiol levels. Immunocytochemical reactions to the AR (Fig. 9C) and ERα (Fig. 9D) show that the epithelial and stromal prostatic cells have greater androgen receptor expression but less frequent expression of the ER-positive cells.

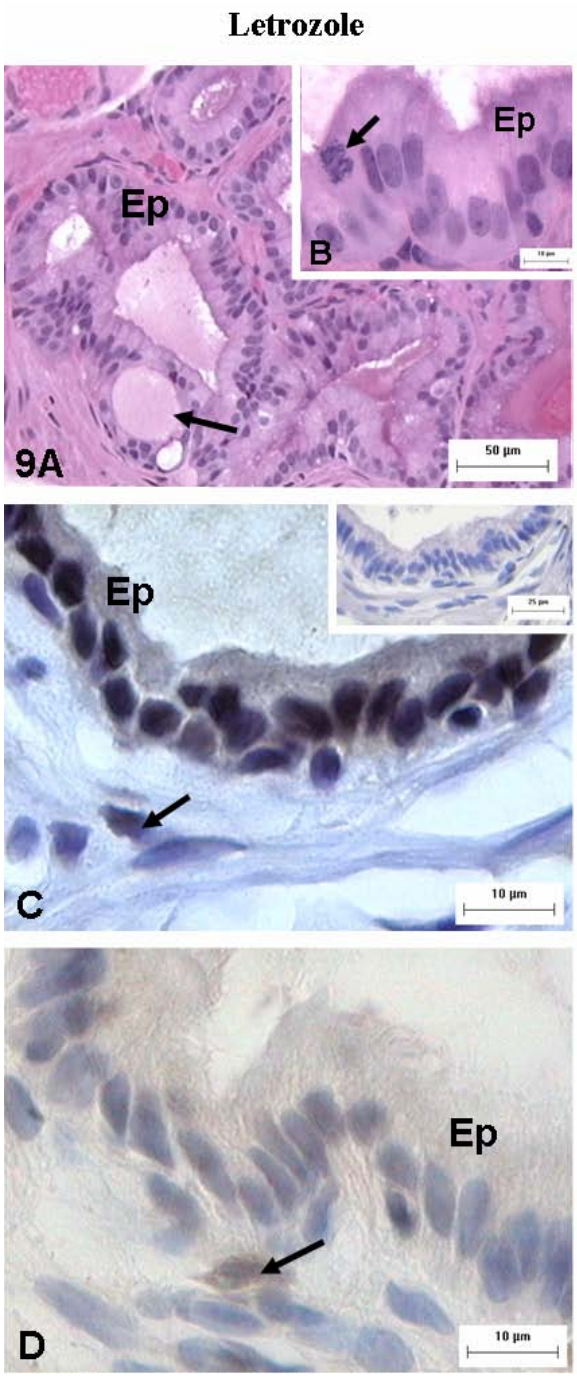

Figure 9. Histological sections of adult female gerbil prostate treated with letrozole. **A**: general view of the gland where an intense glandular hyperplasia and the occurrence of intraepithelial arcs are observed (arrow). **B**: detail of the prostatic epithelium (Ep) showing a great degree of development of epithelial cells and the occurrence of cell proliferation (arrow). **A** and **B** are stained with hematoxylin-eosin. **C**: immunocytochemical reaction to the androgen receptor. Intensely stained cells can be observed in the epithelium (Ep) and stroma (arrow). (inset: negative control). **D**: immunocytochemical reaction to the estrogen alpha receptor. Weak reactions are observed in the epithelial and stromal cells (arrow). **C** and **D** are counterstained with Harris's hematoxylin.

In the prostate, local estrogenic production occurs through testosterone aromatization into estrogen via the aromatase enzyme (Kaburagi *et al.*, 1986; Hiramatsu *et al.*, 1997; Negri-Cesi *et al.*, 1998; McPherson *et al.*, 2001; Risbridger *et al.*, 2003). Hence, it is believed that although serum estradiol levels do not change, letrozole administration causes suppression of estrogen activity in tissue. Therefore, it is suggested that increasing serum testosterone levels, caused by the inhibition of their aromatization into estrogen, is responsible for increasing AR expression and consequently for glandular development and a greater secretory activity of the glands treated with letrozole. In a similar manner, the suppression of estrogen activity in tissue can be related to lower ERα expression in the epithelium and prostatic stroma and to the development of prostatic intra-epithelial neoplasia.

With tamoxifen treatment, the morphologic alterations observed were more severe and consisted of neoplastic disorders and glandular hypertrophy (Santos *et al.*, 2005). The prostatic alveoli presented luminal enlargement and epithelial structural changes (Fig. 10A). Intra-epithelial neoplasia with a pseudocribiform arrangement was found repeatedly in several prostatic

alveoli. The epithelial cells became polymorphic, fully vacuolated, and without traces of a greater secretory activity (Fig. 10B). Low AR (Fig. 10C) and ERα (Fig. 10D) expression was observed in epithelial and stromal cells. Serologic data showed that tamoxifen did not cause significant alterations in serum testosterone or estrogen levels (Santos *et al.*, 2005). Although there were not any serum hormonal alterations with tamoxifen treatment, immunocytochemical data indicate that the tamoxifen action not only disrupted estrogenic activity but also interfered with the prostate gland's response to androgenic stimulus.

Estrogens indirectly participate in prostatic growth and differentiation by modulating AR signaling and regulating the prostatic response to this hormone (McPherson *et al.*, 2001). In male mice that have a deficiency in estrogen production, the absence of this hormone alters AR activity, causing these receptors to be responsible for the development of pre-malignant and malignant lesions (Risbridger *et al.*, 2003). Consequently, it is believed that the tissue changes observed in prostates of female mice treated with tamoxifen are due to alterations in the intraprostatic hormonal environment. By blocking the binding between estrogen and its receptor, the prostatic physiology as a whole can be altered because besides estrogenic suppression, less AR activity was also observed.

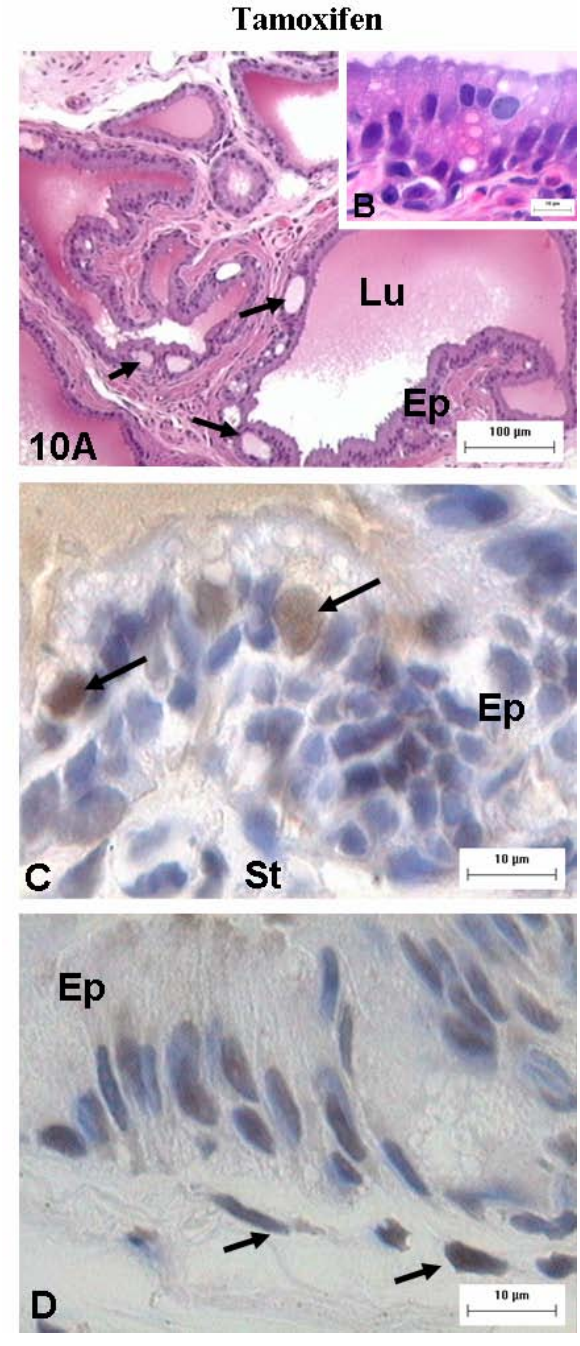

Figure 10. Histological sections of the adult female gerbil prostate treated with tamoxifen. **A**: prostatic alveoli with luminal hypertrophy (Lu) and intraepithelial neoplasia with pseudocribiform pattern (arrows) are shown. **B**: detail of polymorphic epithelial cells showing large amount of vacuoles. **A** and **B** are stained with hematoxylin-eosin. **C**: immunocytochemical reaction to the androgen receptor. Weak reaction are observed in the epithelium (arrows) and stroma (St). **D**: immunocytochemical reaction to the estrogen alpha receptor (ERα). Cells that stained positive for the ERα are observed in the epithelial (Ep) and stromal cells (arrow). **C** and **D** are counterstained with Harris's hematoxylin.

Concluding remarks

Androgens and estrogens participate in hormonal regulation of the female gerbil prostate. While androgens induce the differentiation, development, and secretory activity of the gland, estrogens appear to modulate the androgenic effects and maintain the normal physiology and growth of the prostate. Thus, the balance between these steroid hormones is crucial to prostatic homeostasis. Hormonal imbalance caused by anti-estrogen drugs (letrozole and tamoxifen) can trigger profound alterations in adult prostate morphophysiology. Some of these alterations are similar to those observed in the prostatic glands of post-menopausal women (Sloboda *et al.*, 1998; Islam *et al.*, 2001; Kato *et al.*, 2005) and in senile gerbil females (unpublished data). This corroborates the importance of internal hormonal balance to maintenance of prostatic health.

With the advent of contraceptive pills in recent decades, hormonal reposition drugs, hormonal therapies for breast cancer treatment, and even the exposure to environmental hormones known as *endocrine disruptors*, women are susceptible to severe hormonal alteration that can influence prostatic physiology. Because many health professionals have neglected the existence of a functional prostatic gland in females or even ignored its biological and pathological importance until now, little is known about the effects of long-term exposure to exogenous hormones on prostatic morphology. It is essential to monitor the female prostate frequently, mainly after menopause and during hormonal induction, in order to prevent development of prostatic disorders.

Acknowledgments

This work was funded by FAPESP (São Paulo State Research Foundation; grants 00/11648-1 and 03/08653-1); CNPq (National Council of Scientific and Technological Development; fellowships to SRT) and CAPES (Coordination of Improvement of Personnel of Superior Level; fellowships to FCAS). The authors express their gratitude to Mr. Luis R Falleiros-Jr. and Mrs. Rosana S Souza for technical assistance, to Ricardo S. Sobreira and Peter J. Harris for review of English grammar, to Dr. Luis Henrique Monteiro-Leal (UERJ, Rio de Janeiro) for the free access to the 3D-imaging program, and to Karina Carvalho for help with operation of the 3D-imaging program. Special thanks are due to Dr. Rejane M Góes and Dr. Sérgio L Felisbino (UNESP), Dr. Patricia S L Vilamaior (UNIRP, São José do Rio Preto), to Ms. Ana Maria Galvan Custódio, Ms. Lara S Corradi and Dr. Hernandes F Carvalho (UNICAMP, Campinas) for collaboration and helpful discussions, and to Dr. Milan Zaviačič (Comenius University Bratislava, Slovakia) for providing bibliographic material regarding the human female prostate. This review has been prepared in commemoration of the 15th Anniversary of the Reproduction Biology Group (CNPq/Ibilce/Unesp) coordinated by Dr. Taboga and established in 1991 and to the 9th Anniversary of the first significant publication by the Group's members about prostate biology in 1997. This paper is dedicated *in memoriam* to Dr. Luis Henrique Monteiro-Leal who is recently, prematurely deceased.

References

Addiego F, Belzer EG, Comolli J, Moger W, Perry JD, Whipple B. 1981. Female ejaculation: a case study. *J Sex Res*, 17:1-13.

Ali SZ, Smilari TF, Gal D, Lovecchio JL, Teichberg S. 1995. Primary adenoid cystic carcinoma of Skene´s glands. *Gynecol Oncol*, 57:257-261.

Berstein L, Maximov S, Gershfeld E, Meshkova I, Gamajunova V, Tsyrlina E, Larionov A, Kovalevskij A, Vasilyev D. 2002. Neoadjuvant therapy of endometrial cancer with the aromatase inhibitor letrozole: endocrine and clinical effects. *Obstetr Gynecol*, 105:161-165.

Bieberich CJ, Fujita K, He WW, Jay G. 1996. Prostate-specific and androgen-dependent expression of a novel homeobox gene. *J Biol Chem*, 271:31779-31782.

Cabot MC, Giuliano AE, Volner A, Han TY. 1996. Tamoxifen retards glycosphingolipid metabolism in human cancer cells. *FEBS Lett*, 394:129-131.

Clark MM, Crews D, Galef BG. 1991. Concentrations of sex steroid hormones in pregnant and fetal Mongolian gerbils. *Physiol Behav*, 49:239.

Cunha GR, Hayward SW, Wang YZ. 2002. Role of stroma in carcinogenesis of the prostate. *Differentiation*, 70:473-485.

Custódio AMG, Góes RM, Taboga SR. 2004. Acid phosphatase activity in gerbil prostate: comparative study in male and female during postnatal development. *Cell Biol Int*, 28:335-344.

de Graaf R. 1672. *De mulierum organis generationi inservientibus. Tractatus novus demonstrans tani homines et animália caetera omnia, quac vivípara dicuntut, haud minus quam vivípara ab ovo origenem ducere*. Leyden: [no ed.]. 66p.

Diamandis EP, Yu H. 1997. Nonprostatic sources of prostate-specific antigen. *Urol Clin North Am*, 24:275-282.

Dixon JM, Jackson J, Renshaw L, Miller WR. 2003. Neoadjuvant tamoxifen and aromatase inhibitors: comparisons and clinical outcomes. *J Steroid Biochem Mol Biol*, 86:295-299.

Dodson MK, Cliby WA, Keeney GL, Peterson MF, Podratz KC. 1994. Skene´s gland adenocarcinoma with increased serum level of prostate-specific antigen. *Gynecol Oncol*, 55:304-307.

Dodson MK, Cliby WA, Pettavel PP, Keeney GL,

Podratz KC. 1995. Female urethral adenocarcinoma: evidence for more than one tissue of origin? *Gynecol Oncol*, 59:352-357.

Donjacour AA, Cunha GR. 1993. Assessment of prostatic protein secretion in tissue recombinants made of urogenital sinus mesenchyme and urothelium from normal or androgen-insensitive mice. *Endocrinology*, 131:2342-2350.

Ebisuno S, Miyai M, Nagareda T. 1995. Clear cell adenocarcinoma of the female urethra showing positive staining with antibodies to prostate-specific antigen and prostatic acid phosphatase. *Urology*, 45:682-685.

Flamini MA, Barbeito CG, Gimeno EJ, Portiansky EL. 2002. Morphological characterization of the female prostate (Skene's gland or paraurethral gland) of *Lagostomus maximus maximus*. *Ann Anat*, 184:341-345.

Galadari I, Al-Mazroei M, Alkaabi J. 2004. Prostatic-specific antigen and idiopathic hirsutism in females. *Int J Dermatol*, 43:275-277.

García-Flórez M, Oliveira CA, Carvalho HF. 2005. Early effects of estrogen on the rat ventral prostate. *Braz J Med Biol Res*, 38:487-497.

Gräfenberg E. 1950. The role of the urethra in female orgasm. *Int J Sexol*, 3:145-148.

Gross SA, Didio LJA. 1987. Comparative morphology of the prostate in adult male and female of Praomys (mastomys) natalensis studies with electron microscopy. *J Submicros Cytol*, 19:77-84.

Härkönen PL, Mäkelä SI. 2004. Role of estrogens in development of prostate cancer. *J Steroid Biochem Mol Biol* ,92:297-305.

Haynes BP, Dowsett M, Miller WR, Dixon JM, Bhatnagar AS. 2003. The pharmacology of letrozole. *J Steroid Biochem Mol Biol*, 87:35-45.

Hayward SW, Baskin LS, Haughney PC, Cunha AR, Foster BA, Dahiya R, Prins GS, Cunha GR. 1996. Epithelial development in the rat ventral prostate, anterior prostate and seminal vesicle. *Acta Anat*, 155:81-93.

Hines TM. 2001. The G-spot: A modern gynecologic myth. *Am J Obstet Gynecol*, 185:359-362.

Hiramatsu M, Maehara I, Ozaki M, Harada N, Orikasa S, Sasano H. 1997. Aromatase in hyperplasia and carcinoma of the human prostate. *Prostate*, 31:118-124.

Huang L, Pu Y, Alam S, Birch L, Prins GS. 2004. Estrogenic regulation of signaling pathways and homeobox genes during rat prostate development. *J Androl*, 25:330-337.

Huffman JW. 1948. The detailed anatomy of the paraurethral ducts in the adult human female. *Am J Obstet Gynecol*, 55:86-101.

Huffman JW. 1951. Clinical significance of the paraurethral ducts and glands. *Arch Surg*, 62:615-625.

Isaacs JT, Furuya Y, Berges R. 1994. The role of androgen in the regulation of programmed cell death/apoptosis in normal and malignant prostatic tissue. *Semin Cancer Biol*, 5:391-400.

Islam AHMM, Kato H, Hayama M, Kobayashi S, Ota H, Nishizawa O. 2001. Adenocarcinoma of the female paraurethral duct showing neuroendocrine differentiation. *Urology*, 58:1058.

Kaburagi YK, Marino MB, Kirdani RY, Greco JP, Karr JP, Sandberg AA. 1986. The possibility of aromatization of androgen in human prostate. *J Steroid Biochem*, 26:739-742.

Kato H, Kobayashi S, Islam AM, Nishizawa O. 2005. Female para-urethral adenocarcinoma: histological and immunohistochemical study. *Int J Urol*, 12:117-119.

Kocak M. 2004. Serum levels of prostate-specific antigen and androgens after nasal administration of gonadotropin releasing hormone-agonist in hirsute women. *Gynecol Endocrinol*, 18:179-185.

Leite RP, Santos FCA, Custódio AMG, Góes RM, Taboga SR. 2004. Morphometric evaluation of testosterone effects on the prostatic secretory cells of female gerbil. *In:* Abstracts of the XII Congress of the Brazilian Society for Cell Biology, 2004, Campinas, Brazil. Campinas, Brazil: Brazilian Society of Anatomy. pp.B039.

Marker PC, Donjacour AA, Dahiya R, Cunha GR. 2003. Hormonal, cellular, and molecular control of prostatic development. *Dev Biol*, 253:165-174.

McCluggage WG, Ganesan R, Hirschowitz L, Miller K, Rollason TP. 2006. Ectopic prostatic tissue in the uterine cervix and vagina: report of a series with a detailed immunohistochemical analysis. *Am J Surg Pathol*, 30:209-215.

McCrea LE. 1952. Malignancy of the female urethra. *Urol Surv*, 2:85-149.

McPherson SJ, Wang H, Jones ME, Pedersen J, Iismaa TP, Wreford N, Simpson ER, Risbridger GP. 2001. Elevated androgens and prolactin in aromatase-deficient mice cause enlargement, but not malignancy, of the prostate gland. *Endocrinology*, 142:2458-2467.

Negri-Cesi P, Poletti A, Colciago A, Magni P, Martini P, Motta M. 1998. Presence of 5α-reductase isozymes and aromatase in human prostate cancer cells and in benign prostate hyperplastic tissue. *Prostate*, 34:238-291.

Omoto Y, Imamov O, Warner M, Gustafsson JA. 2005. Estrogen receptor alpha and imprinting of the neonatal mouse ventral prostate by estrogen. *Proc Natl Acad Sci USA*, 102:1484-1489.

Pointis G, Latreille MT, Cedard L. 1980. Gonado-pituitary relationships in the fetal mouse at various times during sexual differentiation. *J Endocrinol*, 86:483-488.

Prins GS, Birch L, Habermann H, Chang WY, Tebeau C, Putz O, Bieberich C. 2001. Influence of neonatal estrogens on rat prostate development. *Reprod Fertil Dev*, 13:241-252.

Pu Y, Huang L, Prins GS. 2004. Sonic hedgehog-patched Gli signaling in the developing rat prostate gland: lobe-specific suppression by neonatal estrogens reduces ductal growth and branching. *Dev Biol*,

273:257-275.

Risbridger GP, Bianco JJ, Ellem SJ, McPherson SJ. 2003. Oestrogens and prostate cancer. *Endocr Relat Cancer*, 10:187-191

Rovuela M, de Miguel MP, Bethencourt FR, Sanches-Chapado M, Fraile B, Arenas MI, Paniagua R. 2001. Estrogen receptors alpha and beta in the normal, hyperplastic and carcinomatous human prostate. *J Endocrinol*, 168:447-454.

Santos FCA, Corradi LS, Taboga SR. 2001. Cytochemical characterization of the stromal compartiment in gerbil female prostate. *In:* Proceedings of the XVIII Congress of the Brazilian Society for Microscopy and Microanalysis, 2001, Águas de Lindóia, Brazil. Brazilian Society of Anatomy. Suppl C, pp.207.

Santos FCA, Carvalho HF, Góes RM, Taboga SR. 2003a. Structure, histochemistry and ultrastructure of the epithelium and stroma in the gerbil (*Meriones unguiculatus*) female prostate. *Tissue Cell*, 35:447-457.

Santos FCA, Leite RP, Góes RM, Taboga SR. 2005. Tamoxifen effects on the gerbil female prostate. *Braz J Morphol Sci Suppl*, 3:51-52

Santos FCA, Corradi LS, Leite, RP, Góes RM, Taboga SR. 2004. Effects of aromatase inhibition on the gerbil female prostate. *In:* Abstracts of the XII Congress of the Brazilian Society for Cell Biology, 2004, Campinas, Brazil. Brazilian Society of Anatomy. pp.B037.

Santos FCA, Leite RP, Custódio AMG, Góes RM, Taboga SR. 2003b. Ultrastructural evaluation of testosterone anabolizing effects on the gerbil female prostate. *In:* Proceedings of the XIX Congress of the Brazilian Society of Microscopy and Microanalysis, 2003, Caxambu, Brazil. Brazilian Society of Anatomy. p.B0108-018.

Santos FCA, Leite RP, Custódio AMG, Carvalho KP, Monteiro-Leal LH, Santos AB, Góes RM, Carvalho HF, Taboga SR. 2006. Testosterone stimulates growth and secretory activity of the adult female prostate of the gerbil (*Meriones unguiculatus*). *Biol Reprod*, 75:370-379.

Sauter ER, Klein G, Wagner-Mann C, Diamandis EP. 2004. Prostate-specific antigen expression in nipple aspirate fluid is associated with advanced breast cancer. *Cancer Detect Prev*, 28:27-31.

Schmidt S, Franke M, Lehmann J, Loch T, Stöckle M, Weichert-Jacobsen K. 2001. Prostate-specific antigen in female urine: a prospective study involving 217 women. *Urology*, 57:717-720.

Schubach G. 2002. The G-spot is the female prostate. *Am J Obstet Gynecol*, 186: 850.

Shapiro E, Huang H, McFadden DE, Masch RJ, NG E, Lepor H, Wu XR. 2004. The prostatic utricle is not a Müllerian duct remnant: immunohistochemical evidence for a distinct urogenital sinus origin. *J Urol*, 172:1753-1756.

Sharifi-Aghdas F, Ghaderian N. 2004. Female paraurethral cysts: experience of 25 cases. *BJU Int*, 93:353-356.

Shehata R. 1974. Urethral glands in the wall of the female urethra of rats, mice and closely related rodents. *Acta Anat*, 90:381-387.

Shehata R. 1975. Female prostate in *Arvicantihis niloticus and Meriones lybicus*. *Acta Anat*, 92:513-523.

Shehata R. 1980. Female prostate and urethral glands in the home rat, *Rattus norvegicus*. *Acta Anat*, 107:286-288.

Skene AJC. 1880. The anatomy and pathology of two important glands of the female urethra. *Am J Obstetr Diss Women Child*, 13:265-270.

Sloboda J, Zaviačič M, Jakubovský J, Hammar E, Johnsen J. 1998. Metastasizing adenocarcinoma of the female prostate (Skene´s paraurethral glands). Histological and immunohistochemical prostate markers studies and first ultraestructural observation. *Pathol Res Pract*, 194:129-136.

Smith AF, Landon GV, Ghanadian R, Chisholm GD. 1978. The ultrastructure of the male and female prostate of Praomys (Mastomys) natalensis. *Cell Tiss Res*, 190:539-552.

Smith IE. 2003. Letrozole versus tamoxifen in the treatment of advanced breast cancer and as neoadjuvant therapy. *J Steroid Biochem Mol Biol*, 86:289-293.

Staack A, Donjacour AA, Brody J, Cunha GR, Carrol P. 2003. Mouse urogenital development: a practical approach. *Differentiation*, 71:402-413.

Steers, WD. 2001. 5α-reductase activity in the prostate. *Urology*, 58(Suppl 6A):17-24.

Taboga SR, Góes RM, Zanetoni C, Santos FCA. 2001. Ultrastructural characterization of the prostate secretory cells: a comparative study between the male and female organs. *In:* Proceedings of the XVIII Congress of the Brazilian Society for Microscopy and Microanalysis, 2001, Águas de Lindóia, Brazil. Brazilian Society of Anatomy. Suppl C, pp.205.

Tepper SL, Jagirdar J, Heath D, Geller SA. 1984. Homology between the female paraurethral (Skenes's) glands and the prostate. *Arch Pathol Lab Med*, 108(5): 423-425.

Thomson AA. 2001. Role of androgens and fibroblast growth factors in prostatic development. *Reproduction*, 121:187-195.

Thomson AA, Timms BG, Barton L, Cunha GR, Grace OC. 2002. The role of smooth muscle in regulating prostatic induction. *Development*, 129:1905-1912.

Timms BG, Petersen SL, Vom Saal FS. 1999. Prostate gland growth during development is stimulated in both male and female rat fetuses by intrauterine proximity to female fetuses. *J Urol*, 161:1694-1701.

Vilamaior PSL, Taboga SR, Carvalho HF. 2006. Postnatal growth of the ventral prostate of Wistar rats: a stereological and morphometric study. *Anat Rec. (*in press).

Vilamaior PSL, Santos FCA, Falleiros-Jr LR, Biancardi MF, Fochi RA, Taboga SR. 2005.

Comparative histology of gerbil and rat female prostate: morphological evidences of different functional state during distinct phases of post-natal development. *Braz J Morphol Sci Suppl*, 3:28.

Wang Y, Hayward S, Cao M, Thayer K, Cunha G. 2001. Cell differentiation lineage in the prostate. *Differentiation*, 68:270-279.

Yu H, Berkel H. 1999. Prostate-specific antigen (PSA) in women. *J La State Med Soc*, 151(14): 209-213.

Wernet N, Albrecht M, Sesterhenn I, Goebbels R, Bonkhoff H, Seitz G, Inniger R, Remberger K. 1992. The "female prostate": localion, morphology, immunohistochemical characteristics and significance. *Eur Urol*, 22:64-69.

Zaviačič M. 1993. Update on the female prostate and the phenomenon of female ejaculation. *J Sex Res*, 30:148-151.

Zaviačič M. 1999. *The female prostate: from vestigial Skene's parauretral glands and ducts to woman's functional prostate*. Bratislava, Slovakia: Slovack Academic Press. 171pp.

Zaviačič M, Ablin RJ. 2000. The female prostate and prostate-specific antigen. Imunohistochemical localization, implications of this prostate marker in women and reasons for using the term "prostate" in human female. *Histol Histopathol*, 15:131-142.

Zaviačič M, Sidlo J, Borovský M. 1993. Prostate specific antigen and prostate specific acid phosphatase in adenocarcinoma of Skene's paraurethral glands and ducts. *Virchows Archiv A Pathol Anat*, 423:503-505.

Zaviačič M, Jakubovská V, Belošovič J, Breza J. 2000a. Ultrastrucuture of the normal adult human female prostate gland (Skene's gland). *Anat Embriol (Berl)*, 201:51-61.

Zaviačič M, Danihel L, Ružičková M, Blažeková J, Itoh Y, Okutani R, Kaway T. 1997a. Immunohistochemical localization of human protein 1 in the female prostate (Skene's Gland) and the male prostate. *Histochem J*, 29:219-227.

Zaviačič M, Ružičková M, Blažeková J, Zaviačič T, Itoh Y, Okutani R, Kawai T. 1997b. Immunohistochemical distribution of rabbit polyclonal antiurinary protein 1 antibody in the female (Skene's gland) and male prostate: new marker for neuroendocrine cells? *Acta Histochem*, 99:267-275.

Zaviačič M, Zajíčková M, Blazeková J, Donárová L, Svetoslav S, Miroslav M, Zaviačič T, Holomán K, Breza J. 2000b. Weight, size, macroanatomy, and histology of the normal prostate in the adult human female: a minireview. *J Histotechnol*, 23:61-69.

Artigo: Experimental endocrine therapies promote epithelial cytodifferentiation and ciliogenisis in the gerbil female prostate. Este trabalho foi aceito pela revista *Cell and Tissue Research* e está em processo de publicação.

Experimental endocrine therapies promote epithelial cytodifferentiation and ciliogenesis in the gerbil female prostate

Fernanda Cristina Alcântara Santos[1],

Luiz Roberto Falleiros-Júnior[2],

Lara Silvia Corradi[1],

Patricia Simone Leite Vilamaior[3],

Sebastião Roberto Taboga[2]

[(1)]Department of Cell Biology, Institute of Biology, UNICAMP, P.O. Box 6109, 13083-864, Campinas, SP, Brazil; [(2)] São Paulo State University – IBILCE/UNESP, Microscopy and Microanalysis Laboratory, Department of Biology, 15054-000, São José do Rio Preto, SP, Brazil; [(3)] Rio Preto Universitary Center – UNIRP, Biology Sciences School , São José do Rio Preto, SP, Brazil.

Running Title: Ciliogenesis in the gerbil female prostate

Correspondence to:

Sebastião Roberto Taboga

Department of Biology - IBILCE/UNESP

Rua Cristovão Colombo, 2265, CEP 15084-000 - São José do Rio Preto, São Paulo, Brazil

Tel +55-17-2212386; Fax: +55-17-2212390 E-mail: taboga@ibilce.unesp.br

Abstract

The incidence of ciliated cells in the gerbil (*Meriones unguiculatus)* female prostate is uncommon and apparently becomes more frequent under androgen (testosterone cypionate) and anti-estrogen (letrozole) endocrine therapies. To evaluate effects of some drugs therapies on ciliogenesis induction in the female prostate glandular epithelium, 90th-days adult females were treated through 14 days with testosterone and letrozole after which the removed glands underwent histological, ultrastructural and serological analyses. The results obtained indicate that the cytodifferentiation of the ciliated phenotype in the alveoli's epithelium became more frequent in the both testosterone and letrozole treatments analyzed and that the ciliogenesis phenomenon of the gerbil female prostate epithelial cells appears to be induced by variation of the androgens levels increase.

Keywords: female prostate; ciliogenesis; testosterone; letrozole; epithelium

Introduction

The Mongolian gerbil (*Meriones unguiculatus*) is a rodent known for its suitability for laboratory use since the 1960s (Williams, 1974). The usefulness of this animal in biomedical research has been recognized in immunology (Nawa et al, 1994), physiology (Nolan et al, 1990), and morphology (Redecker, 1991; Aoki-Komori et al, 1994; Pinheiro et al, 2003; Custódio et al, 2003; Santos et al, 2003 and 2006; Corradi et al, 2004). More recently, gerbil has also been suggested as a suitable model for studies on mammalian aging (Spangler et al, 1997; Pegorin de Campos et al, 2006). Gerbil's prostate has compact lobes, somewhat similar to the human prostate, unlike rats and mice which have distinct lobes (Price, 1963; Pinheiro et al, 2003; Góes et al., 2006). Previous data from our laboratory has demonstrated that histological, histochemical and ultrastructural features of the adult gerbil's prostate are comparable to the human prostate. Besides, we have observed that old gerbils (12 months) may spontaneously develop benign prostate hyperplasia, cancer and other prostate disorders (Pegorin de Campos et al, 2006).

The gerbil adult female prostate is morphologically similar to the gerbil male prostate, because the former is lined by a simple epithelium that varies from cubic to tall prismatic (Santos et al., 2003; Custódio et al., 2004). The cellular types found in the female prostatic epithelium are typical secretory cells (90.5%), clear secretory cells (1.5%) and basal cells (8%) (Santos et al., 2003). Besides, curiously, ciliated cells have been rarely observed in the epithelium of the normal gerbil adult female prostate (Taboga et al., 2005). The genesis of this cellular type in the prostate gland is uncommon, since there are no reports of such occurrence either in animal species or in humans. The function of the ciliated cells in the prostate gland and its significance in this organ are not stated or known. Therapies with androgenic hormones or with anti-estrogenic drugs such as letrozole have caused a change

in the proportion, morphology and physiology of the female prostate secretory cells (Santos et al., 2005; 2006), as well as an apparent increase in frequency of ciliated cells.

The cytodifferentiation in the female genital ducts' epithelium, including ciliogenesis process, have been investigated in several rodents and 17-beta-estradiol is he principal hormone that stimulates cilia formation (Goldberg and Friedman, 1995) and cytodifferentiation of secreting cells (Abe and Oikawa, 1993), in addition the progesterone acts only in the ciliogenesis (Abe and Oikawa, 1993), but this action have been discussed and questioned (Sandoz et al., 1976; Corner et al., 1998).

Based on these statements, the aim of this study is to evaluate the effect of different hormonal therapies on the cytodifferentiation of ciliated cells in the gerbil female prostate, and to infer the possible causes of the development of this cellular type in that organ.

Materials and methods

Samples preparation

The prostate glands of the 15 gerbils (*Meriones unguiculatus*) 90th-days adult females (5 animals per experimental condition): normal (Ct) and treated for 14 days with testosterone cypionate (TT - 1mg/kg/every other day), and letrozole (LET- 1mg/kg/day) were processed by light and transmission electron microscopy. Whole blood was collected for serologic quimioluminescence analyses of steroids levels.

Light microscopy

The urethra and adherent tissues were dissected out after anesthesia by ether inhalation and immediately fixed by immersion in Karnovsky fixative solution (5% parformaldehyde, 2.5% glutaraldehyde in 0.1M phosphate buffer at pH 7.2) for 24 hours. After fixation, the tissues were washed with running tap water, dehydrated in an ethanol series and embedded in glycol methacrylate resin (Leica historesin embedding kit, Leica, Nussloch, Germany) and sectioned at 3 μm on a Leica automatic rotatory microtome (Leica RM2155, Nussloch, Germany). Sections from the female prostate samples were stained with hematoxylin-eosin (Behmer et al., 1976). Observations and light microscopy images were obtained with an Olympus light microscope (Olympus, Hamburg, Germany). In addition, the histological sections were subjected to the prostatic population census according Santos and colleagues (2006). Data were analyzed using the Statistica 6.0 software (Copyright©StarSoft, Inc. 1984-1996). The hypothesis tests used to determine significance were the ANOVA and the Tukey test for multiple comparisons. The significance level was 5% ($p \leq 0.05$).

Transmission electron microscopy

Urethral and paraurethral tissue fragments were fixed by immersion with 3% glutaraldehyde plus 0.25% tannic acid solution in Millonig´s buffer, pH 7.3, containing 0.54% glucose, during 24 hours (Cotta-Pereira, 1976). After washing with the same buffer, the material was post-fixed with 1% osmium tetroxide in same buffer, for 1 hour, washed again, dehydrated in graded acetone series and embedded in Araldite resin. Ultrathin silver sections were cut using a diamond knife and contrasted with 2% alcoholic uranil acetate

and then with 2% lead citrate in sodium hydroxide solution for 10 minutes. Grids were examined under a Leo-Zeiss 906 transmission electron microscope operating at 80 kV.

Serum testosterone concentration

Blood samples were collected from each animal group. The serum was then separated by centrifuge at 3.000 rpm and stored until assayed. Testosterone and estradiol concentration was determined by automatic equipment (VITROS ECi-Johnson & Johnson Ultra-sensitive Quimioluminescent analysis) in a renowned clinical analysis laboratory, using specific reagents supplied by Johnson & Johnson Orthoclinical, USA. The sensitivity of this assay was 0.1-150.0 ng/ml.

Results

The results obtained indicate that the both TT and LET treatments caused important and statistically significant alterations ($p \leq 0.0001$) in the proportion of female prostate ciliated cells in the alveolar epithelium (Fig. 1). The count of the ciliate cells and the relative census showed that means and standard error (Mean±SE) of the Ct group was 0.04% ± 0.02%, the TT treated group was 1.1% ± 0.1% and the LET treated group was 1.1% ± 0.1%. The histological analyses of the secretory epithelium showed two market differentiated cell types, the predominant cylindrical secretory cells and the smaller and less abundant basal cells, which are restrict to the basal compartment of the epithelium. The epithelial cytodifferentiation of the ciliated phenotype were uncommonly visualized in hematoxylin-eosin sections of the Ct (Figures 2a,b), but in the TT treated group (Figure 2c) and LET treated group (Figure 2d) these cell phenotype suffer an increase. At the

transmission electron microscopy, the ciliated cells were characteristically visualized with a typical basal body plus axonemal 9+2 pattern became more frequent in both, TT and LET treatments. Concerning the serologic data, our results reveals that the testosterone levels were significantly ($p \leq 0.05$) higher in both treatments TT and LET. Few oscillations were observed in the serologic levels of estradiol in different treatments, but these alterations were not statistically significant (Table I).

Discussion

Steroid hormones play critical roles in growth, cytodifferentiation and function of gonad cells and hence, in development and physiology of multicellular tissues and organisms (Liu et al., 2005), including female prostate gland (Santos et al., 2006). The hormonal control of ciliogenesis and cytodifferentiation of secretory cells in avian female reproductive tract (Sandoz et al., 1976) and mammalian reproductive ducts (Okada et al., 2004) were very good described. Goldberg and Friedman (1995) reinforced the key role of 17-beta-estradiol in the cytodifferenciation of ciliated cells in rodent oviduct. The author concluded that high estradiol levels was capable of preventing initial epithelial deciliation in vitro and, once deciliation started however, high estradiol was unable to limit the process or induce ciliogenesis. Additional information about the hormonal control of the ciliogenesis was verified by consecutive daily injections of progesterone in ovariectomized rats, which significantly stimulated the ciliogenesis and appearance of ciliated cells but not that of secretory cells (Abe and Oikawa, 1993). Although the testosterone levels produced by the adrenal gland and ovary follicle cells are lower than the male levels, the role of this hormone and its precursors and metabolites is unknown in relation to the ciliogenesis and oviduct epithelium cytodifferentiation.

The present study verified an uncommon presence of typical ciliated cells with normal 9+2 axonemal pattern in the prostatic epithelium of normal gerbil female, besides a significant percentage increase of these cells in the alveoli´s epithelium after the androgenic (TT) and anti-estrogenic (LET) therapies.

The occurrence of atypical solitary cilia exhibiting 9+0 axonemal pattern has been noted in Sertoli cells, fibroblasts and myoid cells of rat testes (Ponzio et al., 1997). Furthermore, ciliogenesis with 9+0 and 8+1 patterns has been observed in epithelia at sites away from the main lesions, such as gastric ones (Kawamata et al., 1986; Rubio et al., 1990) and ovarian adenocarcinoma (Gupta et al., 1985). The authors cited above do not correlate the data with unbalance in steroids levels; they just show the ciliogenesis phenomenon.

In the female prostates treated with androgenic hormones (Santos et al., 2006) and anti-estrogen drugs (Santos et al., 2005) pre-neoplastic and neoplastic alterations were common in the alveolus where ciliated-cell differentiation was evident. Thus, the unusual localization of these ciliated cells may be considered an indicative of a transient epithelial methaplasia process or an early installation of malign and/or pre-malign lesion. Studies of human uterine tube epithelial cells in culture and *in vivo* studies in epithelial cells of rodent's oviducts have been demonstrated that estrogens induce cytodifferentiation and growth of the ciliated epithelial cells and that progesterone suppresses the ciliogenesis phoenomenon (Sandoz et al., 1976; Comer et al., 1998; Hagiwara et al., 2000). It is known that the oscillation of sexual hormone concentrations during the rodent estrus cycle can influence the deciliation and/or stimulate ciliogenesis in oviducts epithelium (Goldberb and Friedman, 1995). However, our results obtained with gerbil female prostate indicate that ciliogenesis appears to be induced by androgen unbalance provoked by both TT and LET therapies. Is known that the LET therapy provoke the inhibition of aromatase enzyme activity, causing the blockage of the testosterone conversion into estrogen. The action of this drug promotes an additional increase of circulating androgen levels (Risbridger et al.,

2003). Thus, the unexpected localization of ciliated cells in the female prostate suggests that androgens endogenously and exogenously originated by blockage of aromatase and TT injections, respectively, may affect the ciliogenesis process in the alveoli's epithelium of that gland. However, confronting the ciliated cell census and the serological levels of testosterone verified that this hormone influence is not dose-dependent, once that the exogenous testosterone did not increase significantly the number of ciliated cells in comparison with the LET therapy.

It is known that the ciliogenesis/deciliation of epithelium oviduct cells is a transient phenomenon dependent of estrogen/progesterone levels oscillation during the estrous cycle. However in our experimental purpose we may not assume if the ciliogenesis is a transient phenomenon or not, but we can affirm that this process is a consequence of a new inducible hormonal environment which promotes an unbalance in the estrogen/progesterone levels. Once that the testosterone concentration in the female is proportionally lower than in male, alterations in this dosage is capable of display the ciliogenesis.

Acknowledgements

This paper is part of the thesis presented by FCAS to the Institute of Biology, UNICAMP, in partial fulfillment of the requirement for a PhD degree, and was supported by grants from the Brazilian agencies CAPES – Coordinating Body for Training University-level Personnel (fellowship to FCAS) and FAPESP – São Paulo Research Foundation (Proc. Nr. 00/11648-1). The authors wish to thank to Mrs. Rosana S. Sousa for their technical assistance and to Biology student Rodrigo P. Leite for help and suggestions, as well as all other researchers at the Microscopy and Microanalysis Laboratory. Acknowledgement is also due to Dr. Peter J. Harris and Ricardo S. Sobreira for English-

language revision of this paper. Special tanks Ana Maria G. Custódio for sugesting and advice.

References

Abe H, Oikawa T. 1993. Effects of estradiol and progesterone on the cytodifferentiation of epithelial cells in the oviduct of the newborn golden hamster. Anat Rec 235(3):390-8.

Aoki-Komori S, Sayto TR, Takahashi KW, Tanogushi K. 1994. Lectin histochemical studies on the scent gland in the Syrian hamster and Mongokian gerbil. Jikken Dobutsu 43(2):181-1990.

Behmer AO, Tolosa EMC, Neto AGF. 1976. Manual de práticas para histologia normal e patológica, 1st ed. Edart-Edusp, São Paulo, pp 144-145.

Pegorin de Campos SP, Zanetoni C, Góes RM, Taboga SR. 2006. Biological behavior of the gerbil ventral prostate during postnatal development. Anat Rec 288A(7): 723-733.

Comer MT, Leese HJ, Southgate J. 1998. Induction of a differentiated cilisted cell phenotype in primary cultures of Fallopian tube epithelium. Hum Reprod 13:3114-3120.

Corradi LS, Goes RM, Carvalho, HF, Taboga SR. 2004. Inhibition of 5-alpha-reductase activity induces stromal remodeling and smooth muscle de-differentiation in adult gerbil ventral prostate. Differentiation 72:198-208.

Cotta-Pereira G, Rodrigo FG, David-Ferreira JF. 1976. The use of tannic acid-glutaraldehyde in the study of elastic related fibers. Stain Technol 51:7-11.

Custódio AM, Góes RM, Taboga SR. 2004. Acid phosphatase activity in gerbil prostate: comparative study in male and female during postnatal development. Cell Biol Int 28:335-44.

Góes RM, Zanetoni C, Tomiosso TK, Ribeiro DL, Taboga SR. 2006. Histological response on dorsal and ventral gerbil prostatic lobes induced by different testosterone withdrawal procedures. Micron. In press.

Goldberg JM, Friedman CI. 1995. Effect of hormonal manipulation on human fallopian tubal epithelium in vitro. J Assist Reprod Genet 12(2):132-5.

Gupta PK, Albritton N, Erozan YS, Frost JK. 1985. Occurrence of cilia in exfoliated ovarian adenocarcinoma cells. Diagn Cytopathol 1:228-231.

Hagiwara H, Ohwada N, Aoki T, Takata K. 2000. Ciliogenesis and ciliary abnormalities. Med Electron Microsc 33:109-114.

Liu H, Zhang C, Tang X, Zeng W, Mi Y. 2005. Stimulating effects of androgen on proliferation of cultured ovarian germ cells through androgenic and estrogenic actions in embryonic chickens. Domestic Animal Endocrinology 28:451–462

Kawamata S, Kubota Y, Sawataishi M, Takaya K. 1986. The fine structure of atypical ciliated cells in the human gastric epithelium. Virchows Arch B Cell Pathol Incl Mol Pathol 51:363-374.

Nawa Y, Horii Y, Okada M, Arizono N. 1994. Histochemical and cytochemical characterization of mucosal and connective tissue mast cells of Mongolian gerbil (*Meriones unguiculatus*). Int Arch Allergy Immunol 104(3):249-254.

Nolan CC, Brown AW, Cavanagh JB. 1990 Regional variations in nerve cell resposnses to the trimethiltin intoxication in Mongolian gerbil. Acta Pathol Microbiol Immunol Scand 81(2):204-212.

Pinheiro PFF, Almeida CCD, Segatelli, TM, Martinez M, Padovani CR, Martinez FE. 2003. Structure of the pelvic and penile urethra-relationship with the ducts of the sex accessory glands of the Mongolian gerbil (*Meriones unguiculatus*). J Anat 202:431-444.

Okada A, Ohta Y, Brody SL, Watanabe H, Krust A, Chambon P, Iguchi T. 2004. Role of foxj1 and estrogen receptor alpha in ciliated epithelial cell differentiation of the neonatal oviduct. J Mol Endocrinol 32:615–625.

Ponzio R, Alonso DF, Gomez DE. 1997. Atypical cilia in testicular cells from normal rats. J Submicrosc Cytol Pathol 29:313-316.

Price D. 1963. Comparative aspects of development and structure in the prostate. Nat Can Inst Monogr 12:1-27.

Redecker P. 1991. Ultrastructural demonstration of neuhaemal contacts in the internal zone of the median eminence of the Mongolian gerbil (*Meriones unguiculatus*) correlation with synaptophysin immunohistochemistry. Histochem 95(5):503-511.

Risbridger GP, Bianco JJ, Ellem SJ, McPherson SJ. 2003. Oestrogens and prostate cancer. Endocrine-Rel Cancer 10:187-191.

Rubio C, Havashi T, Stemmermann G. 1990. Ciliated gastric cells: a study of their phenotypic characteristics. Mod Pathol 3:720-723.

Sandoz D, Biosvieux-Ulrich E, Laugier C, Brad E. 1976. Ciliogenesis in the mucous cells of the quail oviduct. II. Hormonal control. J Cell Biol 71:460-471.

Santos FC, Leite RP, Custodio AM, Carvalho KP, Monteiro-Leal LH, Santos AB, Góes RM, Carvalho HF, Taboga SR. 2006. Testosterone Stimulates Growth and Secretory Activity of the Adult Female Prostate of the Gerbil (*Meriones unguiculatus*). Biol Reprod. DOI 10.1095 In press.

Santos FCA, Góes RM, Carvalho HF, Taboga SR. 2003. Structure, histochemistry and ultrastructure of the epithelium and stroma in the gerbil (*Meriones unguiculatus*) female prostate. Tissue & Cell 35:447-457.

Santos FCA, Leite RP, Góes RM, Taboga SR. 2005. Tamoxifen effects on the gerbil female prostate. Braz J Morphol Sci 22sup:51-52.

Spangler EL, Hengemihle J, Blank G, Speer DL, Brozozowski S, Patel N, Ingram DK. 1997. An assessment of behavioral aging in the Mongolian gerbil. Exp Gerontol 32(6):707-717.

Taboga SR, Falleiros-Jr LR, Góes RM, Santos FCA. 2005. Ciliogenesis in the gerbil female prostate. Braz J Morphol Sci 22sup:28-28.

Williams WM. 1974. The anatomy of the Mongolian gerbil. Tumblebrook Fram, Inc., Massachussets, USA. 107p.

Figure legends

Figure 1. Percentage of ciliated cells in the gerbil female prostate treated by TT and LET. * Tukey test, $p \leq 0.0001$.

Figure 2. Light microscopy of prostate epithelium (ep) of adult gerbil female prostate stained by hematoxylin-eosin method. **a)**: General view of the prostate gland with alveoli´s lumen very large (a). The arrows indicate cilia in the normal epithelium. Bar = 100 μm. **b, c, d)**: Detail on ciliated cells in the Ct female prostate (b) and treated respectively by TT (c) and LET (d). Bars: 10 μm.

Figure 3. Ultrastructural aspect of ciliated cell in normal prostatic secretory ephitelium (Ep). a: ciliated (C) and secretory (S) cells; bar: 2.4 μm. St: stroma, LB: basal lamina. b: detail of apical region of ciliated cell. Basal bodies (arrows); bar: 1.2 μm. c: longitudinal cross section of the axoneme with normal 9+2 pattern; bar: 150 nm.

Table I: Estradiol and testosterone serologic levels in gerbil females Ct and treated with TT or LET for 14 days. The indicated values correspond respectively to the mean and standard error. *ANOVA test, $p \leq 0.05$. [1] $n = 5$ samples per experimental group.

Table I	**Hormone Levels[1]**	
	Estradiol (pg/ml)	***Testosterone (ng/ml)***
Control group (Ct)	22.9 ± 2.6	1.6 ± 0.4
Testosterone treated-group (TT)	29.7 ± 5.4	13.0 ± 1.0*
Letrozole treated-group (LET)	21.8 ± 0.2	5.0 ± 0.5*

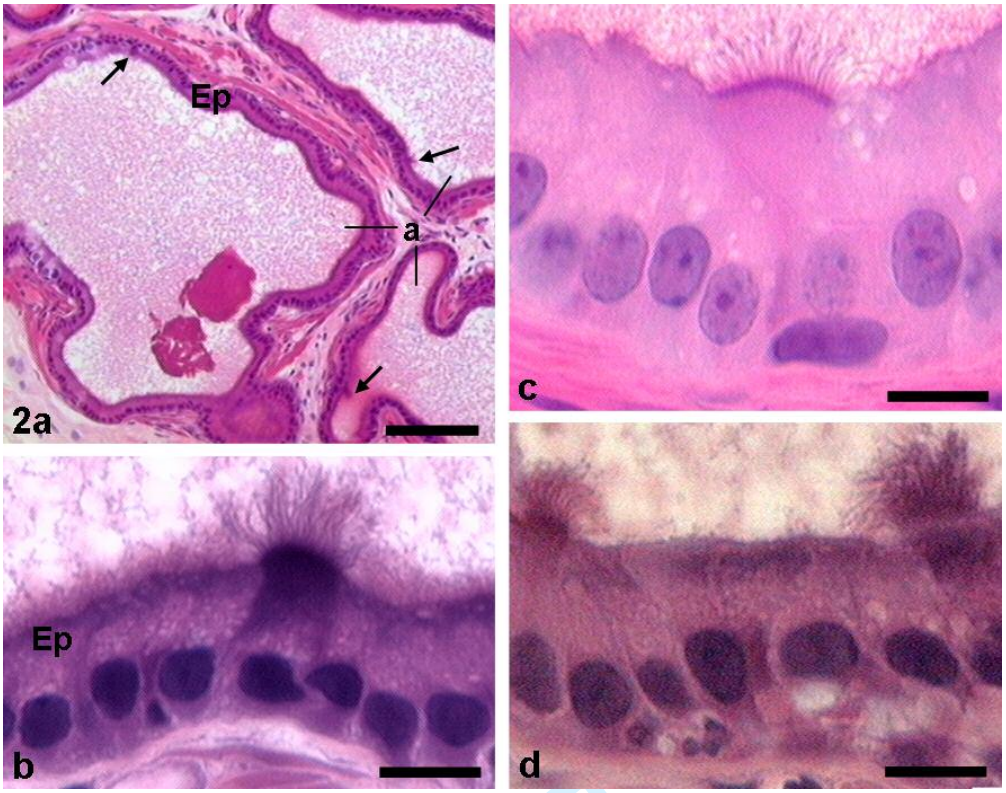

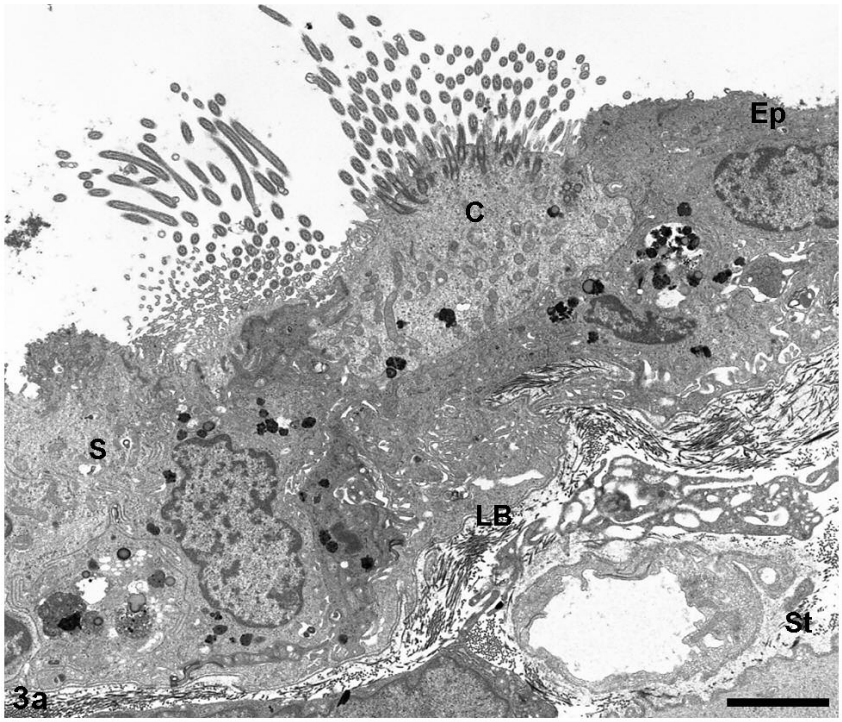
Ep
C
S
LB
St
3a

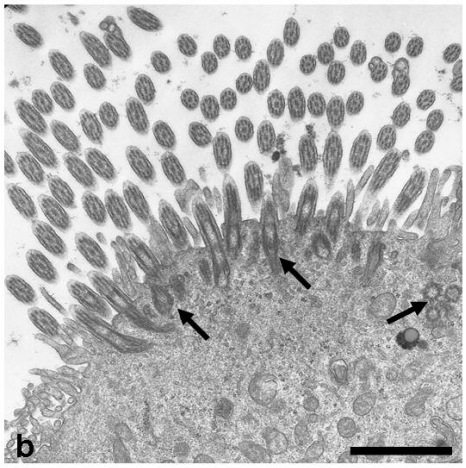
b

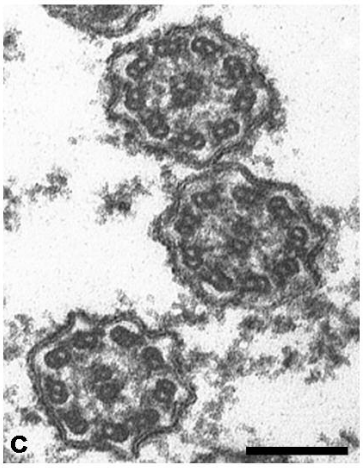
c

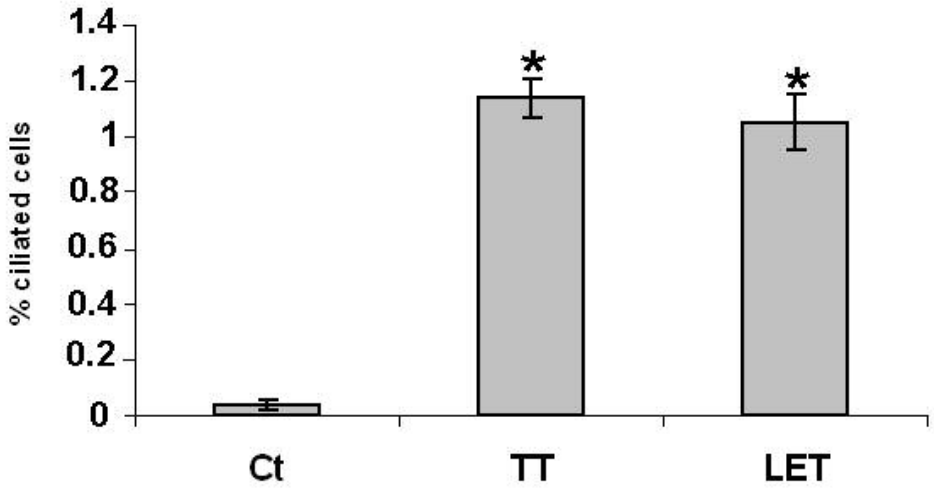

Artigo: A modified method for the selective staining of elastic system fibers in methacrylate tissue section, publicado pelo periódico *Brazilian Journal of Morphological Sciences,* em setembro de 2004.

Este trabalho é uma descrição da modificação do método de coloração pela resorcina-fucsina de Weigert, que foi desenvolvida na tentativa de marcar as fibras do sistema elástico das próstatas femininas analisadas neste trabalho.

SHORT COMMUNICATION

ISSN- 0102-9010

A MODIFIED METHOD FOR THE SELECTIVE STAINING OF ELASTIC SYSTEM FIBERS IN METHACRYLATE TISSUE SECTIONS

Fernanda Cristina Alcântara dos Santos, Lara Sílvia Corradi, Rodrigo Paula Leite, Rejane Maira Góes and Sebastião Roberto Taboga

Laboratory of Microscopy and Microanalysis, Department of Biology, Institute of Biosciences, Letter and Exact Sciences (IBILCE), Paulista State University "Júlio de Mesquita Filho" (UNESP), São José do Rio Preto, SP, Brazil.

ABSTRACT

The elastic system fibers are abundant elements of the extracellular matrix found in organs such as skin, blood vessels, lung and in elastic cartilage and elastic tendons. These fibers have been studied by several selective staining methods, such as resorcin-fuchsin for light microscopy and hematoxylin-eosin plus fluorescence and confocal scanning laser microscopy. However, most of these techniques are only efficient for tissues embedded in paraffin or paraplast, since most dyes show low penetration into glycol methacrylate resins. In this report, we describe a variation of Weigert's resorcin-fuchsin method that involves the pretreatment of resin sections with potassium permanganate. This procedure increased the affinity between the dye and elastic fibers, and stained the elastic fibers in black or dark violet, the nuclei in purple and other structures in light blue. Thus, this modification of the original method provided excellent artifact-free demarcation of elastic fibers in well-preserved tissues.

Key words: Elastic system fiber, extracellular matrix, methacrylate resin, resorcin-fuchsin, selective stain

The elastic system fibers are complex structures that contain elastin, microfibrillar proteins, lysyl oxidase, and, occasionally, proteoglycans. Elastin is the predominant protein of mature elastic fibers and provides the fibers with their characteristic property of elastic recoil. Elastic fibers can be identified in light microscopy by selective staining methods. This selective staining has allowed the visualization of elastic structures in many tissues and organs. In elastic tendons, lung and skin, the fibers are slim, rope-like, and variable in length. In major arteries, such as the aorta, elastic fibers form concentric sheets or lamellae, while in elastic cartilage these fibers are arranged in a three-dimensional network [9].

The elastic fibers in all of these organs and tissues have been studied by several selective staining methods such as resorcin-fuchsin [15] and orcein [14] for ordinary light microscopy, and hematoxylin-eosin staining in conjunction with fluorescence and confocal laser microscopy [3,4,5]. However, most of these techniques are only efficient for tissues embedded in paraffin or paraplast since many dyes show poor penetration into glycol methacrylate resins and their derivates [8].

Various methods have been proposed to facilitate the penetration of stains into resin sections, including microwave irradiation [2] and plasticizing clearing agents [6]. However, these methods are complex and can compromise the quality of the histological sections.

In this report, we describe a modification of resorcin-fuchsin staining method proposed by Weigert in which the resin sections are pretreated with potassium permanganate and oxalic acid. This procedure enhances the dye penetration and improves the detection of elastic fibers.

Male and female adult gerbils (*Meriones unguiculatus*, Gerbilinae, Muridae) were sacrificed by CO_2 inhalation followed by decapitation and the aorta, epiglottis, esophagus, skin and prostate were removed and fixed in Karnovsky fixative (5% paraformaldehyde and 2.5% glutaraldehyde in Sörensën phosphate buffer, pH 7.2), embedded in glycol methacrylate resin (Leica historesin embedding kit) or paraplast (Histosec, Merck) and sectioned (3 μm) on a Leica automatic rotative microtome. The choice of these organs was based on the abundance of elastic system components in their histological architecture.

Correspondence to: Dr. Sebastião Roberto Taboga
Departamento de Biologia, Instituto de Biociências, Letras e Ciências Exatas da Universidade Estadual Paulista "Júlio de Mesquita Filho" (IBILCE/UNESP), Rua Cristóvão Colombo, 2265, Jardim Nazareth, CEP 15054-000, São José do Rio Preto, SP, Brasil. Tel: (55) (17) 221-2386, Fax: (55) (17) 221-2390, E-mail: taboga@bio.ibilce.unesp.br

The sections were subsequently treated with 1% potassium permanganate for 10 min, washed in distilled water for 1 min, immersed in 3% oxalic acid for 1 min and washed again in distilled water for 1 min. After one wash with 95% ethanol for 1 min, the sections were stained with Weigert's resorcin-fuchsin [15] for 5 h, immersed in 95% ethanol for 1 min, counter-stained with Harris' hematoxylin for 3 min, washed in tap water for 10 min, dehydrated in ethanol, clarified in xylol and mounted in Canada balsam. This procedure is summarized in Table I.

Table 1. Steps for the modified Weigert resorcin-fuchsin method for the detection of elastic fibers in hydrophilic resins.

Step	Treatment	Time
1	Potassium permanganate (1%)	10 min
2	Distilled water	1 min
3	Oxalic acid (3%)	1 min
4	Distilled water	1 min
5	Ethanol (95%)	1 min
6	Weigert´s Resorcin-fuchsin	5 h
7	Ethanol (95%)	1 min
8	Harris's hematoxylin	3 min
9	Tap water	10 min
10	Dehydration in ethanol (70%, 95% and 100%)	5 min each
11	Clearing in xylol (3 washes)	10 min each
12	Mounting in Canada balsam	-

Since the elastic fibers of glycol methacrylate resin sections are not stained by hematoxylin-eosin, this stain was used for comparison with Weigert´s original method [1]. Gömöri's reticulin method [1], which employs the same pretreatment as that described here, was used to demonstrate the selectivity of the resorcin-fuchsin stain for elastic fibers. In addition, some sections were stained with resorcin-fuchsin without pretreatment with potassium permanganate in order to demonstrate that prior oxidation was essential for detecting the elastic fibers.

All of the stained sections were observed and documented with either a Zeiss Jenaval or an Olympus light microscope.

Paraplast sections of the prostate muscle artery stained by Weigert's original method are shown in Figure 1a and b. Figure 2a and b shows the same tissue embedded in resin and stained by the Weigert's modified method described here. Both techniques stained the conspicuous internal and external elastic lamina of the *intima* and the thin fibers of the *adventitia*. However, the demarcation and preservation of the elastic fibers was better with the modified method.

Figures 3, 4 and 5 show the aorta wall stained with hematoxylin-eosin, Weigert's modified resorcin-fuchsin and Gömöri's silver impregnation, respectively. The elastic fibers were not stained in the hematoxylin-eosin method, which stains only smooth muscle cells and collagen fibers of the tunica media (Fig. 3). After Gömöri's staining method (Fig. 5), the reticular fibers were stained in black whereas elastic fibers were not stained. On the other hand, Weigert's modified resorcin-fuchsin staining selectively revealed only elastic fibers (Fig. 4). Thus, the differential selectivity of Gömöri's and Weigert's modified resorcin-fuchsin methods is determined by steps subsequent to the pretreatment with potassium permanganate which oxidizes sugar residues.

Figures 6, 7, 8 and 9 show resin sections from epiglottis, esophagus, skin and prostate, respectively, that were stained by the modified Weigert resorcin-fuchsin method. A large amount of strongly stained elastic elements was seen in all cases.

The elastic system fibers cannot be observed by conventional hematoxylin-eosin staining. Rather, these extracellular matrix elements have been observed by selective staining methods such as Weigert's resorcin-fuchsin, Verhöeff´s ferric hematoxylin and Unna´s orcein stains. These methods

Figures 1a,b. A muscle artery from gerbil (*M. unguiculatus*) prostate embedded in paraplast and stained by Weigert's original resorcin-fuchsin method. Bars = a, 52 µm; b, 13 µm. **Figures 2a,b.** A muscle artery from gerbil prostate embedded in historesin and stained by the modified resorcin-fuchsin method. Bars = a, 40 µm; b, 13 µm. **Figure 3.** Elastic elements (**arrows**) in gerbil aorta embedded in historesin and stained with hematoxylin-eosin, which in negatively stains elastic fibers. (**m**) muscle fibers. Bar = 13 µm. **Figure 4.** The modified resorcin-fuchsin method shows intensely stained aortic elastic fibers (**arrows**). Bar = 13 µm. **Figure 5.** Gömöri's reticulin method does not stain aortic elastic fibers (**arrows**), but demarcates reticular fibers in brown (**r**). Bar = 13 µm. **Figures 6-9.** Some organs and tissues from *M. unguiculatus* embedded in historesin and stained by the modified Weigert resorcin-fuchsin method. **6**. Epiglottis with elastic fibers (**el**) around the cartilage (**C**). Bar = 52 µm. The inset shows that staining without pretreatment does not detect the elastic fibers (*****). Bar = 52 µm. **7**. Irregular distribution of elastic fibers in the esophageal submucosa. The association between elastic and skeletal muscle fibers (**mf**) can be seen. Bar = 20 µm. **8**. Histological section of skin showing the relatively thick elastic fibers (**arrows**). Bar = 52 µm. **9**. General distribution of elastic fibers in gerbil prostate. Note the very thin elastic fibers (**arrows**) of the stroma (**s**) and at the base of the epithelium (**ep**). (**v**) blood vessel. Bar = 16 µm.

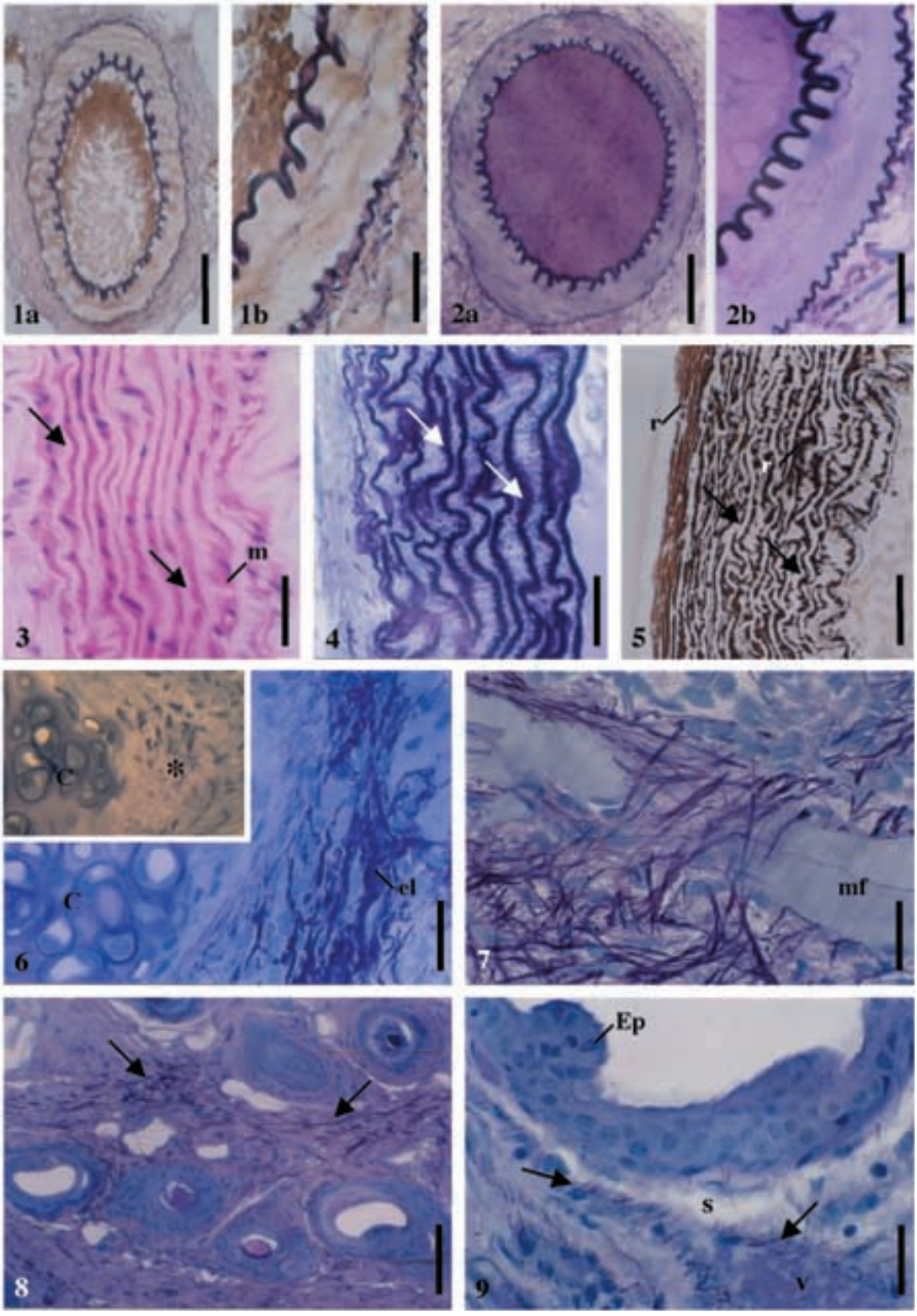
1a
1b
2a
2b
3
m
4
r
5
C
*
C
el
6
mf
7
Ep
s
v
8
9

generally serve only for material embedded in paraffin or paraplast. The use of hydrophilic resins for embedding tissues provides excellent microscopic resolution, but the most histological stains cannot be used with such samples because the resin polymer network limits access of dye molecules to the tissue.

The modification of the staining method described here involves pretreatment with potassium permanganate. This treatment results in the formation of free radical aldehydes. Feulgen and Voit [7] reported the presence of aldehyde groups in elastic fibers. These groups are responsible for cross-linking during elastic fiber maturation [11]. Active aldehyde groups frequently appear during desmosin and isodesmosin formation but are later reduced and may even disappear [13].

Aldehyde groups react positively with Schiff's reagent and resorcin-fuchsin, and are responsible for staining of elastic fibers. Lillie *et al*. [10] and Mc Callum [12] demonstrated that the staining of elastic fibers by resorcin-fuchsin and orcein was mediated by the presence of free aldehyde groups in the elastic extracellular matrix.

The use of potassium permanganate as an oxidizing agent is well established and involves a mechanism known as Casella's reaction [11]. This reaction oxides structures containing carbohydrate to produce aldehydes that are detected by Schiff's reagent.

Since elastic fibers naturally contain aldehydes, the use of Casella's reaction increases the number of free aldehyde groups [11]. This increase in reactive groups facilitates binding of the dye molecule and provides intense staining of elastic and pre-elastic fibers.

The results obtained here were very satisfactory since it was not necessary to remove the resin prior to staining, and excellent artifact-free staining of elastic fibers was observed in well-fixed tissues. This enhanced staining should facilitate morphometric stereological analyses.

ACKNOWLEDGMENTS

The authors thank Dr. Hernandes F. Carvalho (Department of Cell Biology, IB/UNICAMP, Campinas, SP) for constructive suggestions and advice and Luiz Roberto Falleiros Junior for technical assistance. This work was partially supported by Fundação de Amparo à Pesquisa do Estado de São Paulo (FAPESP).

REFERENCES

1. Behmer AO, Tolosa EMC, Neto AGF (1976) *Manual de Práticas para Histologia Normal e Patológica*. Edart-Edusp: São Paulo.
2. Brinn NT (1986) Rapid metallic histologic staining using microwave oven. *J. Histotechnol.* **6**, 125-128.
3. Carvalho HF, Taboga SR (1996a) Fluorescence and confocal laser scanning microscopy imaging of elastic fibers in hematoxylin-eosin stained sections. *Histochem. Cell Biol*. **106**, 587-592.
4. Carvalho HF, Taboga SR (1996b) The applicability of hematoxylin-eosin staining plus fluorescence or confocal laser scanning microscopy to the study of elastic fibers in cartilages. *C. R. Acad. Sci. Paris* **319**, 991-996.
5. Carvalho HF, Taboga SR, Felisbino SL (1999) Fluorescence and confocal laser scanning microscopy of H&E stained sections for the study of elastic fibers in skin and in some skin disorders. *Braz. J. morphol. Sci.* **16**, 97-104.
6. Crowley HH (1989) Improving stain penetration into epoxy resin sections for light microscopy. *Stain Technol*. **64**, 98-100.
7. Feulgen R, Voit K (1924) Über einen weitverbreiteten festen Aldehyd, seine Euststehung aus einer Vorstufe, sein mikrochemischer und mikroskopischer nachweis und die Wege seiner präparativen Darstellung. *Pflügers Arch. Ges. Physiol*. **206**, 389-391.
8. Hayat MA (1993) *Stains and Cytochemical Methods*. Plenum: New York.
9. Kreis T, Vale R (1999) *Extracellular Matrix, Anchor and Adhesion Proteins*. Oxford University Press: New York.
10. Lillie RD, Pizzolato P, Donaldson PT (1972) Elastin IV. Lysinal aldehyde relations, blocking and extraction tests, staining mechanisms. *Acta Histochem.* **44**, 215-219.
11. Lison L (1960) *Histochimie et Cytochimie Animals*. Gautier-Villars: Paris.
12. Mc Callum DK (1973) Positive Schiff reactivity of aortic elastin without prior HIO_4 oxidation: influence of maturity and a suggested source of the aldeyde. *Stain Technol*. **48**, 117-120.
13. Miller EJ, Fullmer HM (1966) Elastin: diminished reactivity with aldeyde reagents in copper deficiency and lathyrism. *J. Exp. Med.* 123, 1097-1108.
14. Unna PG (1891) Notiz, bettreffend die Tänzersche Orceinfarbung des elastischen Gewebes. *Monatsschr. Prakt. Dermatol*. **12**, 394-500.
15. Weigert C (1898) Über eine Methode zur Färbung elastischer Fasern. *Zentralbl. Allg. Pathol*. **9**, 289-292.

Received: October 23, 2003
Accepted: June 2, 2004

1. A administração de testosterona em fêmeas adultas do gerbilo causou importantes alterações prostáticas. As maiores modificações ocorreram no compartimento epitelial da glândula, que apresentou um comportamento bifásico caracterizado por uma resposta proliferativa inicial, seguida por uma fase altamente secretória.

2. O estímulo androgênico exógeno promoveu o crescimento e aumento da atividade secretória da próstata feminina, de maneira semelhante ao que ocorre durante o desenvolvimento da próstata de camundongos e ratos machos. Desse modo, pode-se concluir que a carência em estímulos androgênicos contribui para o pequeno desenvolvimento apresentado pela próstata feminina normal do gerbilo.

3. O curto período de administração androgênica levou à instalação de alterações displásicas como neoplasia intraepitelial prostática, hiperplasia atípica e adenocarcinoma de células mucinosas. Assim, longos períodos de exposição a andrógenos podem resultar em câncer prostático.

4. Condições de hiperandrogenismo ou exposição a andrógenos exógenos causam aumento da atividade prostática, sinais de crescimento displásico, estreitamento da parede uretral, hiperplasia do estroma ovariano e ovários policísticos. Esta série de efeitos pode levar ao comprometimento da saúde das mulheres e, deste modo, a

simples conclusão de que o hiperandrogenismo resulta em ovários policísticos deve ser reconsiderada, visto que outros órgãos também são sensíveis aos andrógenos.

5. A terapia endócrina com letrozol causou uma elevação gradual dos níveis séricos de testosterona, simulando uma condição de hiperandrogenismo. A resposta da glândula prostática feminina do gerbilo a este tratamento foi semelhante à observada no tratamento com andrógenos, compreendendo aumento do peso relativo prostático, acréscimo da atividade secretória, alteração na expressão de receptores androgênicos e estrogênicos e ocorrência de crescimento displásico. No entanto, o letrozol apresentou maior potencial para desenvolver lesões prostáticas do que o tratamento com andrógenos.

6. A condição de hiperandrogenismo causada pelos tratamentos com testosterona e letrozol influenciou o padrão de diferenciação das células epiteliais secretoras, levando a um acréscimo na freqüência de células secretoras claras e de células ciliadas. A diferenciação do fenótipo ciliado revelou-se andrógeno-dependente, porém não foi alterada por diferentes concentrações do hormônio. Por outro lado, a freqüência de diferenciação de células claras foi variável de acordo com a concentração androgênica alcançada.

7. A administração experimental de tamoxifeno em fêmeas adultas do gerbilo resultou em hiperplasia das células epiteliais e estromais, dilatação luminal, diminuição da atividade secretora e crescimento displásico. Estas alterações prostáticas são muito

semelhantes às modificações observadas nas próstatas de roedores machos estrogenizados no período intra-embrionário e neonatal. Assim pode-se concluir que o tamoxifeno atuou como um agonista estrogênico na próstata feminina do gerbilo, embora possa exercer atividade antagonista em outros órgãos reprodutivos.

8. As terapias anti-estrogênicas com letrozol e tamoxifeno, que são amplamente utilizadas como primeira linha de tratamento contra a progressão do câncer de mama ER-positivo, resultam em uma série de efeitos complexos que comprometem a fisiologia de outros órgãos hormônio-dependentes, como a próstata feminina e os ovários.

9. O desequilíbrio hormonal provocado pela administração de letrozol e tamoxifeno resulta em profundas alterações na morfologia prostática, de maneira muito similar ao que ocorre durante o desenvolvimento de lesões espontâneas em mulheres no período pós-menopausa. Assim, a opção por estas terapias deve ser tomada com cautela, visto que longos períodos de tratamento podem resultar em lesões malignas da próstata feminina.

Addiego F, Belzer EG, Comolli J, Moger W, Perry JD, Whipple B. 1981. Female ejaculation: a case study. *J Sex Res*, 17:1-13.

Ali SZ, Smilari TF, Gal D, Lovecchio JL, Teichberg S. 1995. Primary adenoid cystic carcinoma of Skene´s glands. *Gynecologic Oncology*, 57:257-261.

Bhatnagar AS, Hausler A, Schieweck K, Lang M, Bowman LR. 1990. Highly selective inhibition of estrogen biosynthesis by CGS 20267 a new non-steroidal aromatase inhibitor. *J Steroid Biochem Mol Biol*, 37: 1021-1027.

Berstein L, Maximov S, Gershfeld E, Meshkova I, Gamajunova V, Tsyrlina E, Larionov A, Kovalevskij A, Vasilyev D. 2002. Neoadjuvant therapy of endometrial câncer with the aromtase inhibitor letrozole: endocrine and clinical effects. *Obstetrics & Gynecology*, 105:161-165.

Bieberich CJ, Fujita K, He WW, Jay G. 1996. Prostate-specific and androgen-dependent expression of a novel homeobox gene. *J Biol Chem*, 271:31779-31782.

Block, J.L.; Block, N.L.; Lokeshwar, B.L. 1996. Inhibition of aromatase activity and growth suppression by –methoxy-4-androstene-3,7-dione in an androgen sensitive human prostatic carcinoma cell line. *Cancer Letters*, 101: 143-148.

Cabot MC, Giuliano AE, Volner A, Han TY. 1996. Tamoxifen retards glycosphingolipid metabolism in human cancer cells. *FEBS Letters*, 394:129-131.

Clark MM, Crews D, Galef BG. 1991. Concentrations of sex steroids hormones in pregnant and fetal Mongolian gerbils. *Physiol Behav*, 49:239.

Cunha GR, Hayward SW, Wang YZ. 2002. Role of stroma in carcinogenesis of the prostate. *Differentiation*, 70:473-485.

Custódio AMG, Góes RM, Taboga SR. 2004. Acid phosphatase activity in gerbil prostate: comparative study in male and female during postnatal development. *Cell Biology International*, 28:335-344.

de Graaf R. 1672. De mulierum organis generationi inservientibus. Tractatus novus demonstrans tani homines et animália caetera omnia, quac vivípara dicuntut, haud minus quam vivípara ab ovo origenem ducere. Leyden, 66p.

Diamandis EP, Yu H. 1997. Nonprostatic sources of prostate-specific antigen. *Urol Clin North Am*, 24(2):275-282.

Dixon JM, Jackson J, Renshaw L, Miller WR. 2003. Neoadjuvant tamoxifen and aromatase inhibitors: comparisons and clinical outcomes. *J Steroid Biochem Mol Biol*,86:295-299.

Dodson MK, Cliby WA, Keeney GL, Peterson MF, Podratz KC. 1994. Skene´s gland adenocarcinoma with increased serum level of prostate-specific antigen. *Gynecol Oncol*, 55:304-307.

Dodson MK, Cliby WA, Pettavel PP, Keeney GL, Podratz KC. 1995. Female urethral adenocarcinoma: evidence for more than one tissue of origin? *Gynecol Oncol*, 59(3):352-357.

Donjacour AA, Cunha GR. 1993. Assessment of prostatic protein secretion in tissue recombinants made of urogenital sinus mesenchyme and urothelium from normal or androgen-insensitive mice. *Endocrinology*, 131:2342-2350.

Ebisuno S, Miyai M, Nagareda T. 1995. Clear cell adenocarcinoma of the female urethra showing positive staining with antibodies to prostate-specific antigen and prostatic acid phosphatase. *Urology*, 45(4):682-685.

Flamini MA, Barbeito CG, Gimeno EJ, Portiansky EL. 2002. Morphological characterization of the female prostate (Skene's gland or paraurethral gland) of *Lagostomus maximus maximus*. *Annals of Anatomy*, 184:341-345.

Galadari I, Al-Mazroei M, Alkaabi J. 2004. Prostatic-specific antigen and idiopathic hirsutism in females. *International Journal of Dermatology*, 43:275-277.

García-Flórez M, Oliveira CA, Carvalho HF. 2005. Early effects of estrogen on the rat ventral prostate. *Braz J Med Biol Res*, 38(4):487-497.

Gradishar WJ. 2004. Tamoxifen – What next? *The Oncologist*, 9: 378-384.

Gräfenberg E. 1950. The role of the urethra in female orgasm. *Int J Sexol*, 3:145-148.

Gross SA, Didio LJA. 1987 Comparative morphology of the prostate in adult male and female of Praomys (mastomys) natalensis studies with electron microscopy. *J. Submicros. Cytol*, 19 (1):77-84.

Gunson DE, Bell R, Sahota PS, Han Hsu H. 1996. Inhibition of spontaneous mammary tumors by CGS 20267, an aromatase inhibitor, in female Sprague-Dawley rats. *Toxicol Pathol*, 24: 789-794.

Härkönen PL, Mäkelä SI. 2004. Role of estrogens in development of prostate cancer. *J Steroid Biochem Mol Biol* ,92:297-305.

Haynes BP, Dowsett M, Miller WR, Dixon JM, Bhatnagar AS. 2003. The pharmacology of letrozole. *J Steroid Biochem Mol Biol*, 87:35-45.

Hayward SW, Baskin LS, Haughney PC, Cunha AR, Foster BA, Dahiya R, Prins GS, Cunha GR. 1996. Epithelial development in the rat ventral prostate, anterior prostate and seminal vesicle. *Acta Anat*, 155:81-93.

Hines TM. 2001. The G-spot: A modern gynecologic myth. *Am J Obstet Gynecol*, 185(2): 359-362.

Huang L, Pu Y, Alam S, Birch L, Prins GS. 2004. Estrogenic regulation of signaling pathways and homeobox genes during rat prostate development. *J Androl*, 25: 330-337.

Huffman JW. 1948. The detailed anatomy of the paraurethral ducts in the adult human female. *Am J Obstet Gynecol*, 55:86-101.

Huffman JW. 1951. Clinical significance of the paraurethral ducts and glands. *Arch Surg*, 62:615-625.

Ingle JN, Suman VJ 2003. Aromatase inhibitors versus tamoxifen for management of postmenopausal breast cancer in the advanced disease and neoadjuvant settings. *J Steroid Biochem Mol Biol*, 86: 313-319.

Isaacs JT, Furuya Y, Berges R. 1994. The role of androgen in the regulation of ptogrammed cell death/apoptosis in normal and malignant prostatic tissue. *Seminars in Cancer Biology*, 5:391-400.

Islam AHMM, Kato H, Hayama M, Kobayashi S, Ota H, Nishizawa O. 2001. Adenocarcinoma of female paraurethral duct showing neuroendocrine differentiation. *Urology*, 58(6):1058iv-vi.

Kato H, Kobayashi S, Islam AM, Nishizawa O. 2005. Female para-urethral adenocarcinoma: histological and immunohistochemical study. *Int J Urol*, 12:117-119.

Kocak M. 2004. Serum levels of prostate-specific antigen and androgens after nasal administration of gonadotropin releasing hormone-agonist in hirsute women. *Gynecol Endocrinol*, 18(4):179-185.

Marker PC, Donjacour AA, Dahiya R, Cunha GR. 2003. Hormonal, cellular, and molecular control of prostatic development. *Developmental Biology*, 253:165-174.

Markovits JE, Sahota PS. 2000. Aromatase inhibitors prevent spontaneous granular cell tumors in the distal female reproductive tract of Sprague-Dawley rats. *Toxicol Pathol,* 28: 799-801.

McCluggage WG, Ganesan R, Hirschowitz L, Miller K, Rollason TP. 2006. Ectopic prostatic tissue in the uterine cervix and vagina: report of a series with a detailed immunohistochemical analysis. *Am J Surg Pathol*, 30(2):209-215.

McCrea LE. 1952. Malignancy of the female urethra. *Urol Surv*, 2:85-149.

Miller WR, Dixon JM, Macfarlane L, Cameron D, Anderson TJ. 2003. Pathological features of breast cancer response following neoadjuvant treatment with either letrozole or tamoxifen. *Eur J Cancer*, 39: 462-468.

Pointis G, Latreille MT, Cedard L. 1980. Gonado-pituitary relationships in the fetal mouse at various times during sexual differentiation. *J Endocrinol*, 86:483-488.

Pu Y, Huang L, Prins GS. 2004. Sonic hedgehog-patched Gli signaling in the developing rat prostate gland: lobe-specific suppression by neonatal estrogens reduces ductal growth and branching. Dev Biol, 273:257-275.

Risbridger GP, Bianco JJ, Ellem SJ, McPherson SJ. 2003. Oestrogens and prostate cancer. *Endocrine-Related Cancer*, 10:187-191

Santos FCA, Corradi LS, Taboga SR. 2001. Cytochemical characterization of the stromal compartiment in gerbil female prostate. *In* Proceedings of the XVIII Congress of the Brazilian Society for Microscopy and Microanalysis, 2001, Águas de Lindóia, Brazil, Suppl C. pp.207.

Santos FCA, Carvalho HF, Góes RM, Taboga SR. 2003. Structure, histochemistry and ultrastructure of the epithelium and stroma in the gerbil (*Meriones unguiculatus*) female prostate. *Tissue & Cell*, 35:447-457.

Sauter ER, Klein G, Wagner-Mann C, Diamandis EP. 2004. Prostate-specific antigen expression in nipple aspirate fluid is associated with advanced breast cancer. *Cancer Detection and Prevention*, 28:27-31.

Schmidt S, Franke M, Lehmann J, Loch T, Stöckle M, Weichert-Jacobsen K. 2001. Prostate-specific antigen in female urine: a prospective study involving 217 women. *Urology*, 57:717-720.

Schubach G. 2002. The G-spot is the female prostate. *Am J Obstet Gynecol*, 186(4): 850.

Shapiro E, Huang H, McFadden DE, Masch RJ, NG E, Lepor H, Wu XR. 2004. The prostatic utricle is not a Müllerian duct remnant: immunohistochemical evidence for a distinct urogenital sinus origin. *J Urol*, 172:1753-1756.

Sharifi-Aghdas F, Ghaderian N. 2004. Female paraurethral cysts: experience of 25 cases. *BJU International*, 93:353-356.

Shehata R. 1974. Urethral glands in the wall of the female urethra of rats, mice and closely related rodents. *Acta Anat*, 90:381-387.

Shehata R. 1975. Female prostate in *Arvicantihis niloticus* and *Meriones lybicus*. *Acta Anat*, 92:513-523.

Shehata R. 1980. Female prostate and urethral glands in the home rat, *Rattus norvegicus*. *Acta Anat*, 107:286-288.

Singh J and Handelsman DJ. 1999. Imprinting by neonatal sex steroids on the structure and function of the mature mouse prostate. *Biol Reprod*, 61: 200-208.

Skene AJC. 1880. The anatomy and pathology of two important glands of the female urethra. *Amer J Obstetr Diss Women Child*, 13:265-270.

Sloboda J, Zaviačič M, Jakubovský J, Hammar E, Johnsen J. 1998. Metastasizing adenocarcinoma of the female prostate (Skene´s paraurethrl galnds). Histological and immunohistochemical prostate markers studies and first ultraestructural observation. *Pathol Res Pract*, 194:129-136.

Smith AF, Landon GV, Ghanadian R, Chisholm GD. 1978. The ultrastructure of the male and female prostate of Praomys (Mastomys) natalensis. *Cell Tiss Res*, 190:539-552.

Smith IE. 2003. Letrozole versus tamoxifeno in the treatment of advanced breast cancer and as neoadjuvant therapy. *J Steroid Biochem Mol Biol*, 86:289-293.

Staack A, Donjacour AA, Brody J, Cunha GR, Carrol P. 2003. Mouse urogenital development: a practical approach. *Differentiation*, 71:402-413.

Staub NL, Beer MD. 1997. The role of androgens in female vertebrates. *Gen Compar Endocrinology*, 108: 1-24.

Taboga SR, Góes RM, Zanetoni C, Santos FCA. 2001. Ultrastructural characterization of the prostate secretory cells: a comparative study between the male and female organs. *In* Proceedings of the XVIII Congress of the Brazilian Society for Microscopy and Microanalysis, 2001, Águas de Lindóia, Brazil, Suppl C. pp.205.

Taguchi O. 1987. Reproductive tract lesions in male mice treated neonatally with tamoxifen. *Biol Reprod*, 37: 133-116.

Tepper SL, Jagirdar J, Heath D, Geller SA. 1984. Homology between the female parauretrhal (Skenes's) glands and the prostate. *Arch Pathol Lab Med*, 108(5): 423-425.

Thomson AA. 2001. Role of androgens and fibroblast growth factors in prostatic development. *Reproduction*, 121:187-195.

Thomson AA, Timms BG, Barton L, Cunha GR, Grace OC. 2002. The role of smooth muscle in regulating prostatic induction. *Development*, 129:1905-1912.

Timms BG, Petersen SL, Vom Saal FS. 1999. Prostate gland growth during development is stimulated in both male and female rat fetuses by intrauterine proximity to female fetuses. *J Urology*, 161:1694-1701.

Vilamaior PSL, Santos FCA, Falleiros-Jr LR, Biancardi MF, Fochi RA, Taboga SR. 2005. Comparative histology of gerbil and rat female prostate: morphological evidences of different functional state during distinct phases of post-natal development. *Braz. J Morpho. Sci,:* Suppl 3:28.

Wang Y, Hayward S, Cao M, Thayer K, Cunha G. 2001. Cell differentiation lineage in the prostate. *Differentiation*, 68:270-279.

Yu H, Berkel H. 1999. Prostate-specific antigen (PSA) in women. *J La State Med Soc*, 151(14): 209-213.

Wernet N, Albrecht M, Sesterhenn I, Goebbels R, Bonkhoff H, Seitz G, Inniger R, Remberger K. 1992. The "female prostate": localion, morphology, immunohistochemical characteristics and significance. *Eur Urology*, 22:64-69.

Zaviačič M. 1993. Update on the female prostate and the phenomenon of female ejaculation. *The Journal of Sex Research,* 30(2): 148-151.

Zaviačič M, Sidlo J, Borovský M. 1993. Prostate specific antigen and prostate specific acid phosphatase in adenocarcinoma of Skene's paraurethral glands and ducts. *Virchows Archiv A Pathol Anat*, 423: 503-505.

Zaviačič M, Ružičková M, Blažeková J, Zaviačič T, Itoh Y, Okutani R, Kawai T. 1997a. Immunohistochemical distribution of rabbit polyclonal antiurinary protein 1 antibody in the female (Skene's gland) and male prostate: new marker for neuroendocrine cells? *Acta Histochem*, 99:267-275.

Zaviačič M, Danihel L, Ružičková M, Blažeková J, Itoh Y, Okutani R, Kaway T. 1997b. Immunohistochemical localization of human protein 1 in the female prostate (Skene's Gland) and the male prostate. *Histochem J*, 29(3):219-227.

Zaviačič M. 1999. *The Female Prostate: From vestigial Skene's parauretral glands and ducts to woman's functional prostate*. 1.ed. Bratislava, Slovakia: Slovack Academic Press, 171p.

Zaviačič M, Ablin RJ. 2000. The female prostate and prostate-specific antigen. Imunohistochemical localization, implications of this prostate marker in women and reasons for using the term "prostate" in human female. *Histol Histopathol*, 15(1):131-142.

Zaviačič M, Jakubovská V, Belošovič J, Breza J. 2000a. Ultrastrucuture of the normal adult human female prostate gland (Skene's gland). *Anat Embriol (Berl)*, 201(1):51-61.

Zaviačič M, Zajíčková M, Blazeková J, Donárová L, Svetoslav S, Miroslav M, Zaviačič T, Holomán K, Breza J. 2000b. Weight, size, macroanatomy, and histology of the normal

prostate in the adult human female: a minireview. *Journal of Histotechnology*, 23(1):61-69.

Zhang H, McElrath T, Tong W, Pollard JW. 2005. The molecular basis of tamoxifen induction of mouse uterine epithelial cell proliferation. *J Endocrinol*, 184: 129-140.